THE EFFECT OF MAGNETIC FIELD ON COMBUSTION AND EMISSIONS IN GASOLINE ENGINES

BY

Rashid Mohammed Ali Al-Dossary

A Thesis Presented to the

DEANSHIP OF GRADUATE STUDIES

KING FAHD UNIVERSITY OF PETROLEUM & MINERALS

DHAHRAN, SAUDI ARABIA

In Partial Fulfillment of the
Requirements for the Degree of

MASTER OF SCIENCE

In

MECHANICAL ENGINEERING

JUNE 2009

KING FAHD UNIVERSITY OF PETROLEUM & MINERALS

DHAHRAN 31261, SAUDI ARABIA

DEANSHIP OF GRADUATE STUDIES

This thesis, written by **Rashid Mohammed Ali Al-Dossary** under the direction of his thesis advisor and approved by his thesis committee, has been presented to and accepted by the Dean of Graduate Studies, in partial fulfilment of the requirements for the degree of **MASTER OF SCIENCE IN MECHANICAL ENGINEERING.**

Thesis Committee

Dr. A. Al-Farayedhi, Thesis Advisor

Dr. P. Gandhidasan, Member

Dr. K. Ziq, Member

Dr. A. Al-Qutub, Department Chairman

Dr. S. Zummo, Dean of Graduate Studies

30/5/09

Date

عمادة الدراسات العليا
DEANSHIP OF GRADUATE STUDIES

DEDICATION

I would like to dedicate this work to my family for their continuous wonderful love and moral support in all aspects of my life across the years.

I would also like to thank Saudi Aramco, in particular Abqaiq Plants departments, for giving me the opportunity to pursue this degree and continue my education to benefit the company in particular and the country in general.

ACKNOWLEDGMENT

Acknowledgement is due to the King Fahd University of Petroleum & Minerals for supporting this research.

I wish to express my appreciation to Professor Dr. A. Al-Farayedhi who served as my major advisor. I also wish to thank the other members of my thesis committee Dr. P. Gandhidasan and Dr. K. Ziq.

I also want to acknowledge KFUPM staff who helped in this research, particularly M. Adham of the Heat Engine Laboratory for his assistance in setting up the test equipment.

TABLE OF CONTENTS

Page

LIST OF TABLES

LIST OF FIGURES

THESIS ABSTRACT

Name of Student	:	Rashid Mohammed Ali Al-Dossary
Title of Study	:	The Effect of Magnetic Field on Combustion and Emissions in Gasoline Engines
Major Field	:	Mechanical Engineering
Date of Degree	:	June 29, 2009

The current experimental study aims to investigate the effect of magnetic field on internal combustion engines. The study concentrates on engine performance by examining fuel consumption and exhaust emissions. The magnetic field was applied to the fuel supply line of a typical SI engine using unleaded gasoline fuel. Moreover, the magnetic field was generated by electromagnets with a twelve-volts car battery while varying the strength and configuration of the magnetic field. The experiments were conducted at a variety of engine operating conditions by using an engine dynamometer setup. The exhaust gas emissions of CO, NOx, and HC were measured by using an online gas analyzer.

The magnetic effect on SFC reduction was only consistently significant at the lowest load of 20 Nm and both speed extremes of 1000 and 3000 rpm using one magnet. The effect on CO was the most significant reduction of all other emissions at most engine's loads and speeds, especially at lowest speed of 1000 rpm using five magnets. The effect on NOx was the most consistent reduction of all others with the most effect using the 'Spiral' configuration at lowest speed of 1000 rpm. The reduction on HC was most significant at the lowest speed of 1000 rpm using four magnets, while other magnetic fields' strengths and configurations also gave satisfactory reductions at most engines' loads and speeds.

ملخص الرسالة

اســـــم الطالب : راشد محمد علي الدوسري

عنوان الرسالة : تأثير الحقل المغناطيسي على الاحتراق والانبعاثات في محركات البنزين

التخصـــــص : الهندسة الميكانيكية

تاريخ التخرج : 6 رجب 1430 هـ

يهدف هذا البحث التجريبي إلى اختبار تأثير الحقل المغناطيسي على محركات الاحتراق الداخلي. يركز البحث على اداء المحرك بمراقبة استهلاك الوقود ونواتج الاحتراق. وقد تم وضع الحقل المغناطيسي على خط امداد الوقود لمحرك اشتعال بالشرارة مستخدماً وقود لايحتوي على الرصاص. وقد تم احداث الحقل المغناطيسي بواسطة المغناطيس الكهربائي باستخدام بطارية سيارة وتغير قوة وتركيبة الحقل المغناطيسي. وقد تم عمل التجارب في ظروف تشغيل متنوعة على داينمومتر خاص باختبار المحركات. وقد تم قياس نسبة كلٍ من أول أكسيد الكربون وأكاسيد النيتروجين والهيدروكربونات في نواتج الاحتراق وذلك باستخدام جهاز تحليل مستمر.

وقد كان التأثير المغناطيسي على تقليل استهلاك الوقود ثابتاً وبشكل ملحوظ فقط عند أقل حمل على المحرك وأسرع وأبطأ سرعة للمحرك باستخدام مغناطيس واحد. وقد كان التأثير على تقليل أول أكسيد الكربون الافضل أداءً مقارنة بباقي النتائج عند معظم احمال وسرعات المحرك وخصوصاً عند أقل سرعة للمحرك وباستخدام خمسة مغانط. وقد كان التأثير على تقليل أكاسيد النيتروجين الاكثر ثباتاً مقارنة بباقي النتائج وبشكل ملحوظ عند استخدام التركيبة الدائرية وأقل سرعة للمحرك. أخيراً وليس أخراً، قد كان التأثير على تقليل الهيدروكربونات الافضل عند أقل سرعة للمحرك باستخدام أربعة مغانط، كما اعطى تأثير بقية أوضاع الحقل المغناطيسي نتائج مرضية عند معظم احمال وسرعات المحرك.

CHAPTER 1

1 INTRODUCTION

1.1 Background

1.1.1 Internal Combustion Engines

Most automotive applications use internal combustion engines (ICEs) extensively. The combustion process in these engines is a very rapid chemical reaction between a fuel and an oxidizer, which takes place inside a confined space called the combustion chamber. Heat energy is released as a result of the oxidation of the fuel molecules during combustion, which can be transformed into other forms of useful energy such as the mechanical energy used in automotive applications.

The transformation to mechanical energy occurs in rapid repeating periodic cycles of piston movements (strokes) inside the chamber, which exert a rotational force on the crankshaft of the engine as shown in Figure 1-1. The cycle usually consists of four processes: induction, compression, power, and exhaust. The cycle is completed during a number of piston strokes, which depends on the engine design. Since one stroke of the cycle can produce power, a smooth rotation of the crankshaft requires the engine to be built with several cylinders performing the cycle processes at different intervals.

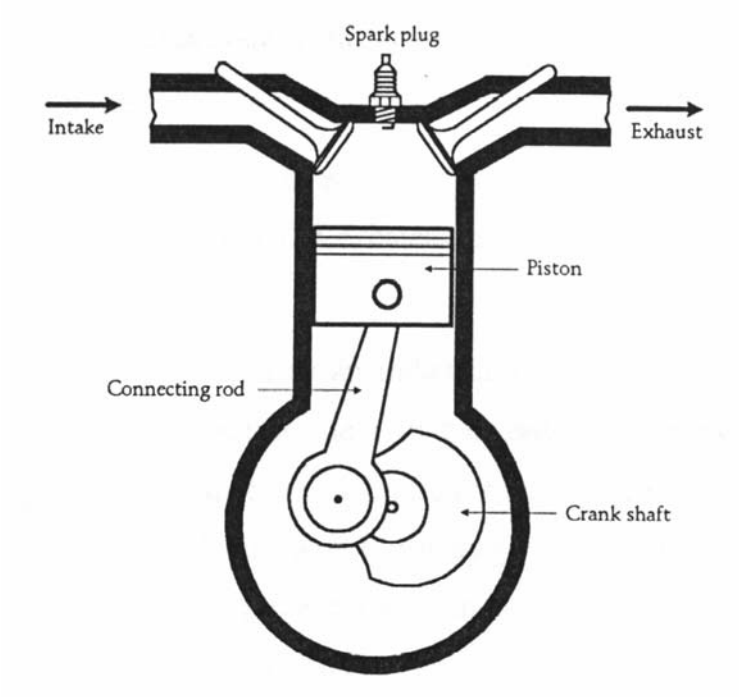

Figure 1-1: Basic structure of a spark ignition (SI) cylinder [1]

ICEs are of two types. Compression Ignition (CI) means introducing fuel into highly compressed air whereas Spark Ignition (SI) means triggering the combustion process by using an external spark. This difference in engine design can affect the performance, combustion efficiency, and exhaust emissions. Moreover, ICEs usually use liquid hydrocarbons such as diesel, gasoline, or natural gas according to the power requirements, and gases in hydrocarbon flames are usually ionized.

The engine completes the combustion cycle processes with the pistons in two upward and two downward positions. This can be accomplished in two crankshaft revolutions as shown in Figure 1-2. In the first stroke (Intake), the piston moves from the most upward position, called top centre (TC), to the most downward position, called bottom centre (BC), in order to induce the fuel and air mixture through the inlet valve. In the second stroke (Compression), the piston moves upward in order to compress the mixture to a

small fraction of its initial volume, while both valves are closed. Before the end of the compression stroke, the combustion process is triggered by using an internal spark. In the third stroke (Expansion), the piston moves downward to BC due to the high temperature, high pressure gases, and it forces the crankshaft to rotate. In the fourth and last stroke (Exhaust), the piston moves from BC to TC, and it forces all the combustion gases out through the exhaust valve.

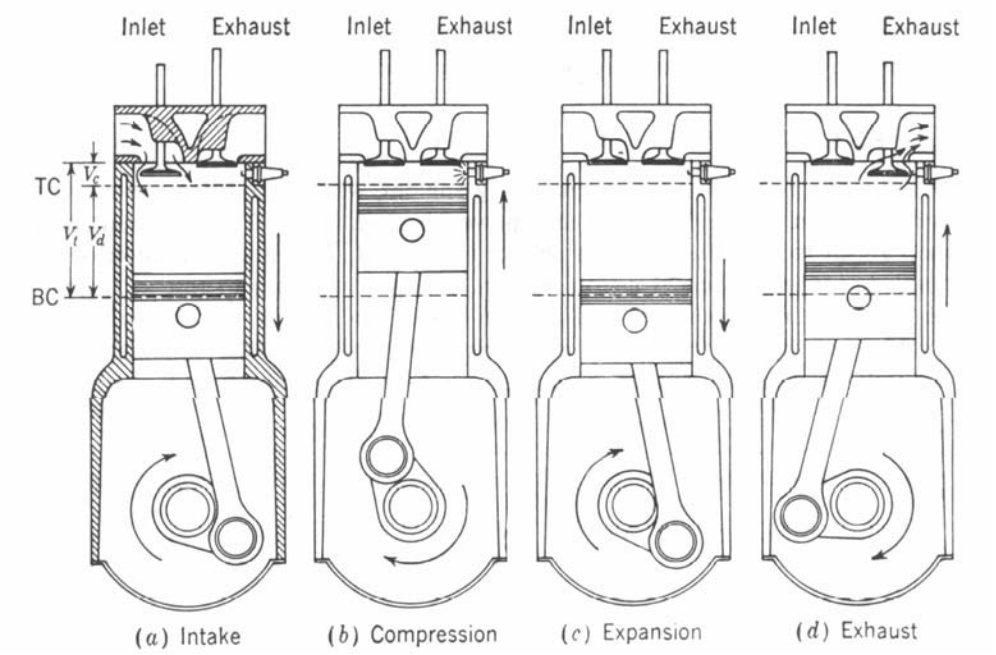

Figure 1-2: Four-stroke operating cycle of a Spark Ignition (SI) engine [2]

The combustion process can be affected by other operating variables such as the equivalence ratio, spark timing, engine speed, and load condition. The equivalence ratio is the ratio between the stoichiometric and actual air/fuel ratio. Combustion stoichiometry occurs when the chemically correct or theoretical proportions of fuel and air are introduced in the combustion chamber [1, 2, 3, 4, 5].

A four-stroke ICE with six cylinders, spark ignition, and fuel injection was used in this study with unleaded gasoline fuel. The magnetic effect was applied on the fuel supply line just before the induction stage to maximize its effect throughout the combustion process. The experiments were conducted at different load and speed settings while keeping all the other engine variables controlled automatically at its best performance.

1.1.2 Fuel Consumption

Most of the heat generated by this combustion process, about 67% of the total energy produced, is lost in the cylinder walls and exhaust process. Moreover, due to incomplete combustion, not all the energy in the supplied fuel is released. Part of the energy produced is consumed by the engine itself during the cycle processes and mechanical friction in the moving internal components of the cylinders. The effectiveness of the engine to convert fuel energy into mechanical work is measured by the brake thermal efficiency η_{bt} as shown in Equation 1-1, where P_{brake} is the engine brake power, $\dot{m}_f$ is the fuel consumption rate, and Q_{LHV} is the fuel low heating value.

$$\eta_{bt} = \frac{P_{brake}(kW)}{\dot{m}_f(kg/s)Q_{LHV}(kJ/kg)} \quad \text{(Equation 1-1)}$$

As shown in Equation 1-2, another important parameter to measure the engine efficiency is the Specific Fuel Consumption (SFC) which is used in this study for comparison since the fuel utilized in all experiments have the same energy content.

$$SFC(g/kWh) = \frac{\dot{m}_f(g/h)}{P_{brake}(kW)} = \frac{3600}{\eta_{bt}Q_{LHV}(MJ/kg)} \quad \text{(Equation 1-2)}$$

The maximum torque exerted on the crankshaft is usually the measure for engine output. However, the brake mean effective pressure (bmep) is a more useful measure since it does not depend on engine size. For a four-stroke engine as shown in Equation 1-3, it depends on engine displacement volume V_d and engine rotational speed N [1, 2, 3, 4, 5].

$$bmep(kPa) = \frac{P_{brake}(kW) \times 2000}{V_d(Liter)N(rev/s)} \quad \text{(Equation 1-3)}$$

1.1.3 Exhaust Emissions

The combustion processes and their emission formulation are extremely complex and difficult to control. Complete combustion of the hydrocarbon fuel is very hard to be accomplished. Some of the reasons of this incomplete combustion are chamber deposits, flame quenching, improper fuel and air mixture, and variation of flame temperature. Noxious emissions such as unburned hydrocarbons (HC), nitrogen oxides (NOx), and carbon monoxides (CO) are formed due to these reasons. Each of these gases has certain properties and negative impacts on all living organisms and the environment. The application of a magnetic field might make the combustion process more complete, and consequently reduce these noxious gases emissions [1, 2, 3, 4, 5, 6].

Furthermore, HC can cause eye irritation and cancer. HC are classified by their chemical reaction with the surroundings as reactive or non-reactive hydrocarbons. Saturated hydrocarbons such as paraffins and naphthenes are classified as non-reactive hydrocarbons. On the other hand, unsaturated hydrocarbons such as olefins and aromatics are classified as reactive hydrocarbons [2].

Nitrogen oxides formation is caused by the combustion flame high temperature. Nitrogen oxide (NO) is the major emission from these oxides, especially in SI engines. In addition,

small quantities of nitrogen dioxide (NO_2) are also emitted, which react with atmospheric oxygen (O_2) to form ozone (O_3). Moreover, nitrogen oxides react with atmospheric water vapour to form acid rain, which is mainly nitric acid (HNO_3), which can inhibit plant growth [1, 3, 6, 7].

Carbon monoxide is formed by incomplete oxidation of the fuel, which depends on the oxygen availability during combustion. CO is an odourless, colourless, poisonous gas, which delays the oxygen transportation from the lungs to the rest of the body, and subsequently causes dizziness and death.

These gases along with others react with the atmosphere in the presence of sunlight to form the photochemical smog. This smog will cause eye irritation, bad odour, and visibility reduction. Furthermore, these gases are highly oxidizing to the environment when reacted with each other.

Different methods have been invented to reduce these emissions by enhancing the combustion process or treating the exhaust gas. Proper fuel and air mixture has been produced by using fuel injection systems. Fuel additives have been introduced to promote combustion. Exhaust gas recirculation has been introduced to control the combustion temperature, and subsequently controlling the NOx formation. Oxidizing the incomplete burned gases has been accomplished by injecting air in the exhaust manifold. Catalytic converters have been produced to oxidize and reduce HC, NOx, and CO emissions [3, 6].

1.1.4 Magnetic Field

Magnetic field is usually the result of electrical charge in motion. In permanent magnets, there is no conventional electric current. However, the spins and orbital motions of electrons within the magnet material (called “Amperian Currents”) are the main cause for

magnetization within the material and magnetic field outside the material. These magnetic fields apply a force on the current-carrying conductors and permanent magnets [8].

Magnetic force and electrical force are similar in the attraction and repulsion properties. Similar poles of different magnets and similar electrical charges repel each other, whereas opposite poles of different magnets and opposite electrical charges attract each other. On the other hand, electrical charges can be isolated, and magnetic poles always exist in pairs [9].

Magnetic materials are classified into three categories based on their susceptibility (receptiveness or sensitivity) and permeability (porosity): diamagnets, paramagnets, and ferromagnets. Diamagnets such as copper, silver, and gold have low and negative susceptibility and they are usually used as superconductors. Paramagnets such as aluminium, platinum and manganese have low but positive susceptibility. Ferromagnets such as iron, cobalt, and nickel have high and positive susceptibility, which will produce higher magnetic induction and flux. Ferromagnets are the most widely recognized magnetic materials [8].

Magnetic field is an inherited material property in permanent magnets. However, magnetic fields can also be produced by solenoids or electromagnets. A solenoid is usually made by winding an insulated electrical conductor wire such as copper over an insulated core, called the former, in a helical pattern. On the other hand, an electromagnet uses a soft ferromagnetic material such as iron to be the former. The ferromagnetic core generates a higher magnetic induction for the same magnetic field. Increasing the number

of windings per unit length is more effective in producing a higher magnetic field than increasing the coil current [8].

Magnetic field lines around a cylindrical solenoid or an electromagnet are always moving from the north pole (field source) to the south pole (field sink) as shown in Figure 1-3 [8]. Winding the coil tightly around the former will produce a uniform magnetic field pattern, which resembles that of a permanent magnet, while loose windings will produce an inductor as shown in Figure 1-4 [9].

Magnetic field effect has been used in a number of good applications. Some of these applications are preventing lime scale build-up inside pipes, filtering solid particles from liquids, and separating charged particles (usually ions) based on their mass in mass spectrometers. The molecular arrangement and molecular energy of the fuel and the oxidizer atoms can be affected by the application of a magnetic field [10, 11, 14, 15, 16, 17, 18, 19].

The effect of a magnetic field can be applied at any of these cycle processes. However, applying the magnetic effect at the induction stage can last throughout the other cycle's processes too. The magnetic effect on combustion and emissions of internal combustion engines can vary, depending on the engine design and type of fuel used. The magnetic field impact on combustion and emissions can differ in other applications such as boilers, gas turbines, and diffusion flames.

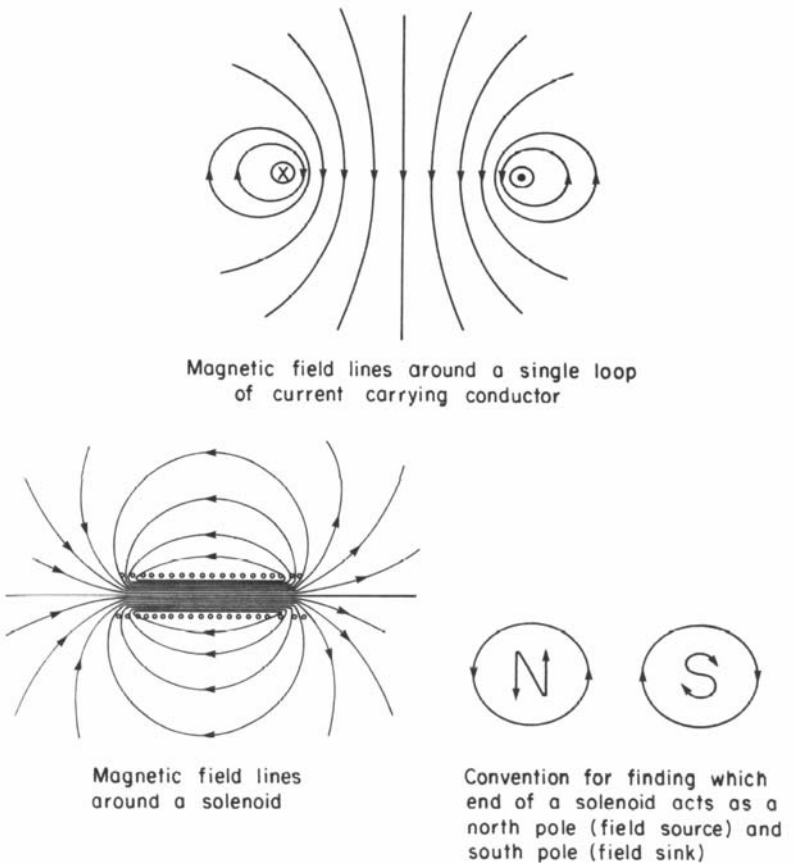

Figure 1-3: Magnetic field lines around a solenoid and a conductor [9]

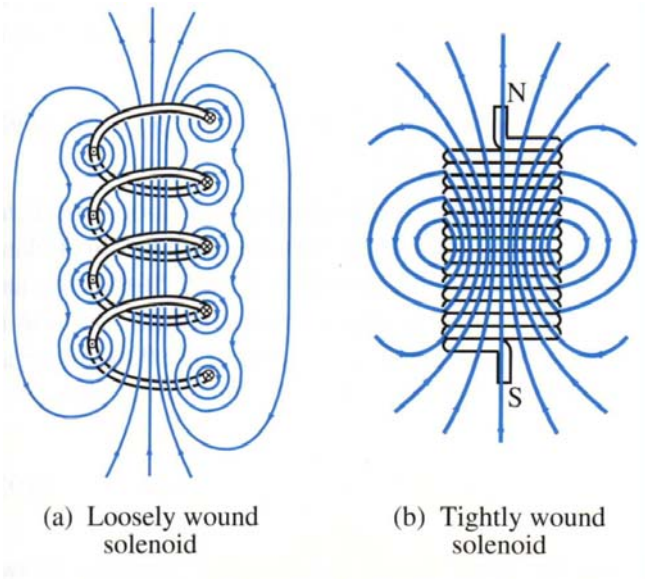

Figure 1-4: Magnetic field lines of two different types of windings [9]

1.2 RESEARCH OBJECTIVES

The present experimental study is aimed to investigate the effect of magnetic field on engine performance by examining fuel consumption and exhaust emissions of typical automotive engines. It was conducted with an internal combustion SI engine with unleaded gasoline fuel at different speed and load conditions. The study compares the effect of different magnetic field strengths and configurations on engine performance and emissions.

The magnetic field was produced by using electromagnets which were constructed and applied on the fuel supply line before the induction stage. The fuel line's test section was constructed from permeable material in order to maximize the magnetic field effect on the fuel. Moreover, the magnetic field effect on the test section was manipulated with different number of magnets, orientations, and polarities.

The engine performance was monitored mainly by examining SFC and exhaust emissions such as unburned HC, CO, and NOx which were measured and analyzed by utilizing an online computerized system.

In the current study, the engine performance parameters and exhaust emissions were studied extensively in a very broad range of operating conditions. The experiments were designed to give an objective basis for comparison between magnetic field strengths and configuration on engine performance and exhaust emissions.

CHAPTER 2

2 LITERATURE REVIEW

Magnetism is one of the least understood forces of nature that are still under exploration by many scientists and researchers. Studying this phenomenon leads to complex equations of quantum physics, which remains controversial in theory [17]. The application of a magnetic field on a pipe helps to prevent lime scale build-up inside the pipe, but, the world's top scientists cannot agree on the actual reason for such phenomenon. The effect of magnetism on fluids has also been proven by Bloch and Purcell, which won them the Nobel Prize [16].

Few scientific publications have explored the effect of magnetic field on the combustion process. However, several commercial publications and patents claim that this effect in significant. The present literature review deals only with scientific publications which study the effect of magnetic field on combustion characteristics.

Ueno and Harada in 1986 [10] found that the application of a magnetic field on the combustion of alcohol with platinum catalyst, which had magnetic induction strength of 0.5-1.4 T and magnetic field gradient on the order of 20-200 T/m, lowered the combustion temperature rapidly by 100-200 ^{o}C. Moreover, Ueno and Harada in 1987 [11] found that the application of a magnetic field on gas flow, which had magnetic induction strength of 1.6-2.2 T and a magnetic field gradient on the order of 220-300 T/m, had formed a "wall of oxygen" or an "air curtain" that depresses back flames and gas flow.

Both studies concentrated on the alignment of the paramagnetic molecules of oxygen with the magnetic field, and they each show a negative impact on the combustion process.

Aoki in 1989 [12] observed an increase in the emission concentration of OH, CH, and C_2, and a decrease of soot production from diffusion flames exposed to a non-uniform magnetic field. However, Aoki in 1990 [13] reported a decrease in the emission concentration of OH, CH, and C_2 for diffusion flames exposed to uniform and non-uniform magnetic field regions. This decrease in the later study was attributed to the arrangement used to produce the uniform magnetic field. Both studies still hold great promise for the positive impact of a magnetic field on the combustion process.

Wakayama in 1993 [14] found that the combustion reaction of diffusion flames can be promoted and controlled with the application of inhomogeneous magnetic field. He also noticed that the effect of inhomogeneous magnetic fields is larger in diffusion flames than in partially premixed flames. The effect of magnetic field on flames is mainly attributed to the response of the paramagnetic oxygen gas in air around the flame. Moreover, Wakayama et al. in 1996 [15] discovered that the presence of a magnetic field reduced the formation of soot in diffusion flames under microgravity, which usually formed large soot particles without the presence of a magnetic field. Both studies concentrated on the potential ability of magnetic control of air flows around diffusion flames (Magneto-Aerodynamics), and they showed significant positive impacts on the combustion process.

A company called Energy Management Solution (EMS) in 1996 [16] claimed that the application of a strong permanent magnetic field on fuel supply line will prepare the

hydrocarbon molecules to react easily with free radicals in the combustion process. This will make the fuel burn completely with the air mixture, which will produce more energy with the same amount of fuel, which will consequently lead to a reduction in the noxious emissions. They also claim that many independent users of strong permanent magnets proved their ability to increase the potential performance of thermal process plants. In addition, these magnets do not need any maintenance or power supply, and they do not interfere with the supply or production of the system.

Nayyar in 1998 [17] claimed that many experiments and observations showed the effect of magnetism on combustion, but the reason for this effect is still an area of study in pure physics. Moreover, he recalled the use of electromagnets on aviation fuel to combat the fuel inconsistency fifty years ago. He claimed that the reason might be the agitation of the fuel molecular structure, which will cause the positive charge on the electron 'to precess'. This precession is believed to make the fuel mix more readily with the oxygen during combustion. He supported his claim with several experiments, conducted in laboratories and industrial applications, that increased the efficiency and decreased the emissions by 20%. He also claimed that the strong permanent magnets, if placed strategically, can improve fuel economy by 8-24%, and reduce emissions by 30%.

Baker and Saito in 2000 [18] recalled that the impact of magnetic fields on combustion has been noticed since the time of Faraday. They related this impact to the nature of the diamagnetic and paramagnetic gases involved in the combustion process. They claimed that the presence of a magnetic field will produce net dipole moments in diamagnetic gases and align the dipole moments in the paramagnetic gases. This will result in a repulsion force in diamagnetic gases and an attraction force in paramagnetic gases, and

will thus lead to the arrangement of these gases. They developed an expression for the Gibbs free energy, which includes a magnetic field contribution. They examined changes in the equilibrium composition quantitatively for the combustion of methane in air with the presence of a uniform magnetic field. These equilibrium characteristics were determined, by minimizing the Gibbs free energy, to be around zero. They suggested that the magnetic field must be strong enough, around 0.04 T (400 Gauss), in order to observe a significant impact on the equilibrium combustion characteristics. They discovered that the presence of magnetic field at certain temperature ranges decreased the mole fraction in the majority of the product species, but it increased the mole fraction in a few of the product species. They also observed that the NO emissions were reduced dramatically in comparison to other equilibrium mole fractions in the presence of a strong magnetic field (around 0.04 T) at high temperatures (around 3000 K). That study showed a promising positive impact, especially for the harmful emission such as NO and CO.

Pankhurst and Parkin in 2001 [19] claimed that the effect of a magnetic field on liquids and gases are already known. The magnetic field can influence the chemical reactions during combustion since oxygen in the fuel-air mixture has paramagnetic behaviour that affects the brightness of the flame in rocket engines according to the magnitude of the magnetic field gradient imposed.

Most of the above studies showed a promising positive impact of magnetic field on the combustion processes and their emission formulations. This encourages researchers to conduct more extensive studies in this field in order to benefit the world financially and environmentally.

CHAPTER 3

3 EXPERIMENTAL SETUP

3.1 BACKGROUND

In the present study, the experiments were designed to investigate the impact of magnetic field on engine performance by examining fuel consumption and exhaust emissions such as CO, NOx, and HC. These experiments were conducted on a spark ignition internal combustion engine with unleaded gasoline fuel. They were conducted at different engine speed and load conditions with different numbers of electromagnets at different orientations and polarities.

The engine output energy was controlled and measured by applying an external load on the crankshaft by using a dynamometer. A dynamometer acts like a braking device by means of friction, hydraulic, or magnetic force, which absorbs the engine energy. The fuel consumption was measured by determining the rate of fuel flow to the engine, utilizing the simplest method of timing a calibrated volume with a stopwatch (A more complicated approach would use a gravimetric metering unit, which weighs the supplied fuel to the engine over a certain time interval). The exhaust emissions were monitored and analyzed by using a specialized gas analyzer, which uses different analyzing techniques for each sampled gas.

3.2 TEST FACILITIES

The test engine and the dynamometer are controlled by a microcomputer equipped with a high-speed data acquisition and logging system. This controlling system receives the operational data from various sensors fitted on the engine and the dynamometer. These sensors measure and report different parameters such as engine load, engine speed, spark timing, intake air temperature, exhaust gas temperature, oil temperature, and cooling water temperature. Several actuators are also fitted on the testing facilities in order to execute the controller commands. All data received from these testing facilities are displayed on the controller monitor and logged at the same time to another microcomputer to be stored and traced over time. A schematic diagram illustrating the major testing facilities used in this experimental study is shown in Figure 3-1 for clarification, and it is detailed in the following sections.

3.2.1 Engine

The test engine used in this experimental study is a four stroke, spark ignition internal combustion engine. It was manufactured by Mercedes-Benz and it is located in the Heat Engine Laboratory at KFUPM. The engine consists of six cylinders, with a swept volume of 2960 cm^3. It has a bore diameter of 88.5 mm, a stroke length of 80.2 mm, a compression ratio of 9.2, and a maximum power output of 132 kW at 5700 rpm. The engine is equipped with the KE-Jetronic continuous fuel injection system, which injects the fuel directly before the intake valve of each cylinder. The engine has an electronic ignition system with an electronic spark timing adjustment. The cooling water and lubrication oil temperatures are adjusted and controlled by two fitted heat exchangers.

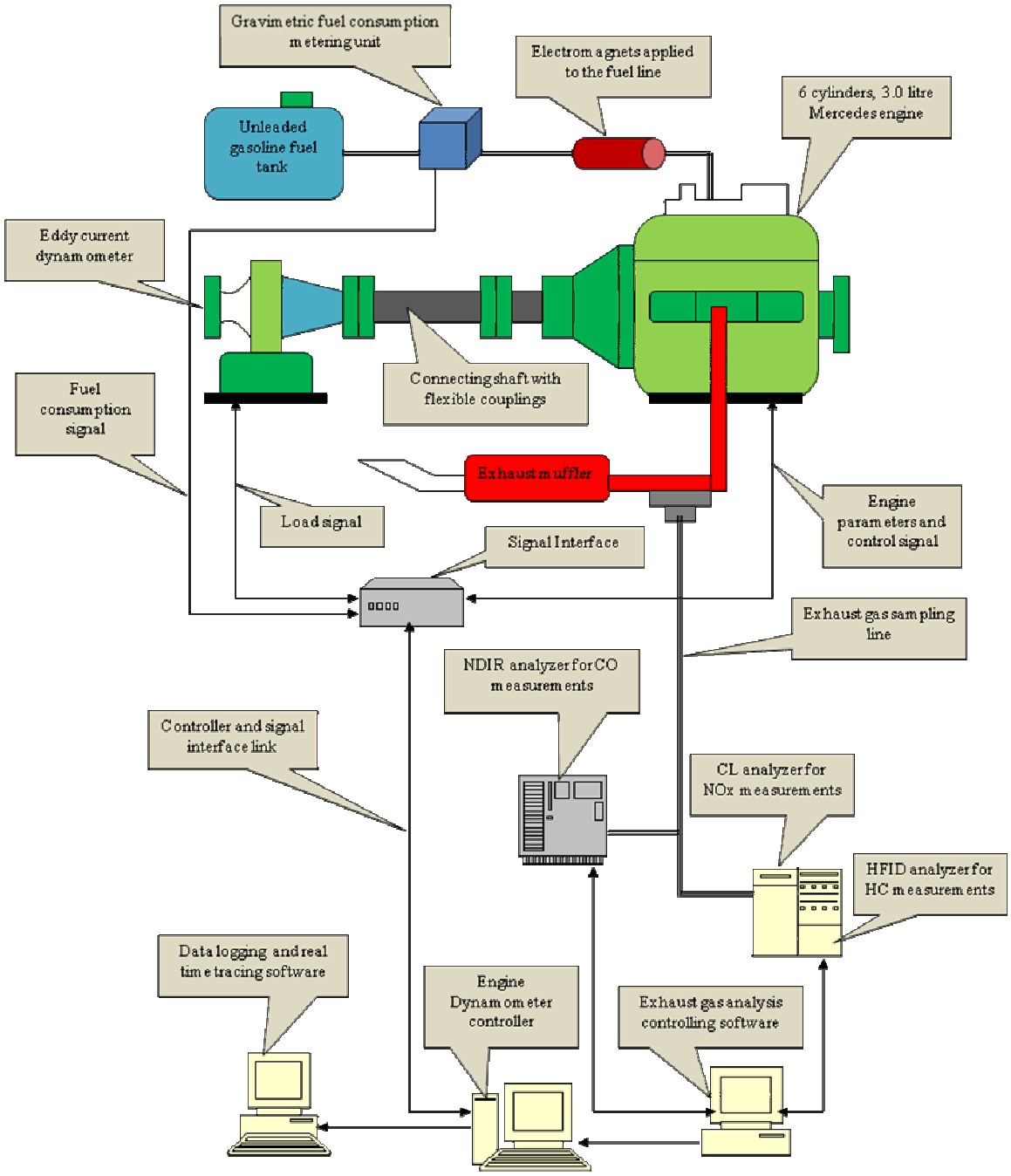

Figure 3-1: Schematic diagram illustrating the major testing facilities

3.2.2 Dynamometer

The engine is coupled to an eddy-current water-cooled dynamometer, which attains the braking effect through a magnetic field produced by the supplied electrical current. The dynamometer's revolving part dissipates the engine power in the form of heat, which is proportional to the strength of the magnetic field. The dynamometer has a maximum power of 257 kW, a maximum torque of 1400 Nm, and a maximum speed of 8000 rpm.

3.2.3 Gas Analyzer

The unburned hydrocarbons (HC) concentration is measured by the Heated Flame Ionization Detector (HFID), which proportionally relates a current of ions produced by a hydrogen flame to the amount of carbon atoms contained in the exhaust sample. The measurement range for this analyzer is 0.01 to 5 vol%. The nitrogen oxides (NOx) concentration is measured by a Chemi-Luminescent (CL) analyzer, which proportionally relates the photon lights from the reaction between nitrogen oxide (NO) and ozone (O_3) to the concentration of NO in the exhaust sample. The small amounts of nitrogen dioxide (NO_2) are converted to NO prior to the reaction with ozone. The measurement range of this analyzer is 10-10000 ppm. The carbon monoxide (CO) concentration is measured by the Non-Dispersive Infra-Red (NDIR) analyzer, which proportionally relates the CO absorption of a certain infrared radiation wavelength to the concentration of CO in the exhaust sample. The measurement range of this analyzer is 10-5000 ppm.

All three analyzers have less than ±1% span repeatability (relative scale) and less than ±1% span drift (full scale over 24 hour period). These measurement results are displayed

on the exhaust analysis controller, and transferred at the same time to the system controller through the local area network (LAN) cable.

3.3 TEST MAGNETS

Five electromagnets were constructed by winding copper wires around deformed iron rods with a certain shape as shown in Figure 3-2. Electrical current running through the winded copper wire was supplied by a twelve volts (12V) car battery in order to generate the magnetic field. The battery was recharged regularly to eliminate any power discrepancies which might influence the magnetic field effect.

The electromagnet iron core magnified and concentrated the magnetic fields at the ends, which are pointed toward the fuel supply line. A suitable copper wire grade (0.3 mm) was selected which can be wound without difficulty or breakage. Sufficient windings were produced to generate the desired magnetic field strength without burning the wire. The wire was wound tightly in order to generate a uniform magnetic field. The magnetic field was measured by using a Gauss meter, to be around 800 Gauss for each electromagnet. The ends of the cooper wire were detachable to manipulate polarity of the generated magnetic field.

A permeable test section made of copper was constructed on the fuel supply line before the fuel injection point in order to maximize the magnetic field effect on the fuel before combustion. The number of electromagnets controlled the magnetic field strength to be placed directly on the test section. The orientation and polarity of each magnet controlled the configuration to manipulate the magnetic field effect on the supplied fuel.

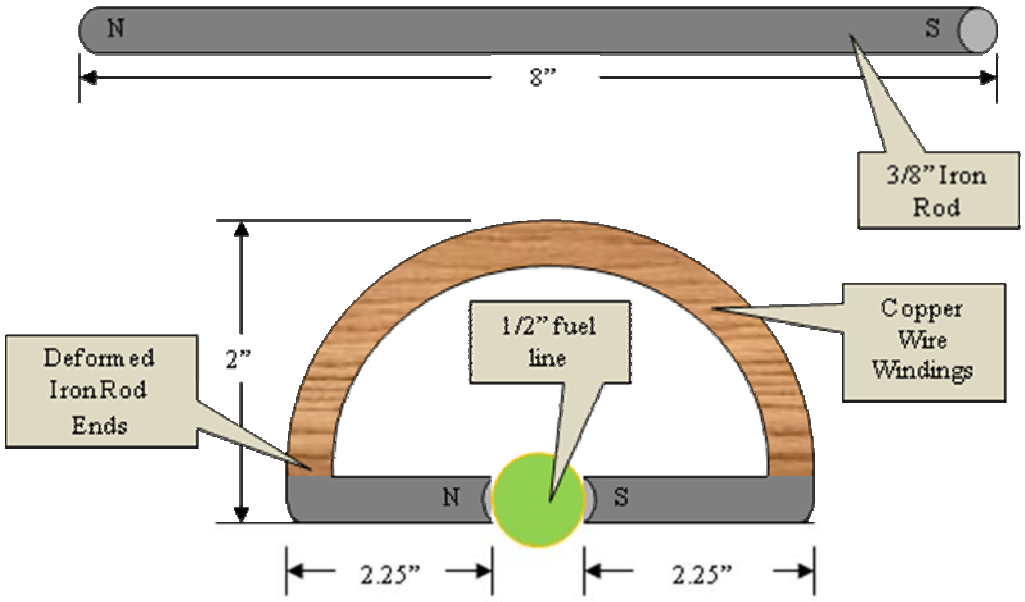

Figure 3-2: Single constructed electromagnet

3.4 TEST CONDITIONS

The engine, dynamometer, and gas analyzer measurements can be affected by many engine operational parameters such as spark timing, air/fuel ratio, and cooling water temperature. These measurements can be also affected by test room conditions such as temperature, atmospheric pressure, and humidity. The best engine parameters were adjusted in order to achieve optimum engine performance for each condition. This was also accomplished by conducting all settings of the engine load and speed at each magnetic field strength or configuration setup during the same day to avoid discrepancy.

3.5 TEST PROCEDURE

The engine was first tested without a magnetic field effect in order to establish the base line for the following experiments that have different magnetic effects. Each test was

conducted by fixing one of the independent variables constant and varying the other one with certain increment intervals. The engine speed was varied five times at 500 rpm increments from 1000 rpm to 3000 rpm. The load on the engine was also varied five times at 40 Nm increments from 20 Nm to 180 Nm.

The magnetic field strength was increased five times at 800 Gauss increments from 800 Gauss to 4000 Gauss by adding another magnet each time. All magnetic field strengths were varied by using the same 'Attraction' configuration where opposite poles attracted each other. Furthermore, the orientation of the five magnets (4000 Gauss) was made perpendicular on each other to get the 'Spiral' Configuration as shown in Figure 3-3 (a). Moreover, the polarities of the strongest magnetic field of 4000 Gauss in parallel setup were made to be the same, in order to get the 'Repulsion' configuration as shown in Figure 3-3 (b).

All test readings were given enough time to stabilize before being recorded at each load and speed setting and different magnetic field strengths and configurations.

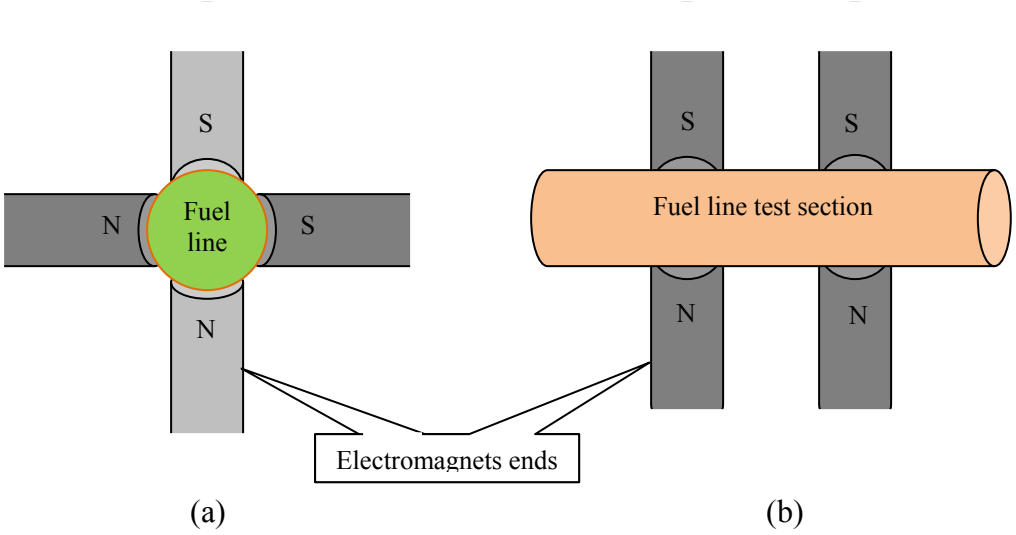

Figure 3-3: Electromagnets (a) orientation and (b) polarity

CHAPTER 4

4 SPECIFIC FUEL CONSUMPTION (SFC)

4.1 Magnetic Field Strength Effect

4.1.1 Constant Load Simulation

The variation of Specific Fuel Consumption (SFC) against varying speeds at a constant load of 20 Nm and different aligned magnetic field strength in 'Attraction' configuration is shown in Figure 4-1. It is observed that, with a zero magnetic field strength, the SFC follows a parabolic relation with a minimum value of 660 g/kWh at 1900 rpm. As the magnetic field is turned on, a marked reduction of 10% in SFC is observed for most of the magnetic field strengths at the lowest and highest engine speeds, where the SFC is the highest value depicted in the base curve. However, no convincing dependence is observed on the magnitude of magnetic field strength, since one magnet of 800 Gauss shows the most favourable effect compared to all the others. At the intermediate speeds where the SFC is lower, the magnetic field effect tends to diminish within the error of ±1%. All the curves with magnetic effect follow a more linear trend, slightly dissimilar to the curve corresponding to the base line.

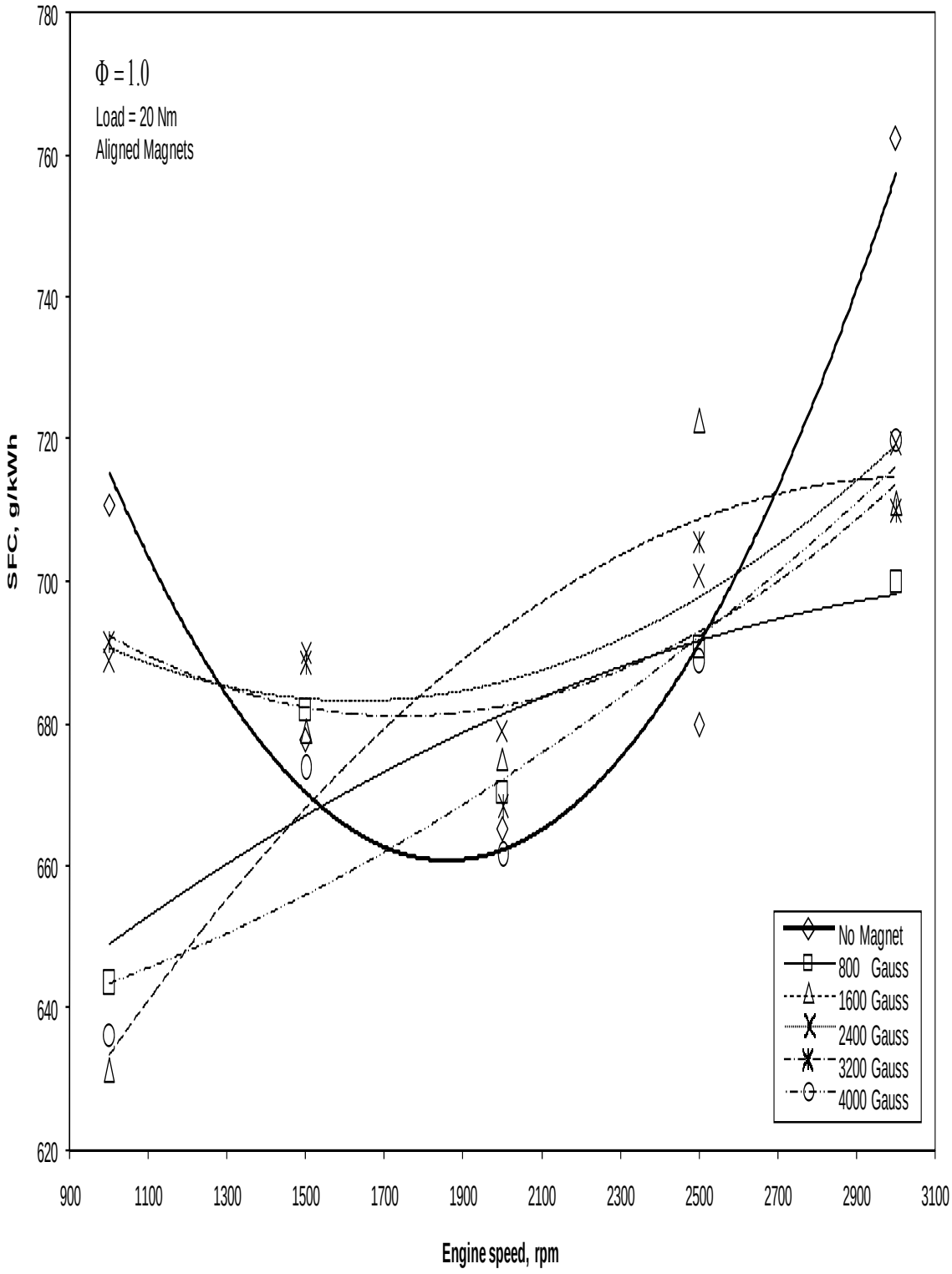

Figure 4-1: Magnetic strength effect on SFC at constant load of 20 Nm

Figure 4-2 shows the relationship between the same variables but at a load of 60 Nm, where it is noticed that the SFC decreases substantially by half at all engine speeds at this increased load. The curve corresponding to zero magnetic field strength still follows the same parabolic trend with less variation and a minimum value of 365 g/kWh at the same speed of 1900 rpm. As the magnetic field is turned on, only a slight reduction of 2% is observed from the base curve for the lowest speed. All curves can be regarded as representing a highly insensitive dependence of SFC on engine speed due to the low variation across.

Figure 4-3 shows the same curves but at a load of 100 Nm, where it is observed that the application of the magnetic field has little effect if any on the dependence of SFC on engine speed. Moreover, the magnitude of the magnetic field strength does little to change this. All the curves follow the same trend, with slight deviations within the error at various engine speeds. The difference in the maximum and minimum SFC magnitudes increases but the overall SFC values decreases somewhat at all engine speeds as compared to the previous figure.

The same trend continues with engine loads of 140 and 180 Nm as depicted in Figure 4-4 and Figure 4-5. The overall decrease in the SFC value at all engine speeds with increasing load continued, but the amount of decrement is decreasing with the increase in load. The application of the magnetic field has little effect on reducing the SFC magnitude at all engine speeds, and the magnitude of the magnetic field strength does little to change this. The difference between the maximum and minimum magnitudes of SFC for any given load increases with increasing load, with the exception of the lowest load of 20 Nm as shown in Figure 4-1.

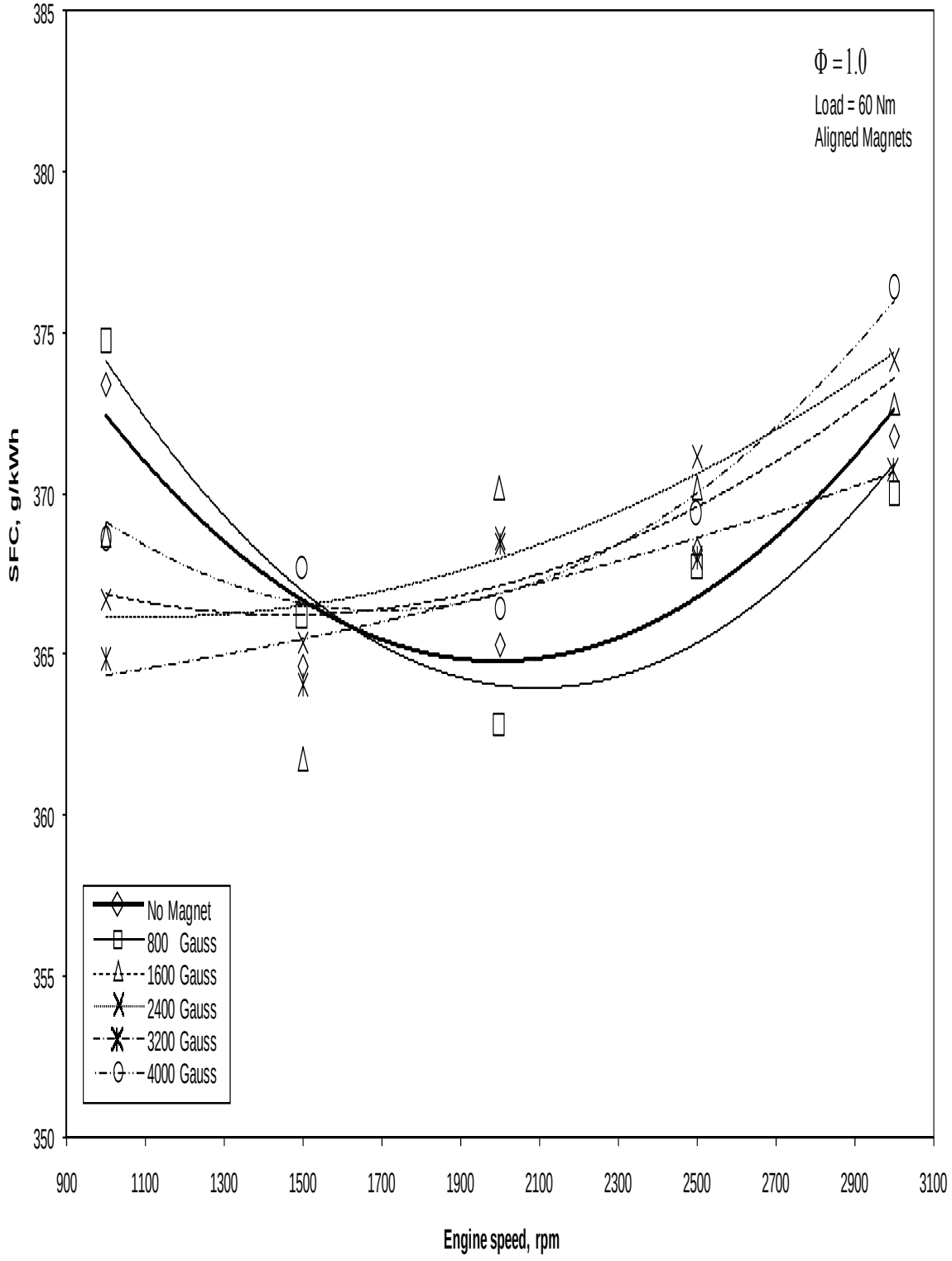

Figure 4-2: Magnetic strength effect on SFC at constant load of 60 Nm

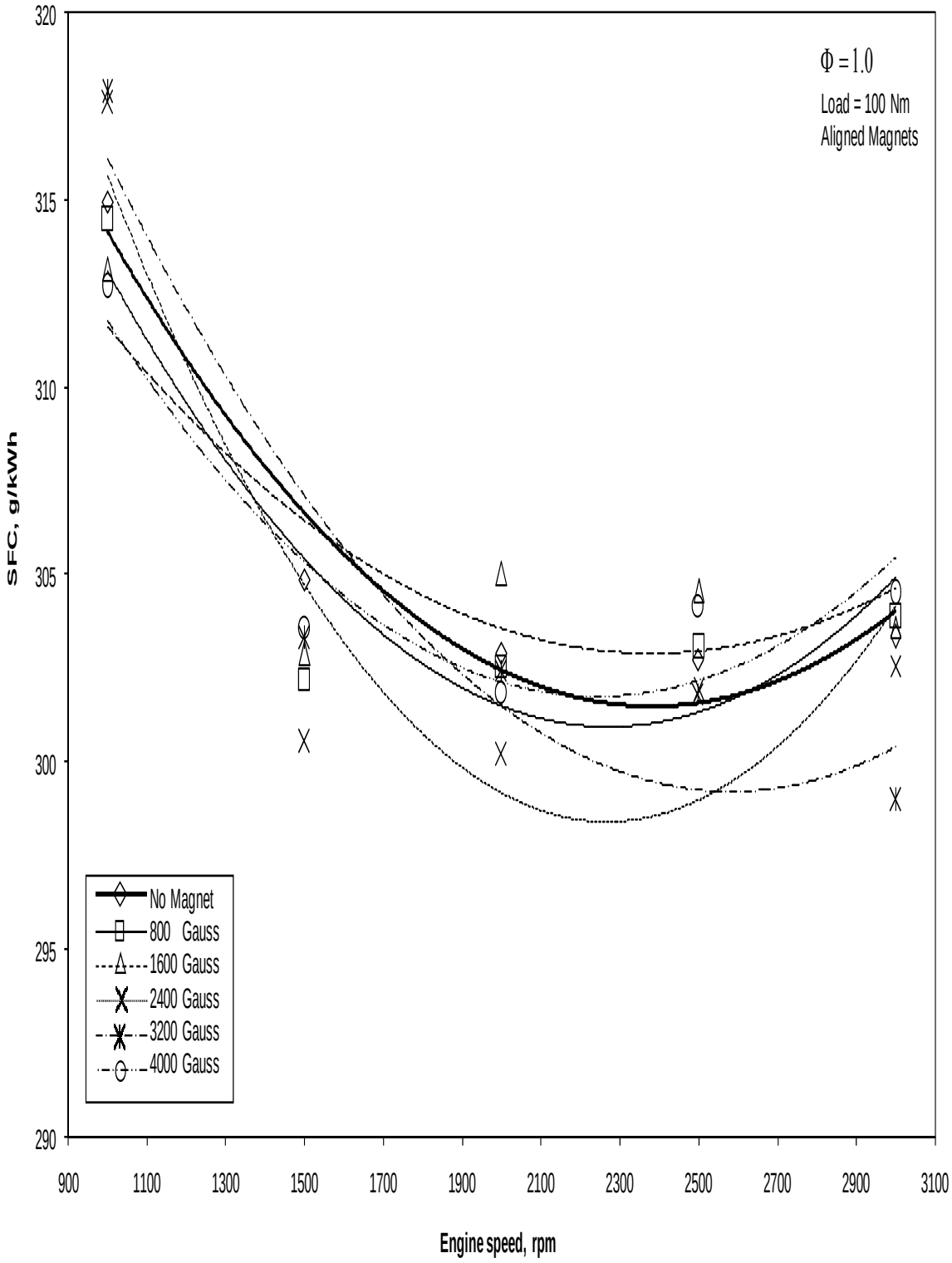

Figure 4-3: Magnetic strength effect on SFC at constant load of 100 Nm

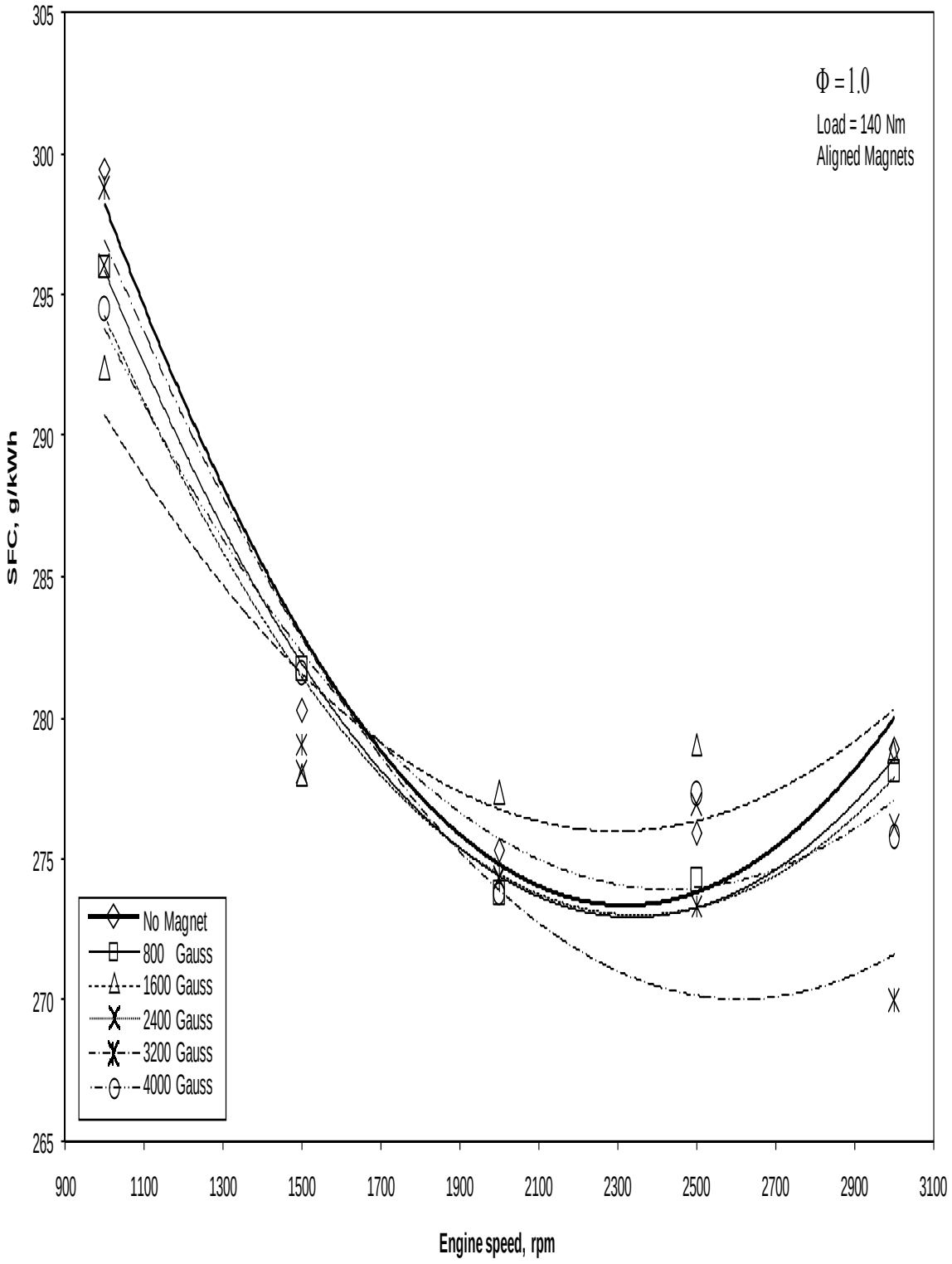

Figure 4-4: Magnetic strength effect on SFC at constant load of 140 Nm

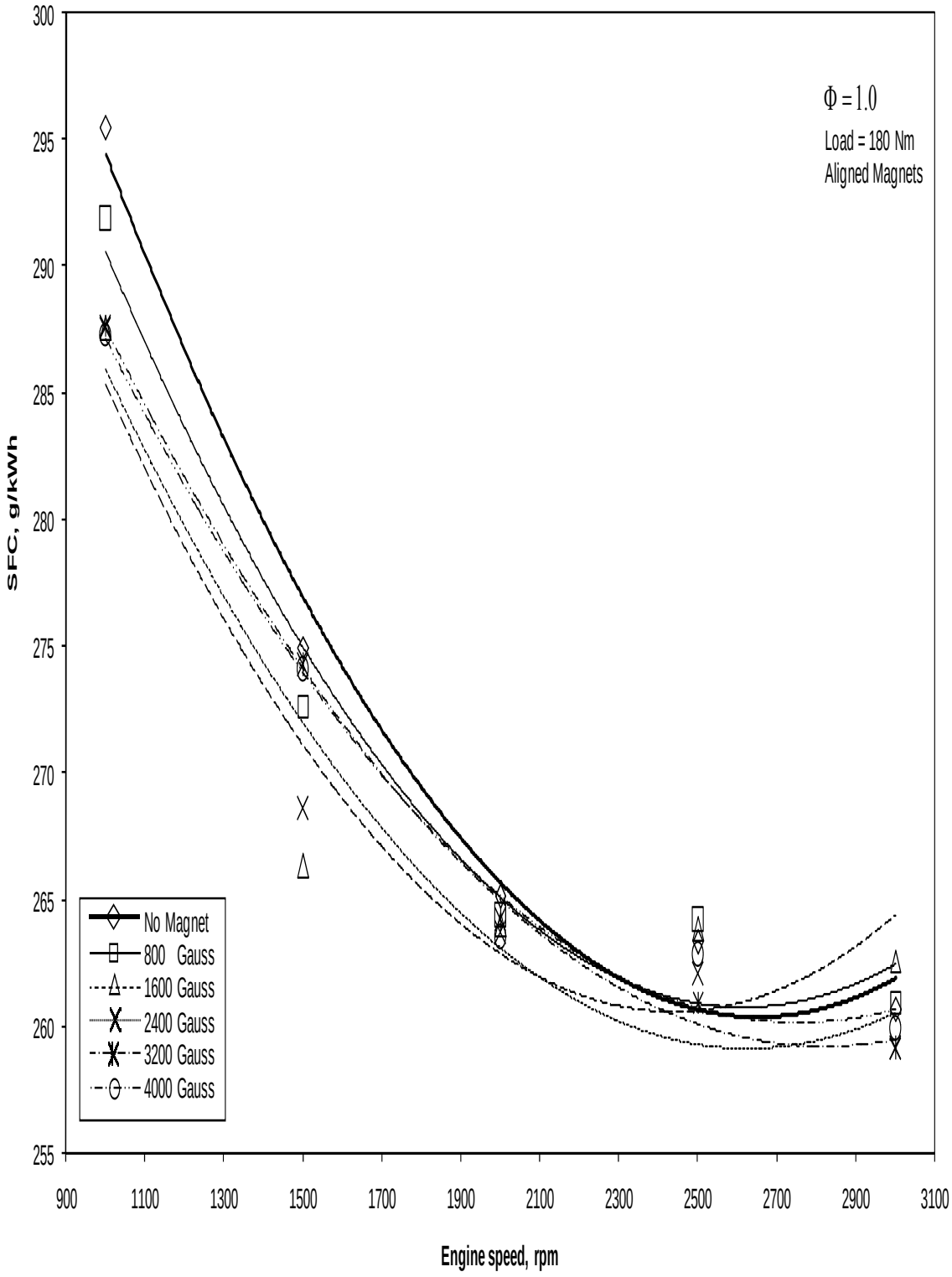

Figure 4-5: Magnetic strength effect on SFC at constant load of 180 Nm

4.1.2 Constant Speed Simulation

The variation of the engine's SFC against different loads at a constant speed of 1000 rpm and different aligned magnetic field strengths in 'Attraction' configuration is shown in Figure 4-6. With no magnetic field, it is observed that the specific fuel consumption decreases monotonically with increasing engine load. The rate of decrease of SFC is high at low engine loads, but it decreases with increasing loads. At high engine loads, it approaches a constant value asymptotically. When the magnetic field is turned on, no appreciable effect is observed on SFC at most engine loads with increasing magnetic field strength. However, at the lowest engine load of 85 kPa, there is a slight but noticeable reduction effect of 10% as observed earlier at this lowest speed of 1000 rpm.

Figure 4-7 and Figure 4-8 show the relationship between the same variables at engine speeds of 1500 and 2000 rpm respectively. Here, the magnetic field imparts no appreciable effect on SFC variation at all engine loads. However, it is observed that, with increasing engine speed, there is a slight decrease in SFC at virtually all engine loads.

Figure 4-9 and Figure 4-10 show the same relation at engine speeds of 2500 and 3000 rpm respectively. Increasing the magnetic field strength shows no effect at on SFC variation at most engine loads as observed in the previous figures. However, the maximum value of SFC starts to increase with increasing engine speed at the lowest load, with a slight but noticeable magnetic field effect of 10% as observed earlier at the highest speed of 3000 rpm.

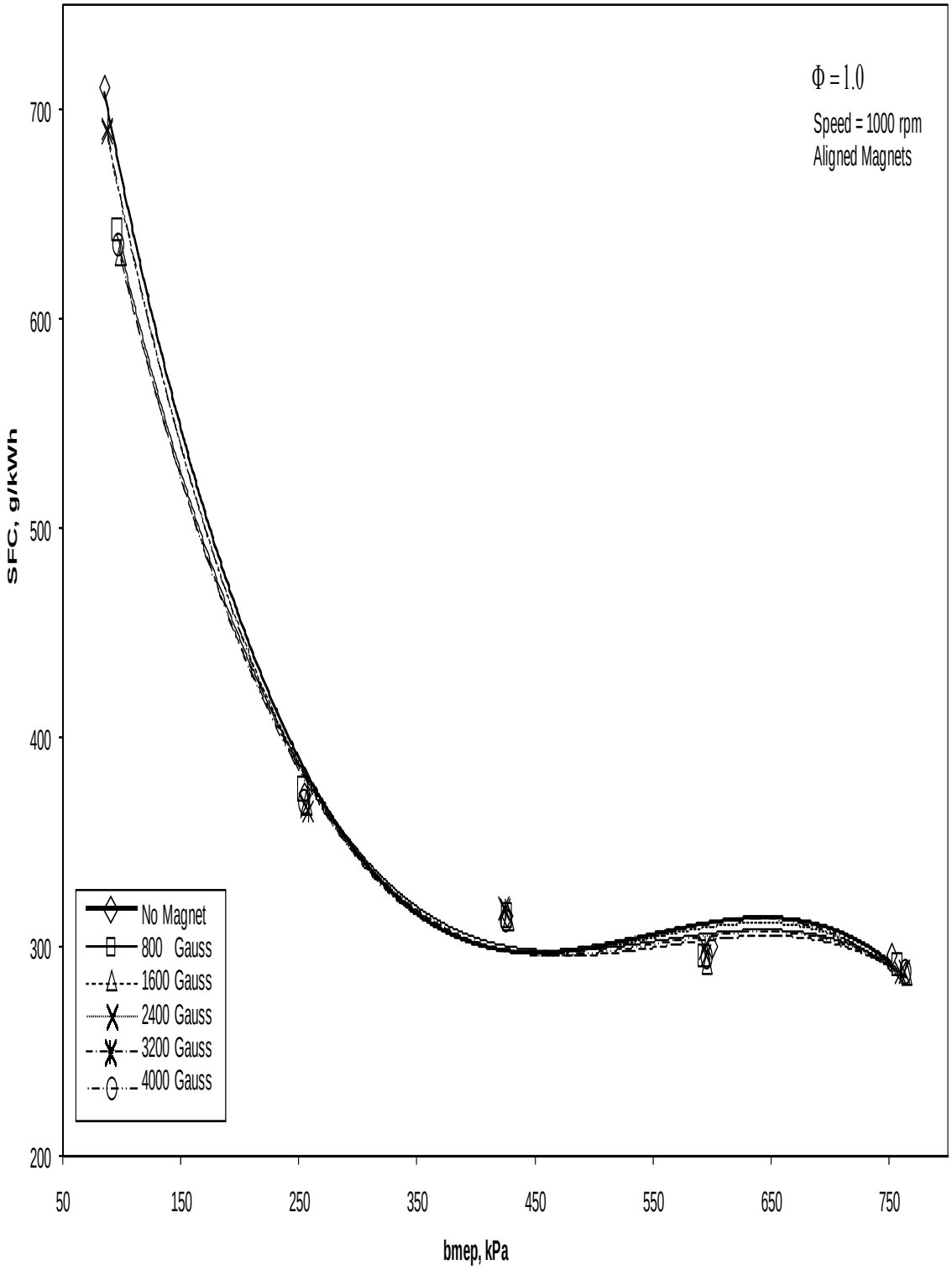

Figure 4-6: Magnetic strength effect on SFC at constant speed of 1000 rpm

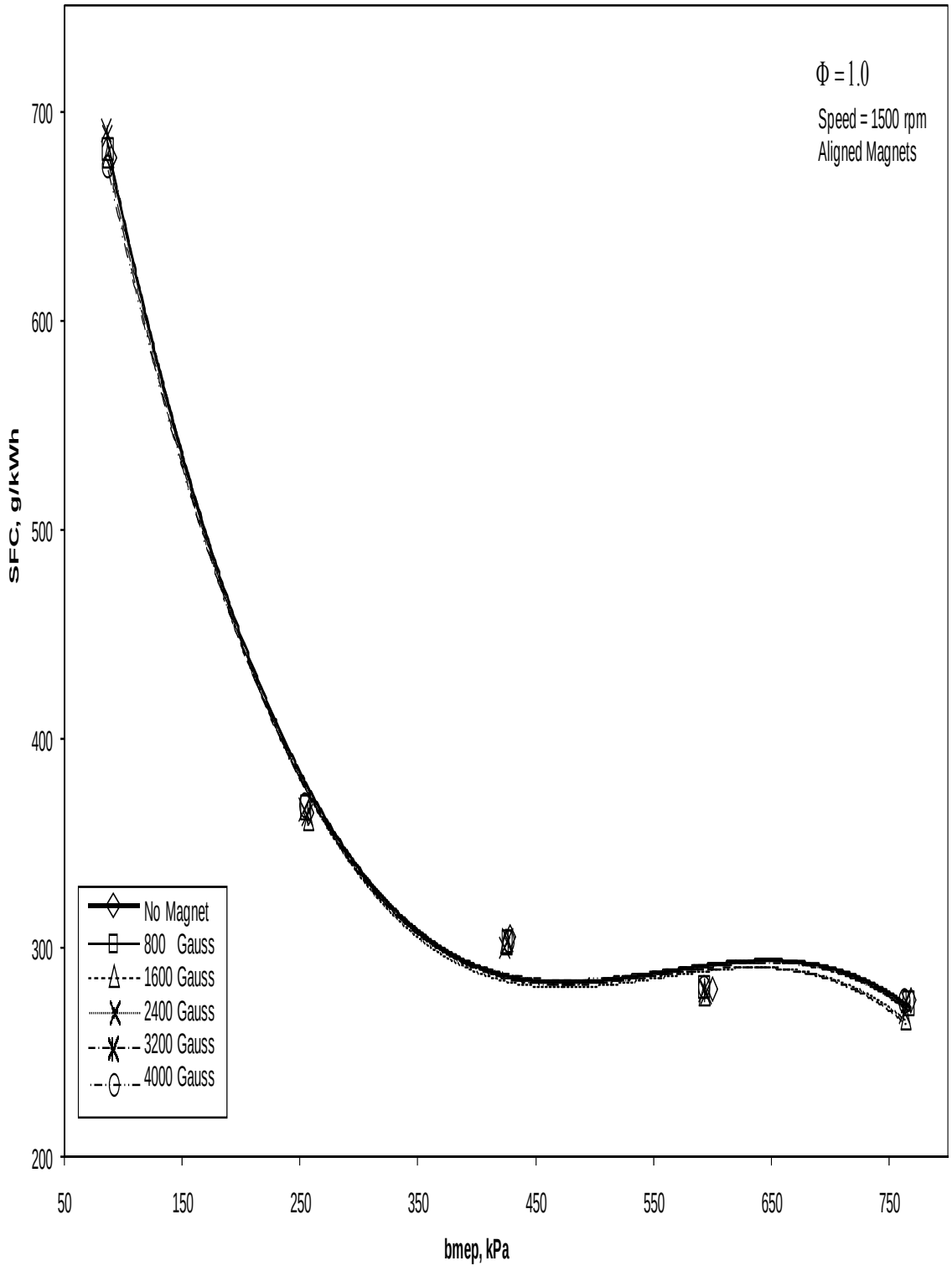

Figure 4-7: Magnetic strength effect on SFC at constant speed of 1500 rpm

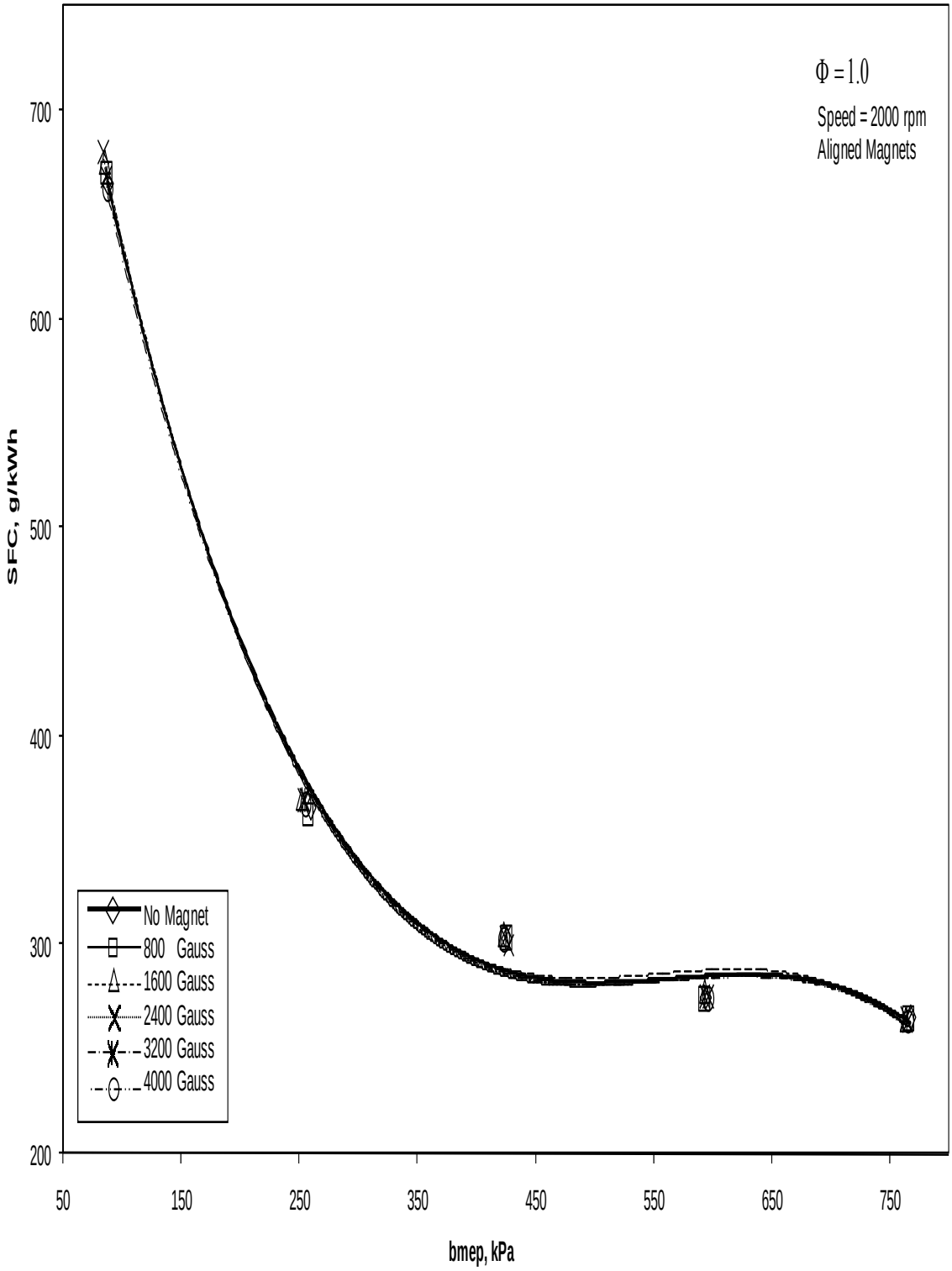

Figure 4-8: Magnetic strength effect on SFC at constant speed of 2000 rpm

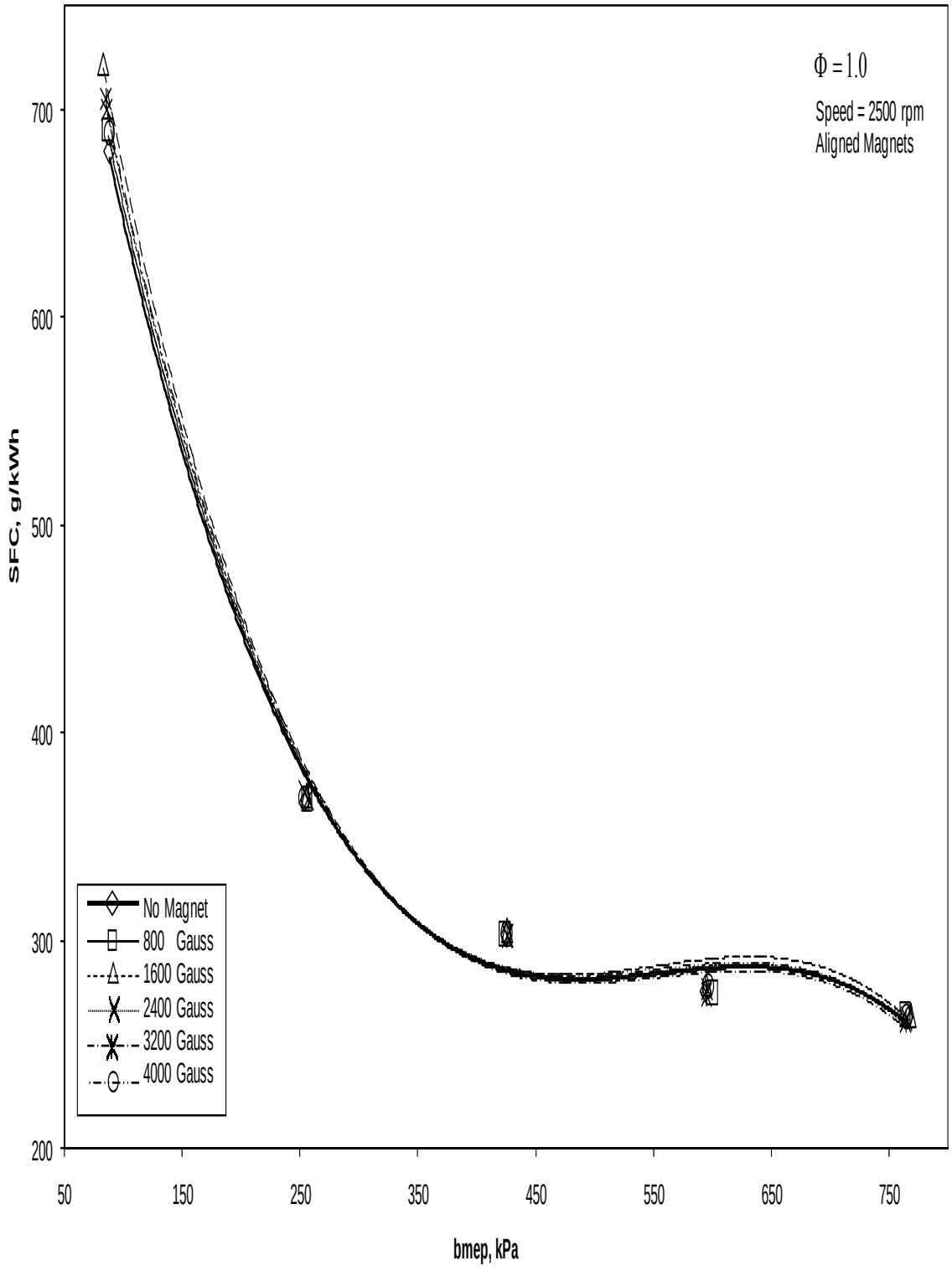

Figure 4-9: Magnetic strength effect on SFC at constant speed of 2500 rpm

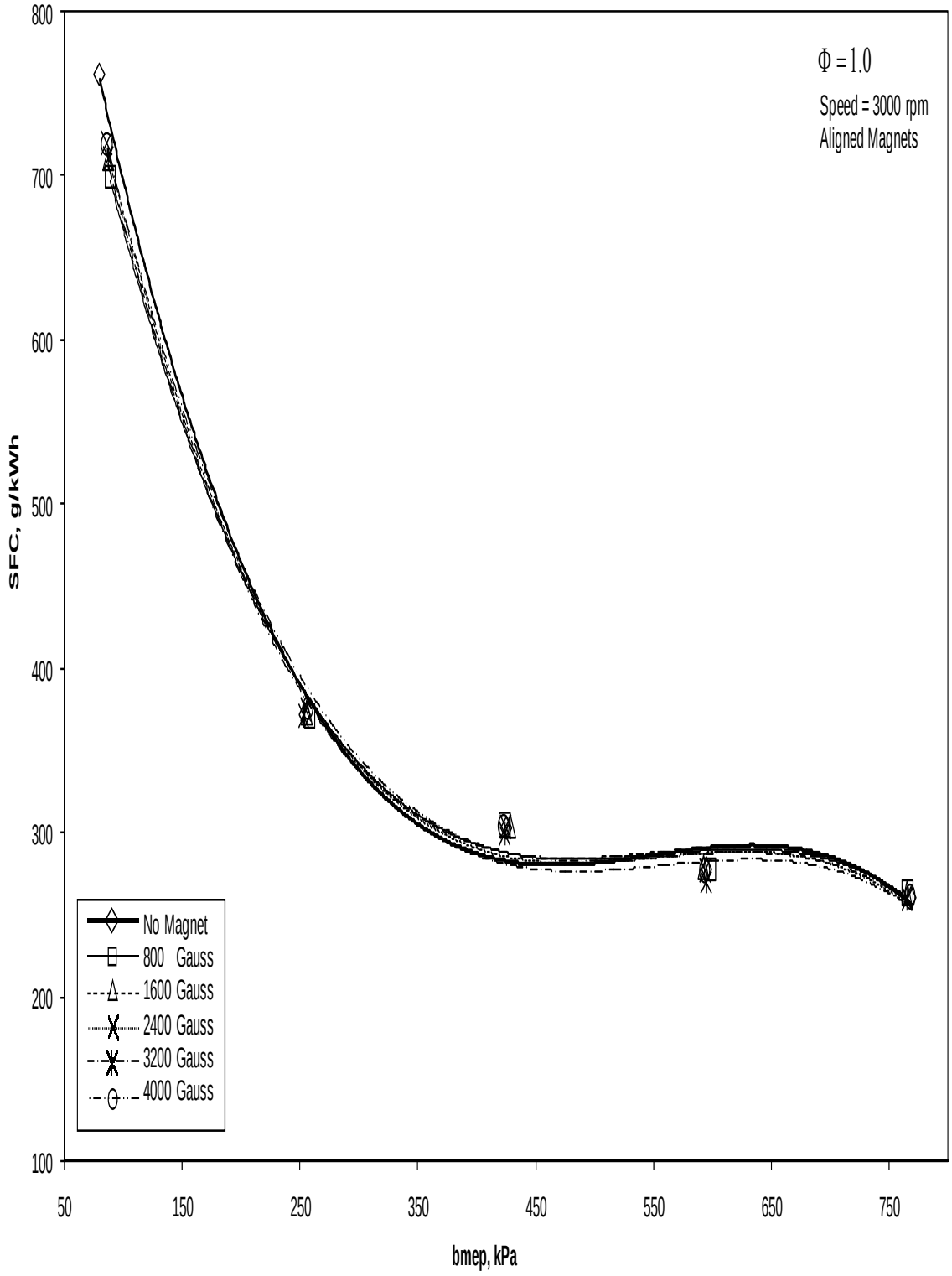

Figure 4-10: Magnetic strength effect on SFC at constant speed of 3000 rpm

4.2 Magnetic Field Configuration Effect

4.2.1 Constant Load Simulation

The variation of SFC against varying engine speeds at a constant load of 20 Nm and constant magnetic field strength of 4000 Gauss with three different magnetic field configurations is shown in Figure 4-11. It is seen that with the magnetic field turned off the SFC initially decreases with increasing engine speed, reaching a minimum value of about 660 g/kWh at 1900 rpm. Then, it starts to increase and reaches a value of 765 g/kWh at the highest engine speed. As the magnetic field is turned on, a significant reduction of SFC is observed only at the lowest and highest engine speed for all configurations. In marked contrast, the 'Attraction' configuration shows the best improvement at almost all engine speeds. Moreover, the 'Repulsion' configuration performs slightly better at the highest speed of 3000 rpm to reach a reduction of 10%. However, the 'Spiral' configuration shows less favourable performance at almost all engine speeds.

Figure 4-12 shows the relationship between the same variables as the previous figure but now at a different load of 60 Nm. It is seen that again in general all the curves behave in a manner analogous to a parabola. However, now it is seen that no marked improvement occurs when the magnetic field is turned on except for the lowest speed of 1000 rpm. In fact, the performance becomes slightly worse at most other speeds, except the 'Repulsion' configuration, where it tends to perform slightly better for all engine speeds. With this increase of load, the overall SFC goes down drastically for all values of the engine speed.

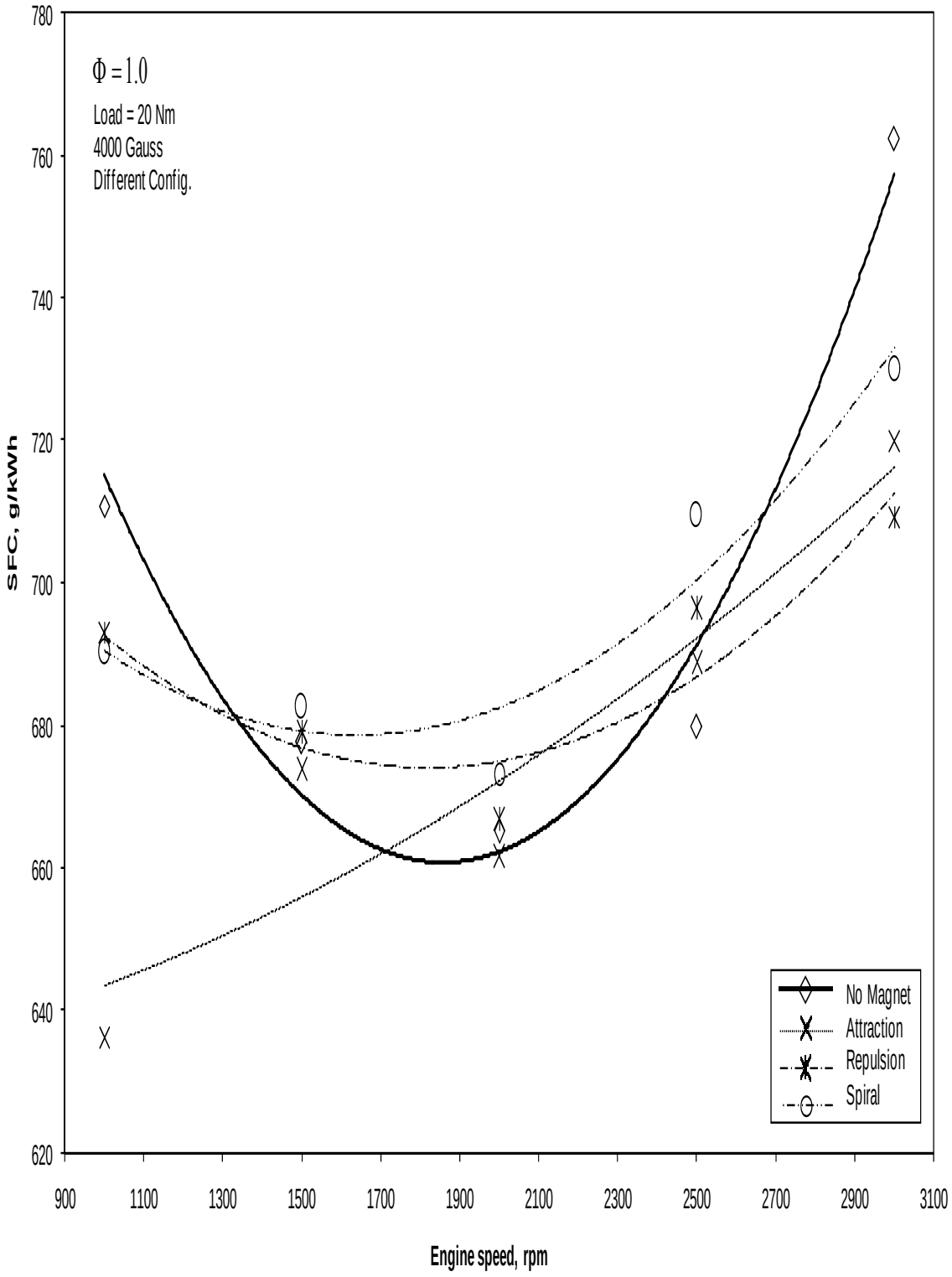

Figure 4-11: Magnetic configuration effect on SFC at constant load of 20 Nm

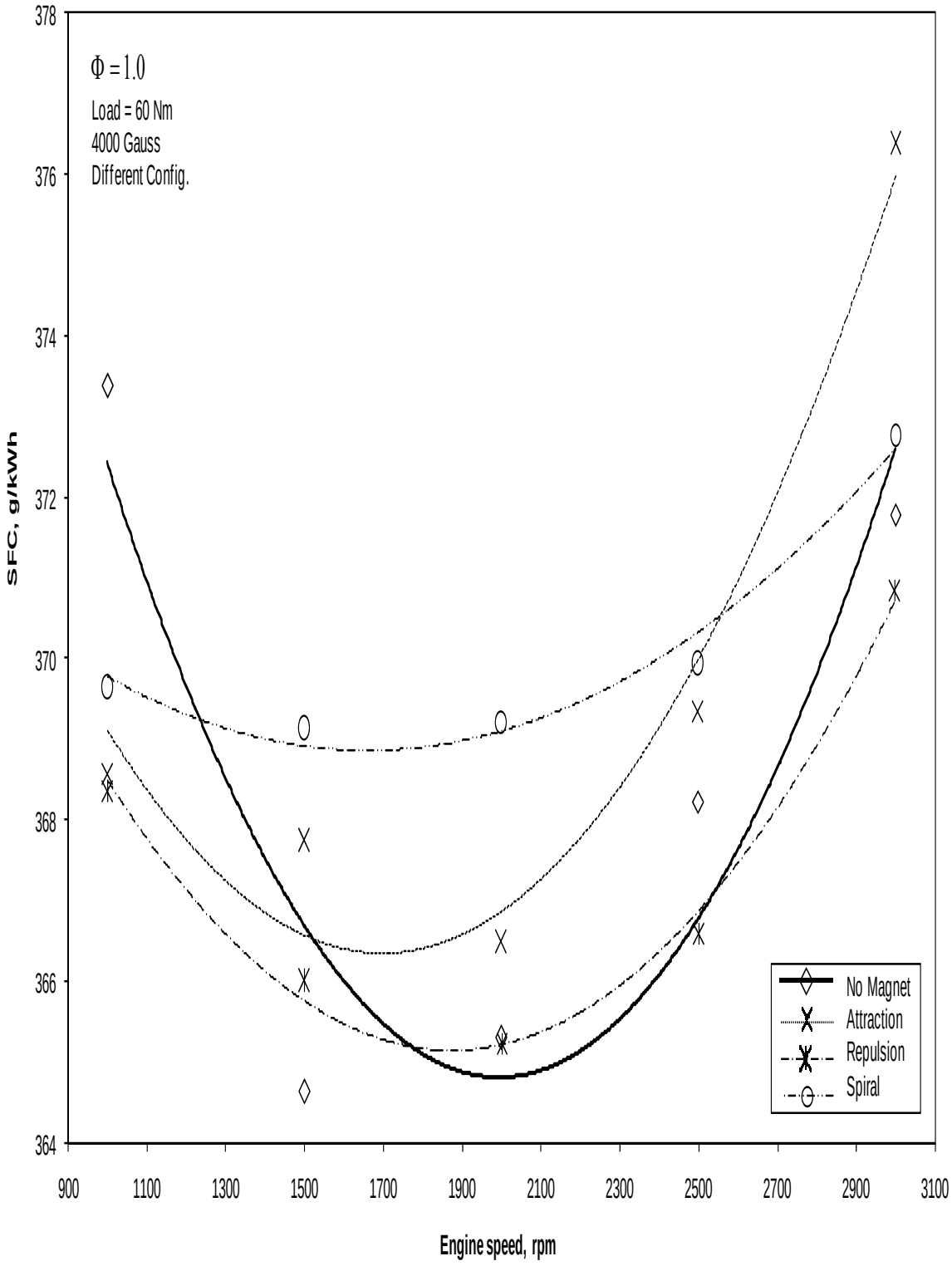

Figure 4-12: Magnetic configuration effect on SFC at constant load of 60 Nm

As the load is increased further to 100 Nm, as depicted in Figure 4-13, a further decrease in the overall SFC values occurs at all engine speeds. No marked improvement or worsening results from the introduction of the magnetic field at all engine speeds.

Further increase of load to 140 Nm and 180 Nm, shown in Figure 4-14 and Figure 4-15, produces the same result. There is an overall decrease of SFC at all engine speeds with an increase in load, but no marked improvement with the introduction of the magnetic field at most engine speeds of any field configuration.

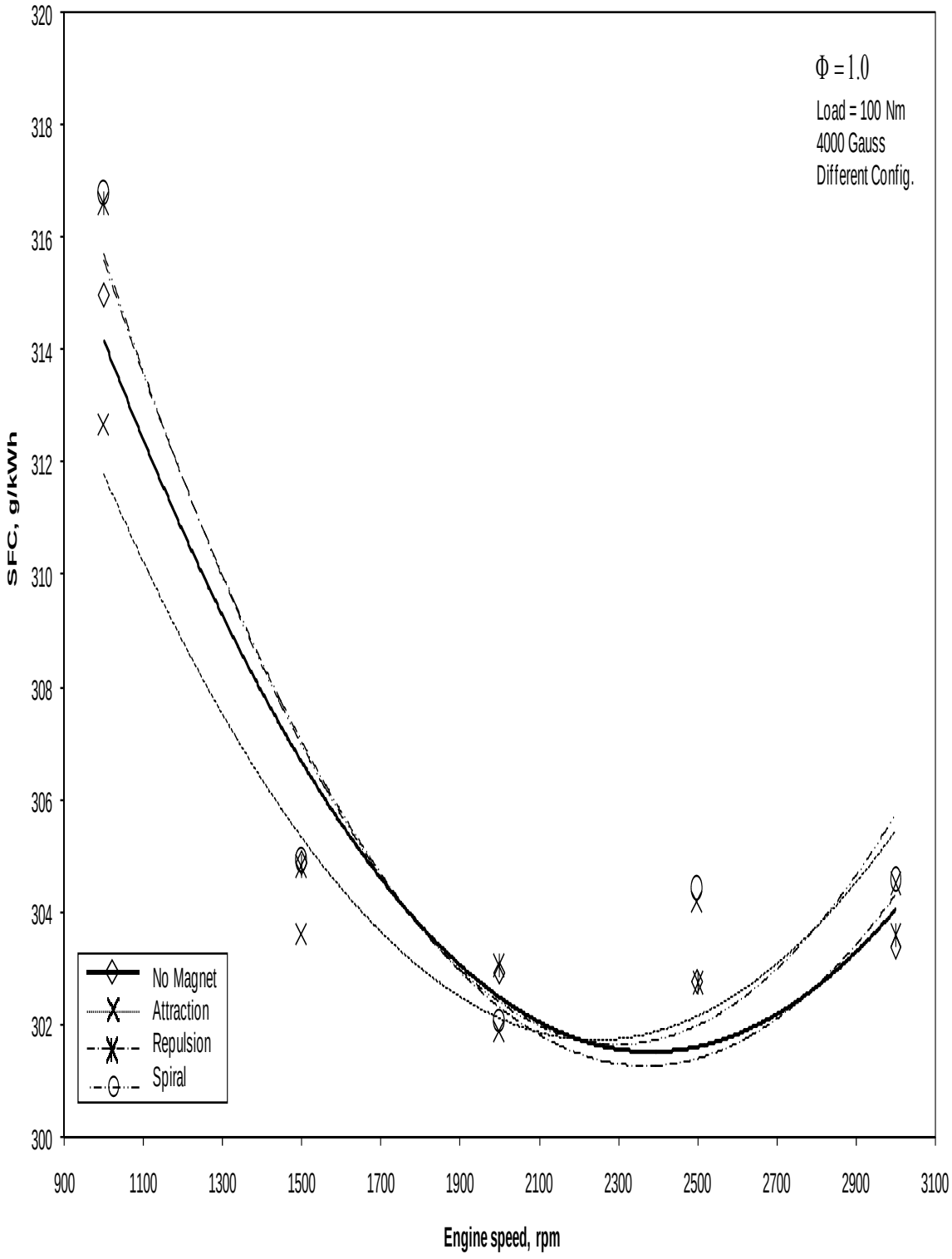

Figure 4-13: Magnetic configuration effect on SFC at constant load of 100 Nm

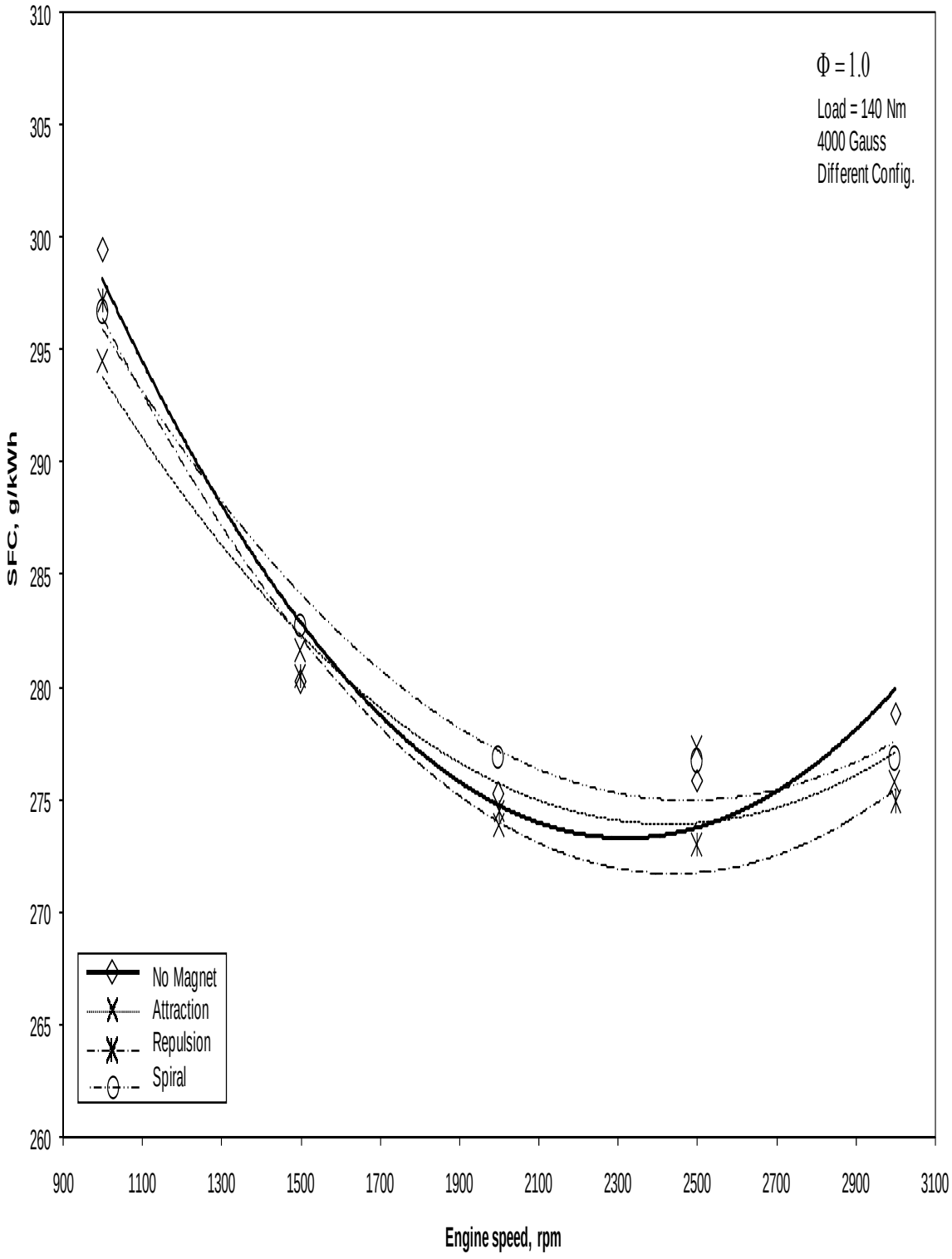

Figure 4-14: Magnetic configuration effect on SFC at constant load of 140 Nm

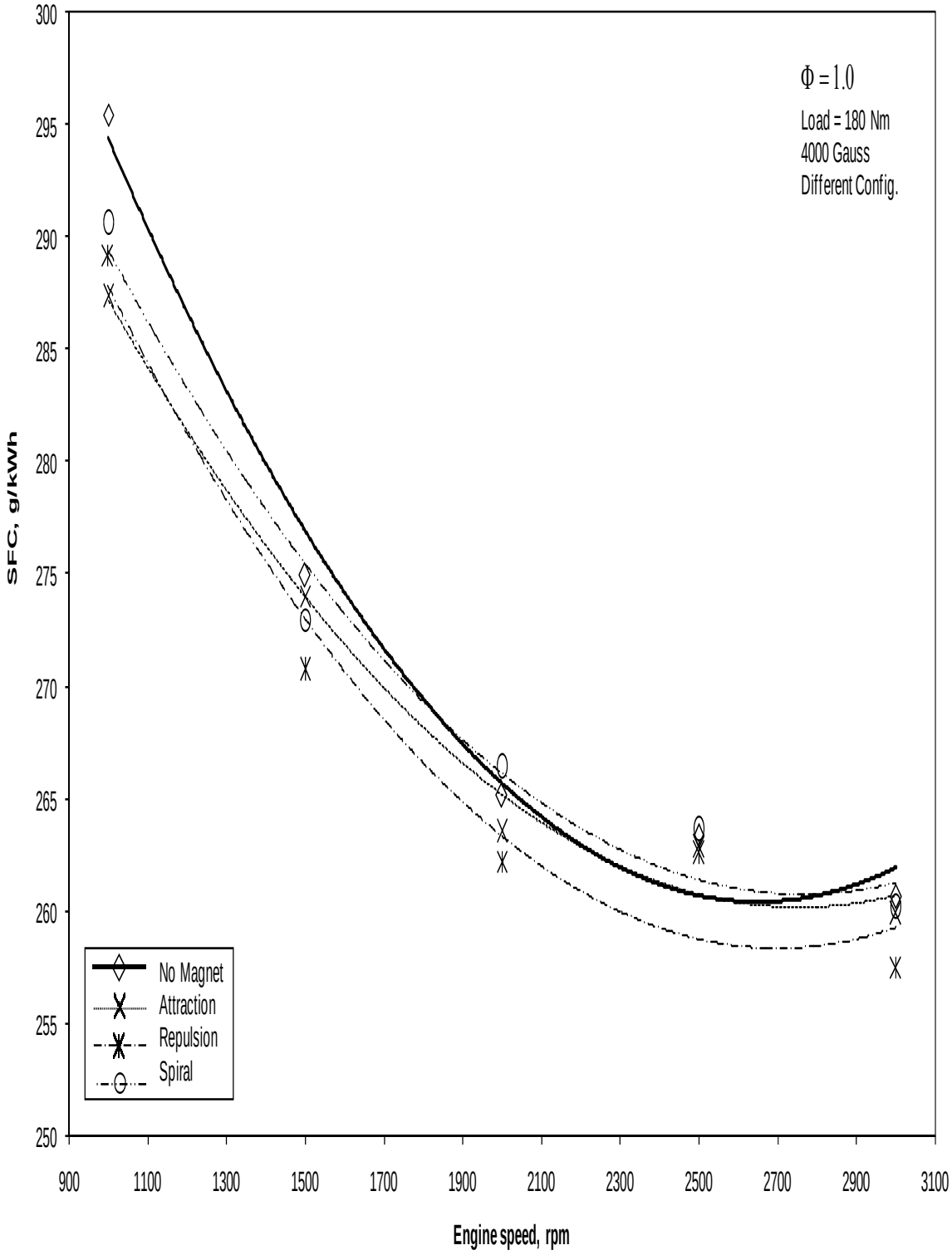

Figure 4-15: Magnetic configuration effect on SFC at constant load of 180 Nm

4.2.2 Constant Speed Simulation

The variation of the engine's SFC against different loads at a constant speed of 1000 rpm and constant magnetic field strength of 4000 Gauss with three different magnetic field configurations in 'Attraction', 'Repulsion', and 'Spiral' is shown in Figure 4-16. First of all, we note that, as the load increases, initially the SFC decreases rapidly, but with further increase of load, the SFC decreases with a steadier rate and reaches a constant value asymptotically. The overall SFC decreases monotonically with increasing load from around 700 (g/kWh) to nearly 270 (g/kWh). It can be easily observed that all four curves are virtually identical, with slight dissimilarity occurring only near the lowest engine loads, specifically for the 'Attraction' configuration. This slight and unobvious effect might be caused by the large SFC variation range across these different loads.

Figure 4-17 through Figure 4-20 correspond to an increase of the engine speed to 1500, 2000, 2500 and 3000 rpm respectively, while all other parameters are unchanged. These curves are observed to be virtually identical to Figure 4-16, where the magnetic field configuration effect is observed to be minimal.

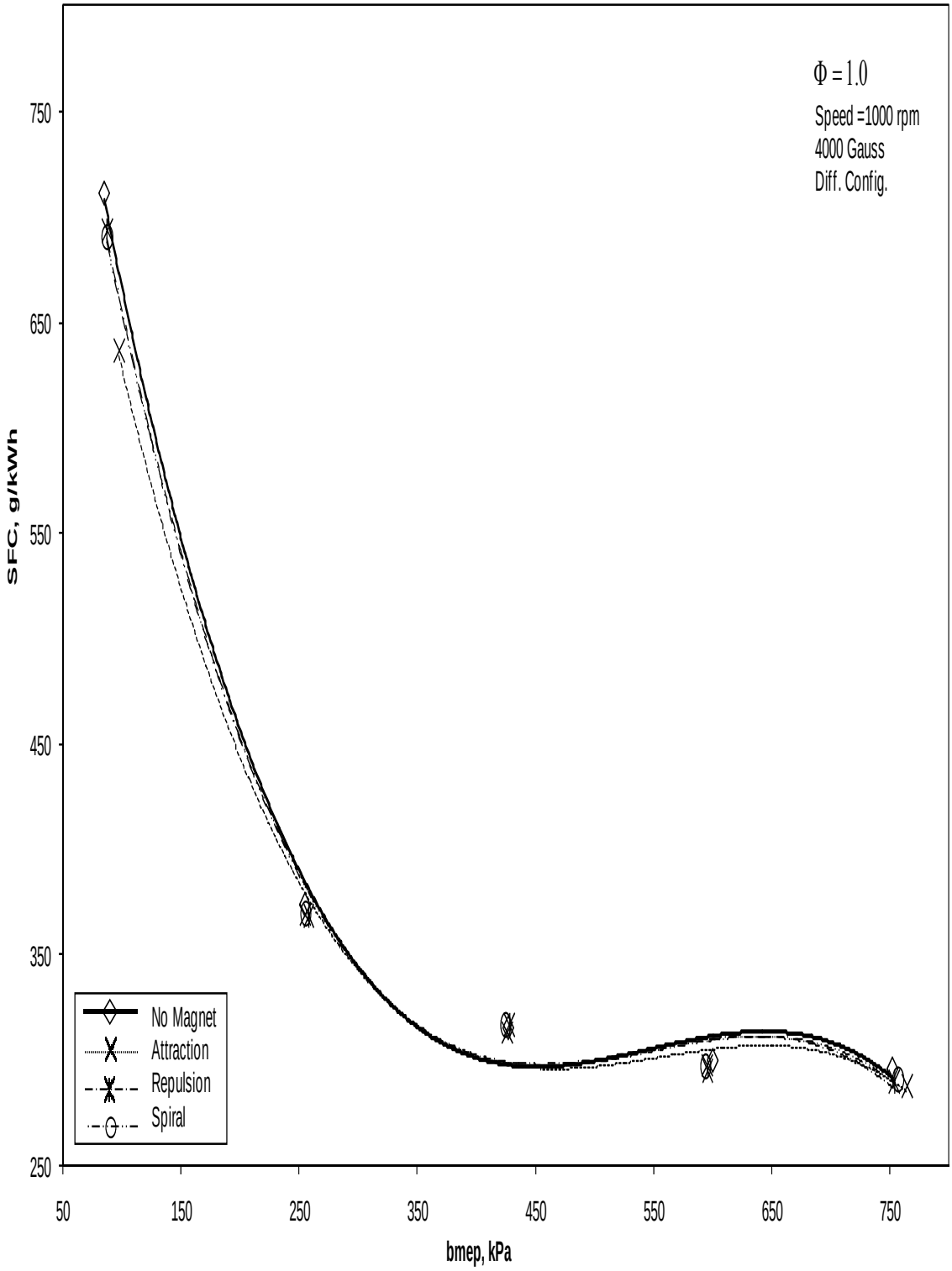

Figure 4-16: Magnetic configuration effect on SFC at constant speed of 1000 rpm

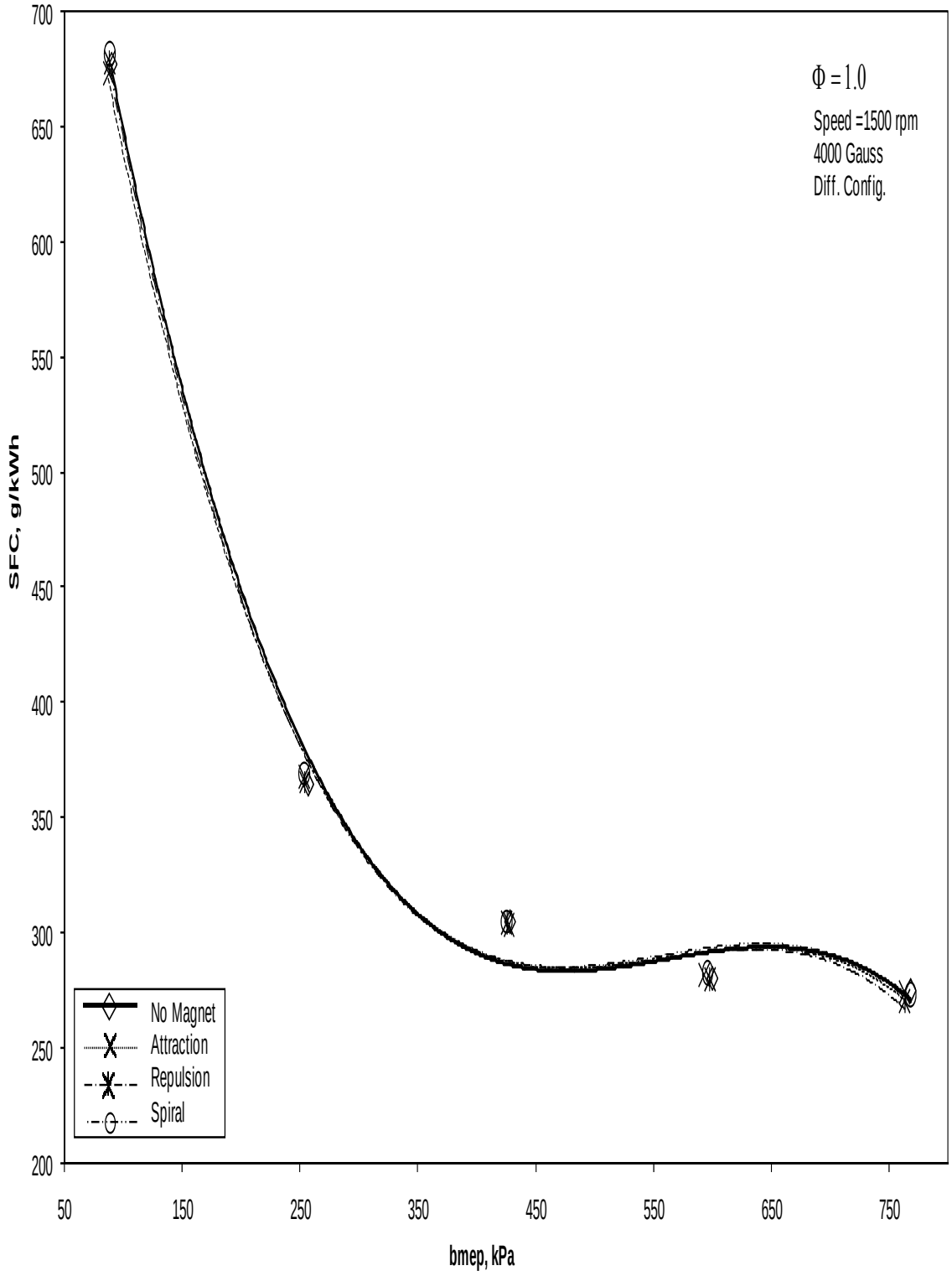

Figure 4-17: Magnetic configuration effect on SFC at constant speed of 1500 rpm

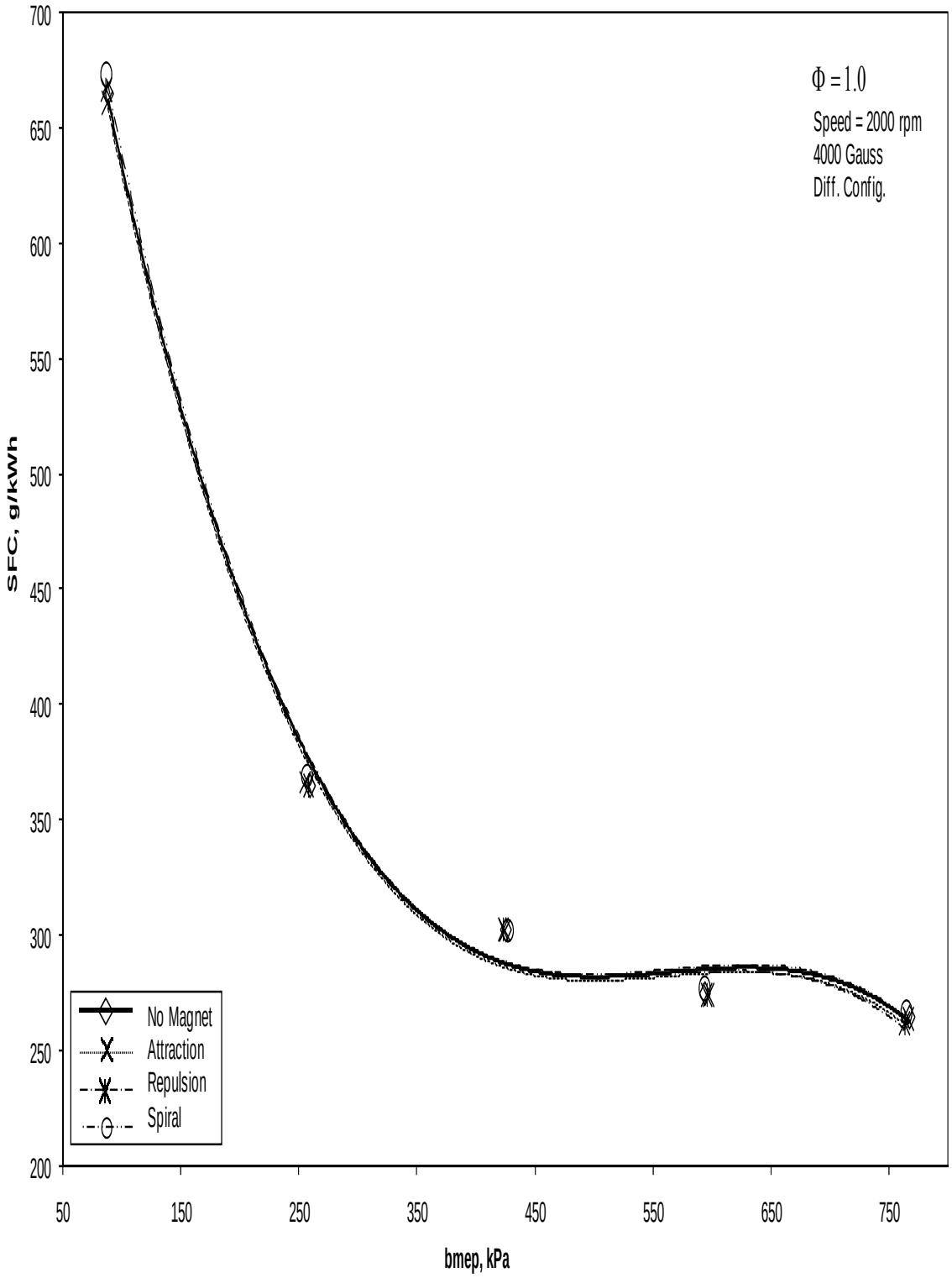

Figure 4-18: Magnetic configuration effect on SFC at constant speed of 2000 rpm

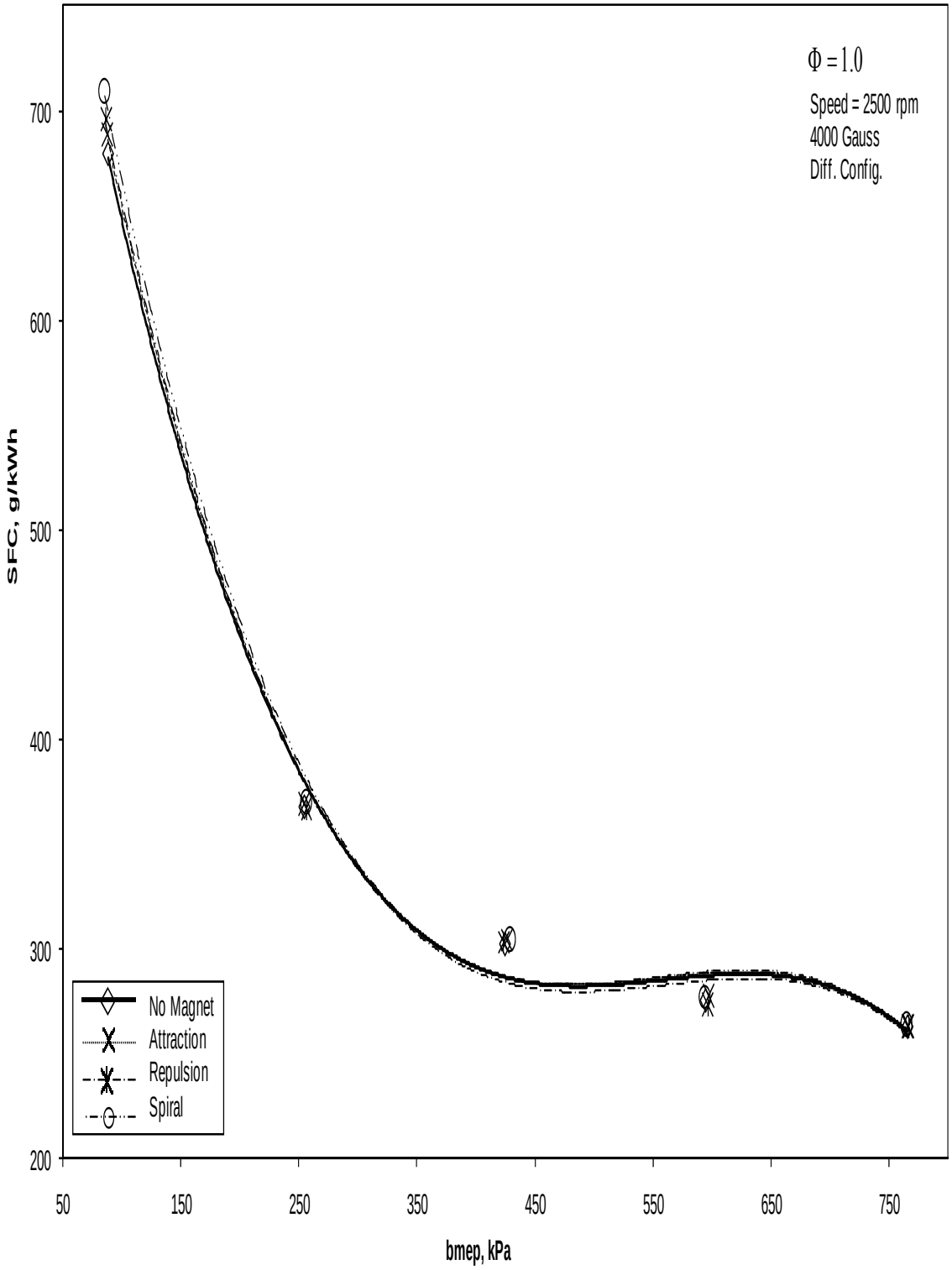

Figure 4-19: Magnetic configuration effect on SFC at constant speed of 2500 rpm

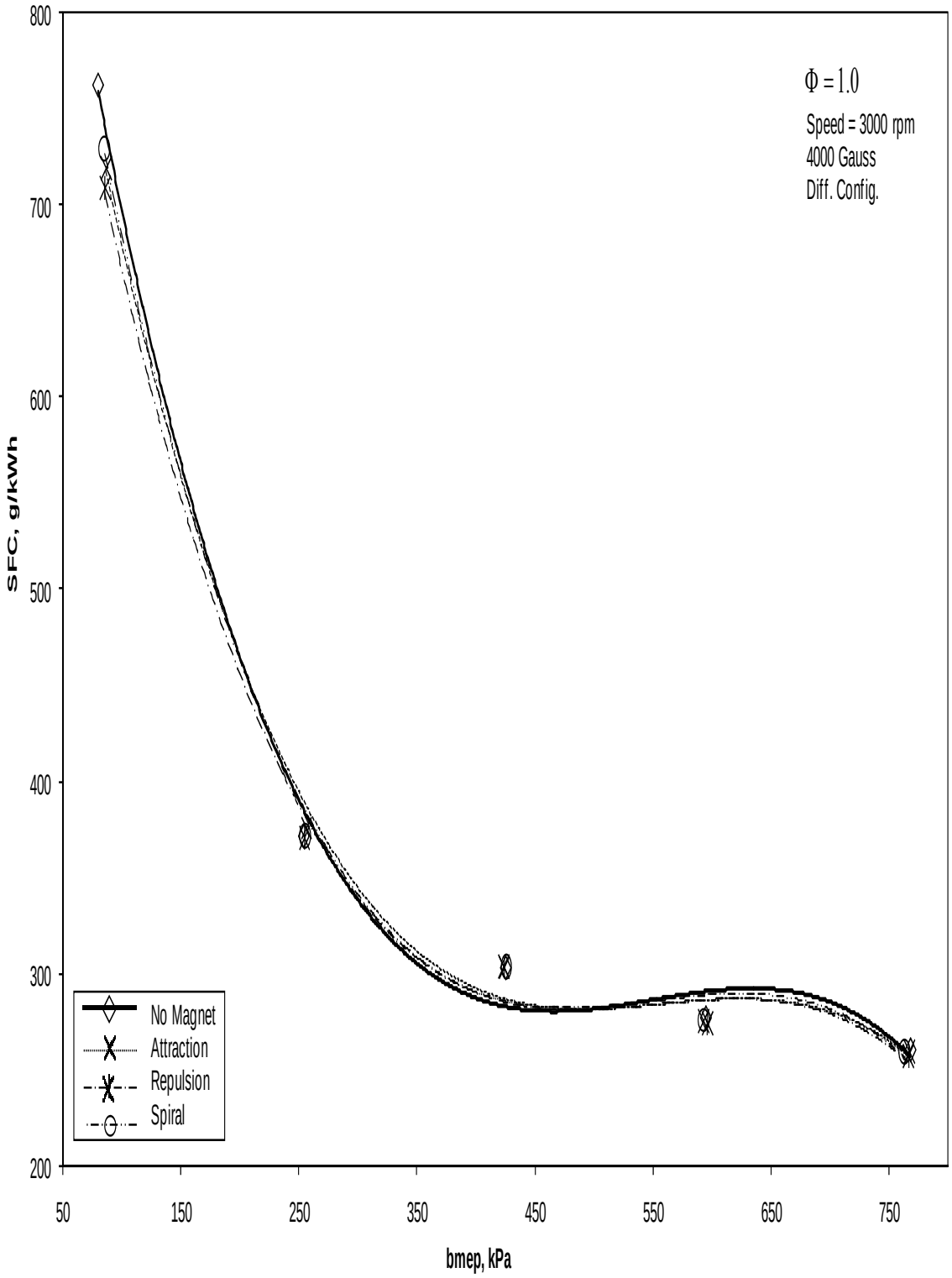

Figure 4-20: Magnetic configuration effect on SFC at constant speed of 3000 rpm

CHAPTER 5

5 CARBON MONOXIDE EMISSIONS (CO)

5.1 Magnetic Field Strength Effect

5.1.1 Constant Load Simulation

The variation of CO emissions in ppm against varying speeds at a constant load of 20 Nm and different aligned magnetic field strength in 'Attraction' configuration is shown in Figure 5-1. The CO emissions initially have a very high value of more than 3000 ppm at the lowest engine speed of 1000 rpm without any magnetic effect. As the engine speed is increased, CO emissions go down with smaller variation after 1500 rpm to stabilize at 2150 ppm. As the magnetic field is turned on, a remarkable decrease of 49% in CO emissions level is observed at the lowest engine speed of 1000 rpm. The increase in the magnetic field strength shows no distinctive effect in the emission level at most engine speeds. The curves corresponding to the different magnetic field strengths follow the same trend as the base curve, where they stabilize around a lower average value of 1900 ppm after 1500 rpm with an average decrease of 10% from the base curve.

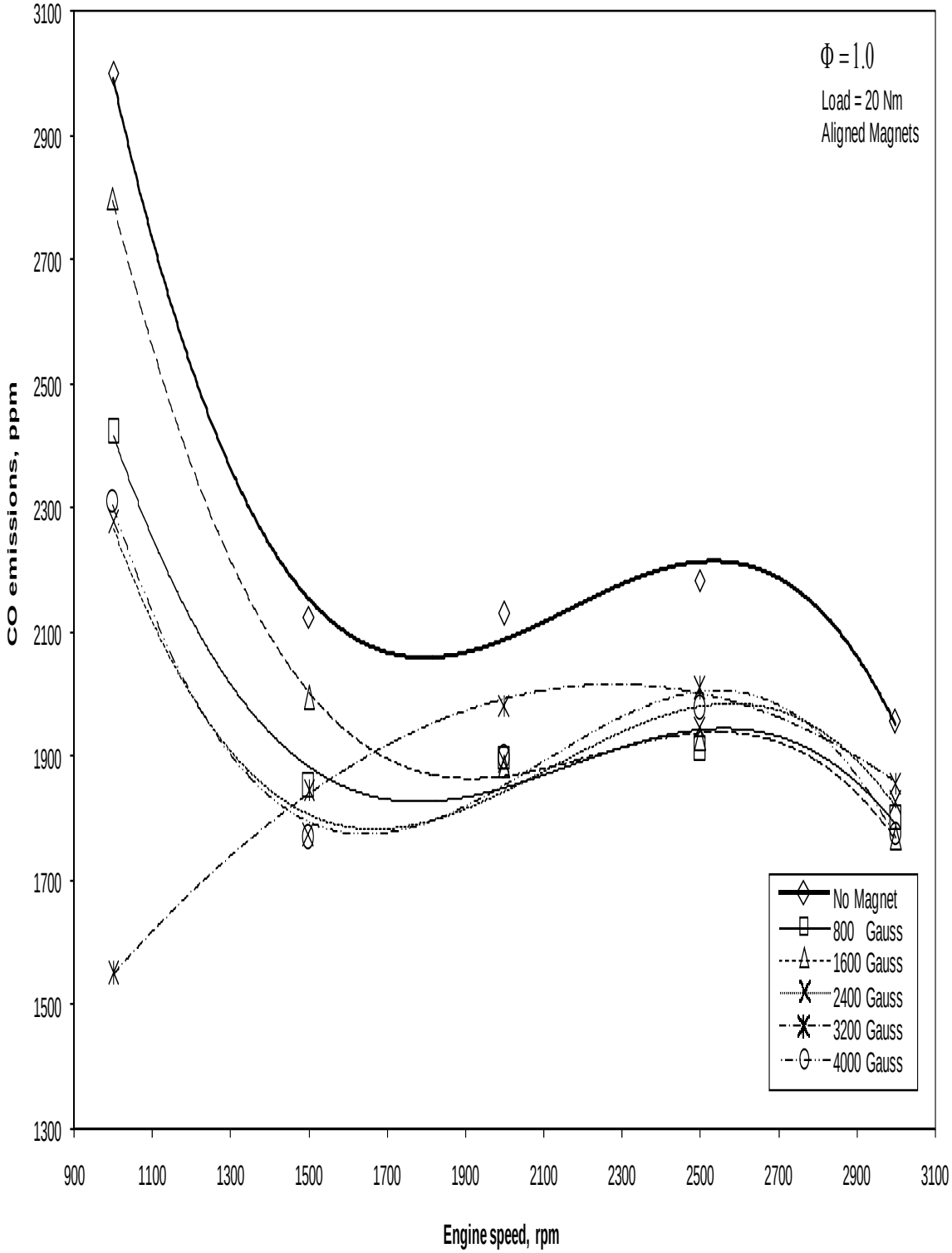

Figure 5-1: Magnetic strength effect on CO at constant load of 20 Nm

As the load is increased to 60 Nm, as shown in Figure 5-2, the qualitative behaviour of all the curves changes dramatically. Now, the CO emissions correspond to a mostly monotonically increasing curve as the engine speed increases, reaching a maximum of 2300 ppm near the highest engine speed of 3000 rpm. In general, the overall CO emissions level decreases considerably. Application of the magnetic field produces a similar appreciable reduction of 10% in the higher engine speed range. Increase in the magnitude of the magnetic field strength shows little variation. All the curves follow the same trend as that corresponding to zero magnetic strength.

Figure 5-3 shows the same relationship, but with an increased engine load to 100 Nm, where the qualitative behaviour remains almost the same as with the previous load. Application of the magnetic field again results in a similar decrease of 10% in the emissions level, where it is also more pronounced at higher engine speeds. The magnitude of the magnetic field strength has little effect on the emissions level.

Figure 5-4 shows the previous relationship at an increased load of 140 Nm where a shift in the qualitative behaviour is observed, similar to Figure 5-1. The CO emissions level goes down initially from 1800 ppm to a minimum value of 1200 ppm at 1500 rpm. Then, it increases to a maximum of 1900 ppm at 2500 rpm before it decreases slightly again. Application of the magnetic field produces somewhat more decrease in the emissions level compared to previous loads at almost all engine speeds. This can be seen especially at the lowest speed of 1000 rpm where the reduction reaches 40% with five magnets. In addition, different magnetic field strengths do not show a clear distinction for their effect on CO emissions.

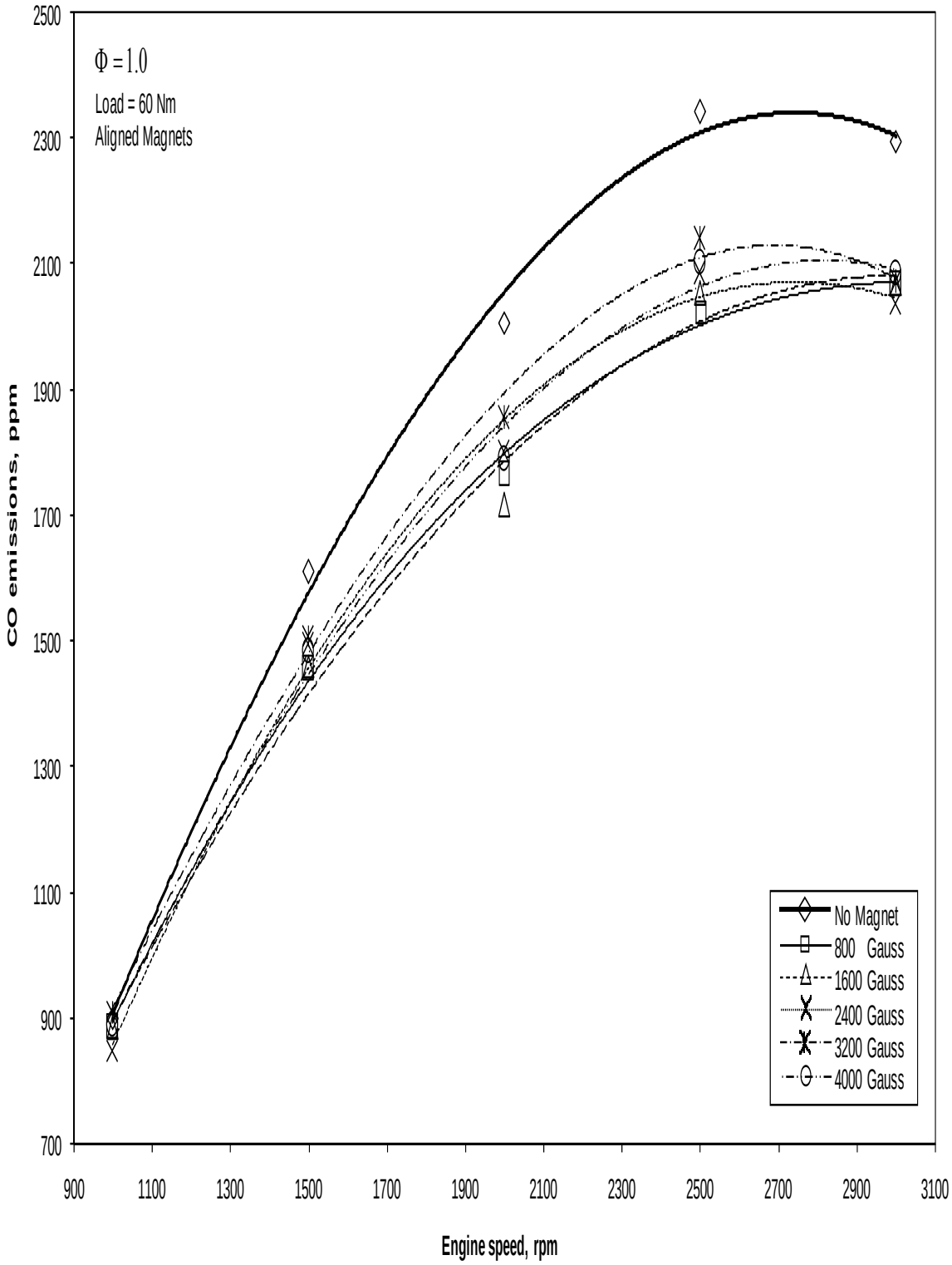

Figure 5-2: Magnetic strength effect on CO at constant load of 60 Nm

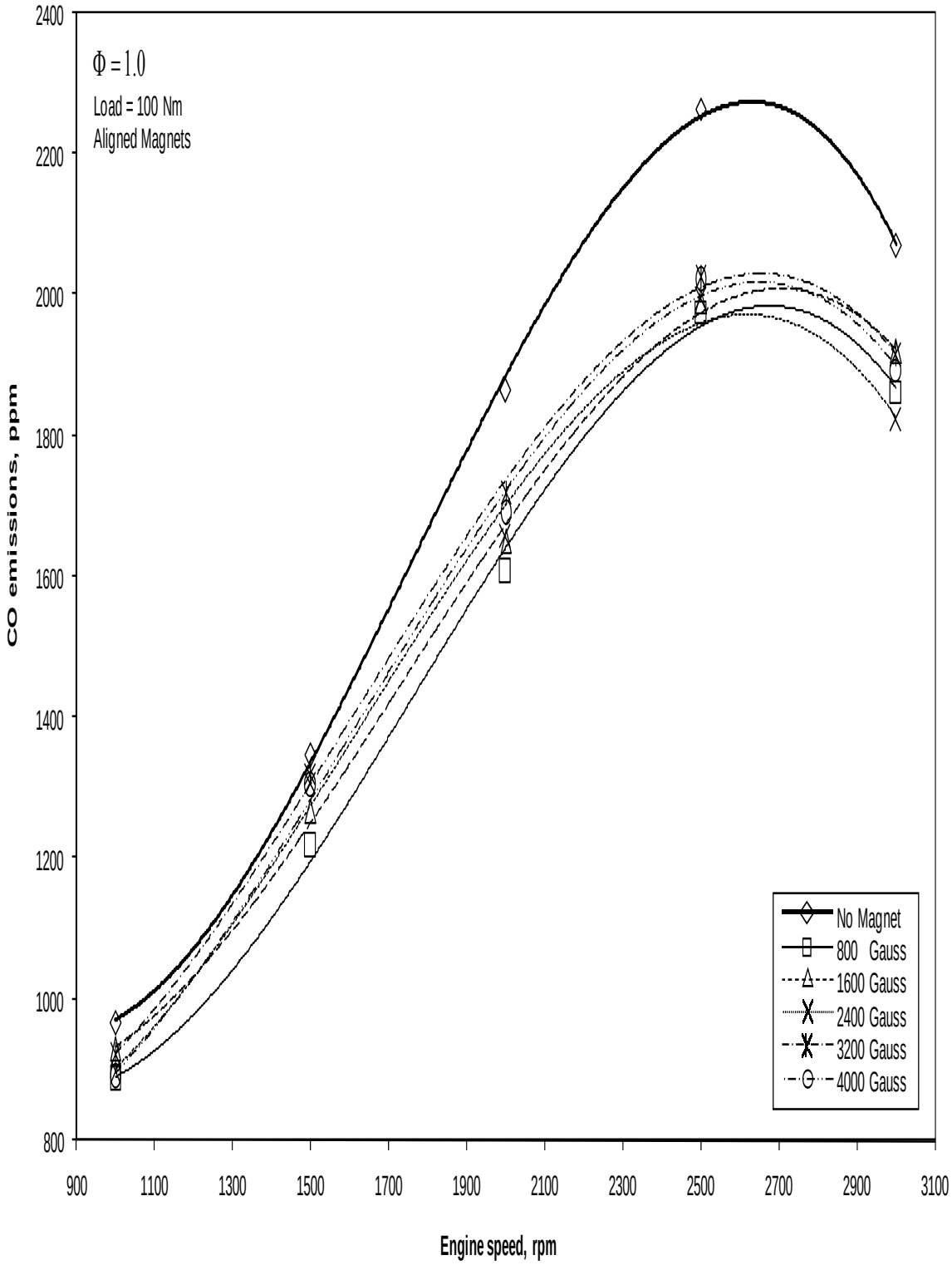

Figure 5-3: Magnetic strength effect on CO at constant load of 100 Nm

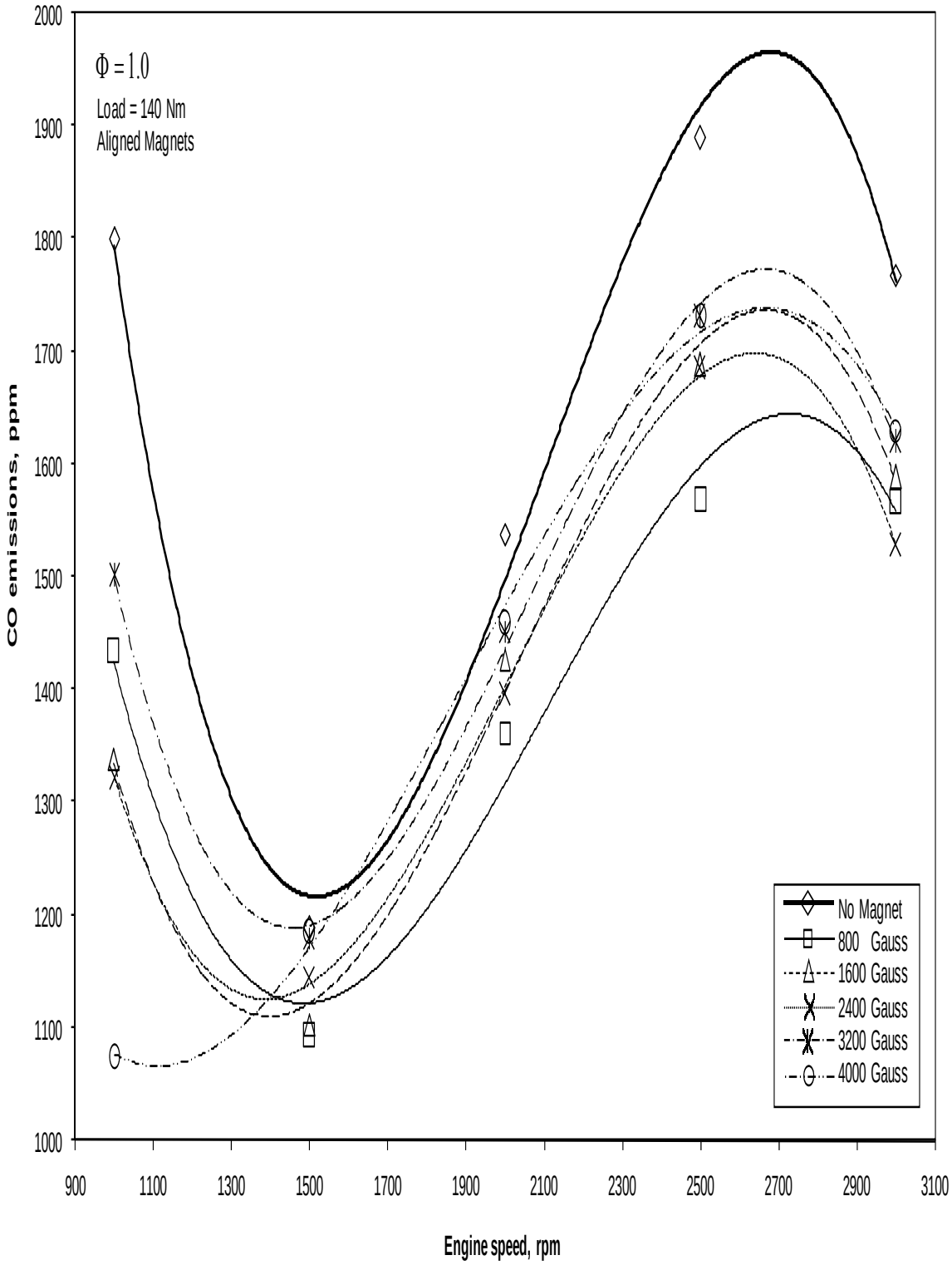

Figure 5-4: Magnetic strength effect on CO at constant load of 140 Nm

A further increase in engine load to 180 Nm, as depicted in Figure 5-5, shows a return to the qualitative behaviour observed in Figure 5-1. The CO emissions level goes down sharply and stabilizes at around 1900 ppm above 1500 rpm, which is considerably less than the value reached at a load of 20 Nm. However, the CO emissions increase dramatically to a higher value of 3400 ppm at the engine speed of 1000 rpm. Application of a magnetic field shows even more decrease in the emissions level at almost all engine speeds. This can be seen especially at the lowest speed of 1000 rpm where the reduction reaches 45% with five magnets. The effect of magnetic field strength is more obvious at this load, since the strongest field shows the most favourable effect consistently across all engine speeds. All curves follow the same trend as that shown by the base curve.

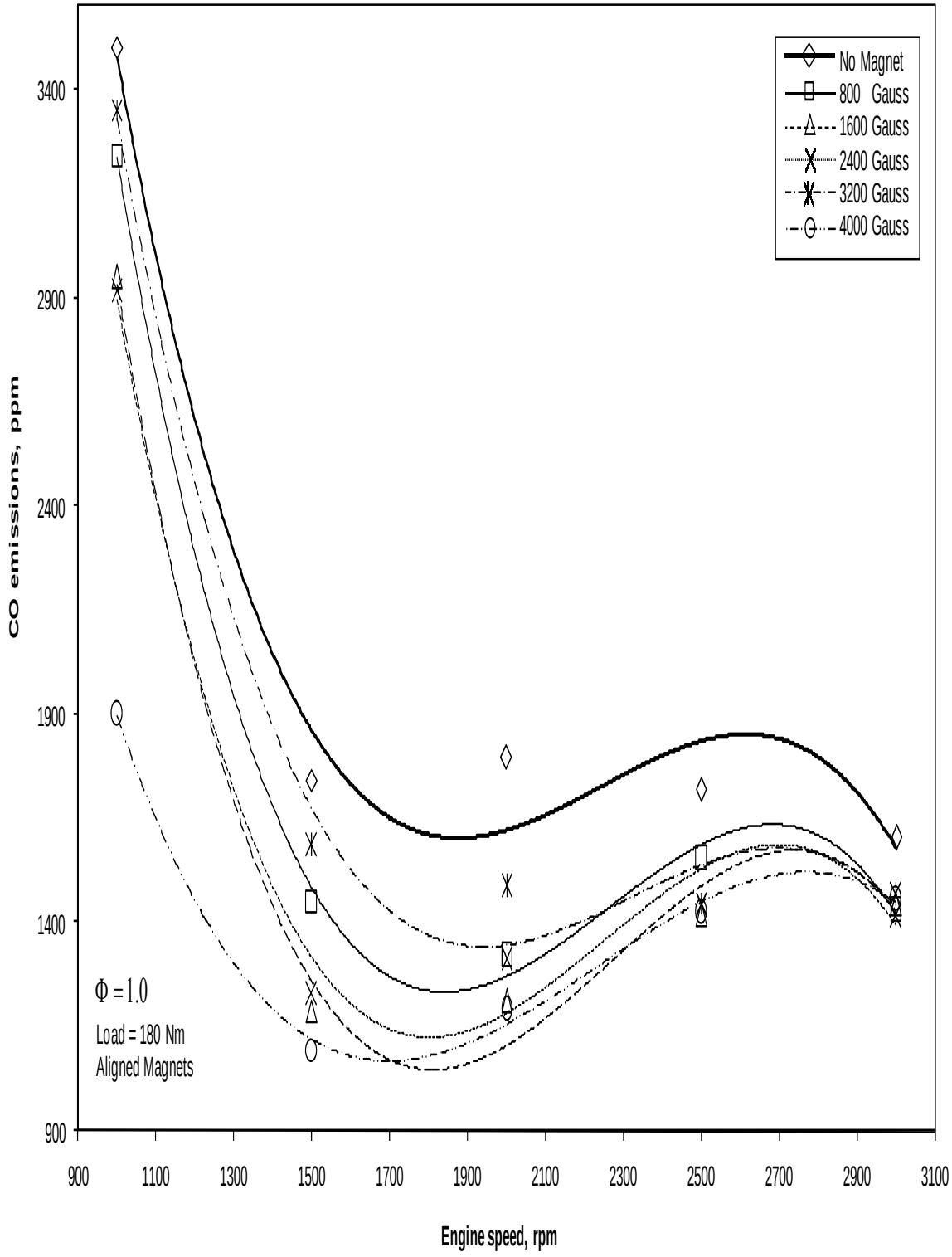

Figure 5-5: Magnetic strength effect on CO at constant load of 180 Nm

5.1.2 Constant Speed Simulation

The variation of CO emission against different loads at a constant speed of 1000 rpm and different aligned magnetic field strengths in 'Attraction' configuration is shown in Figure 5-6. With no magnetic field, it is observed that the CO emission decreases initially with increasing engine loads until it reaches a minimum of around 650 ppm at 350 kPa of engine load. Thereafter, the emission increases to a maximum of 3500 ppm at the highest load of 750 kPa. The shape of the curve is seen to resemble a parabola. When the magnetic field is turned on, a noticeable effect is observed for most engine loads, especially at higher and lower engine load values. As the engine load increases beyond the minimum emission point, a higher positive effect is also observed for all magnetic field strengths, especially for the 4000 Gauss field. The best favourable effect of more than 40% emission reduction is observed at both ends of the load spectrum.

Figure 5-7 shows the relationship between the same variables, while the engine speed is increased to 1500 rpm. With no magnetic field, the CO emission behaviour does not change much, while the minimum emission point shifts towards a higher engine load of 500 kPa, and the difference between the maximum and minimum values is reduced substantially. Similarly, when the magnetic field is turned on a remarkable effect is observed for most engine loads, especially at the highest and lowest engine loads. In addition, the highest magnetic field strength still shows the best reduction, reaching 35% at the highest load of 180 Nm and 15% reduction at lowest load of 20 Nm.

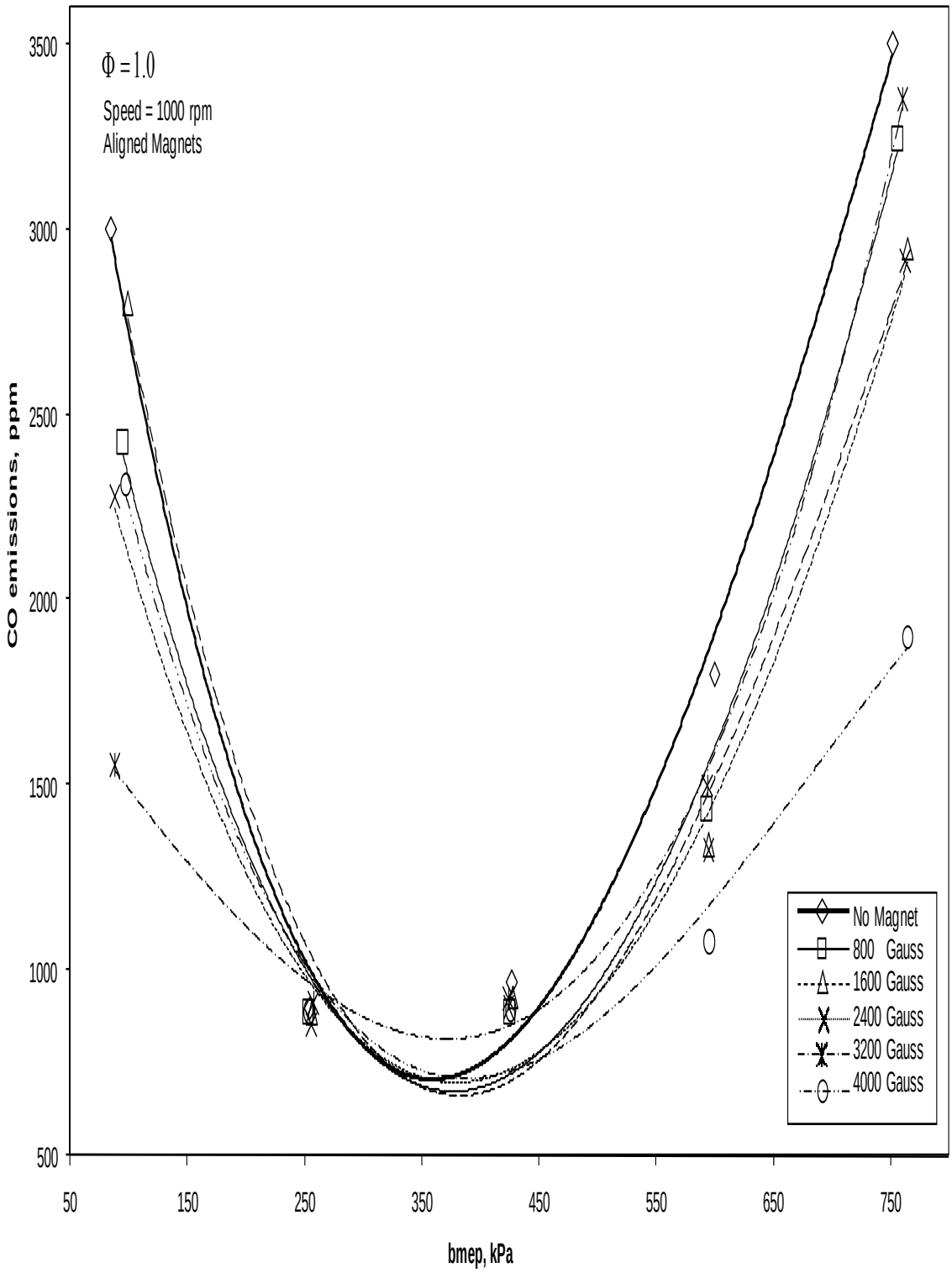

Figure 5-6: Magnetic strength effect on CO at constant speed of 1000 rpm

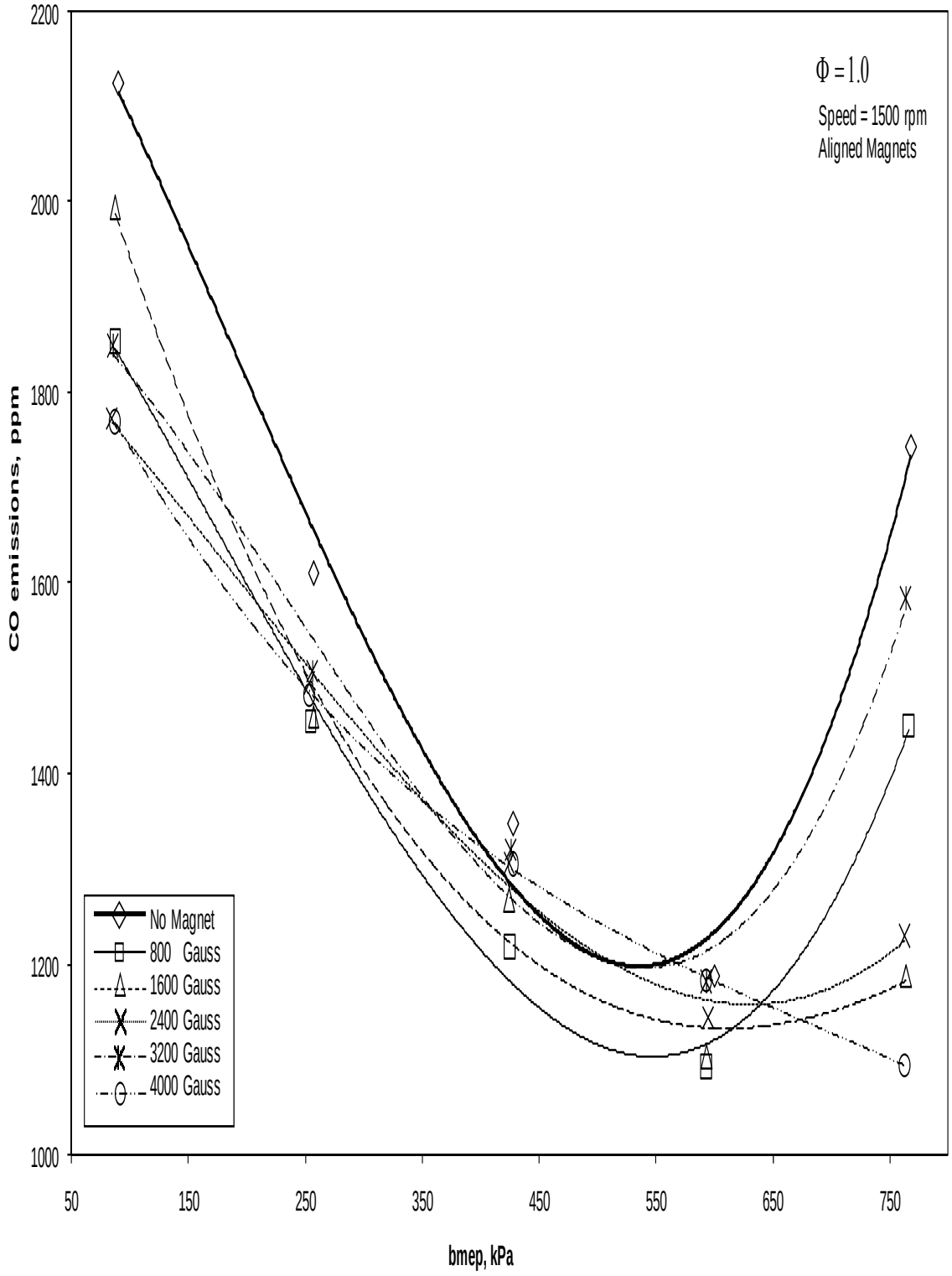

Figure 5-7: Magnetic strength effect on CO at constant speed of 1500 rpm

Figure 5-8 shows the same graph as before but at an engine speed of 2000 rpm. With no magnetic field, the CO emissions continue their trend of reduction in the maximum value and increase in the minimum, where the parabolic trend is becoming flatter. Also, the higher minimum emission value of 1600 ppm now occurs at a higher engine load of 600 kPa. Similarly, at this engine speed, when the magnetic field is turned on, an appreciable reduction of CO emissions is still observed at all engine loads and at all magnetic field strengths. In addition, the dependence of CO emission on magnetic field strength seems very complex and apparently unpredictable at this load. Moreover, the maximum emission reduction reaches 35% at the highest load of 180 Nm.

Figure 5-9 shows the variation in the same variables at an engine speed of 2500 rpm. At zero magnetic field, the curve changes its engine load dependence. The maximum CO emissions now increase from the previous engine speed setting by 200 ppm, but the minimum remains near its previous value of 1700 ppm. When the magnetic field is turned on, an appreciable reduction between 10-20% in CO emissions is observed consistently at all engine loads and at all magnetic field strengths. This reduction in CO emissions does not seem to depend noticeably on the magnetic field strength.

Similar observations are reported for an engine speed of 3000 rpm as shown in Figure 5-10. The only difference is that the CO emission now starts to decrease at almost all engine loads. The qualitative behaviour remains essentially the same. With the application of the magnetic field, the CO emission reduction of 10% is observed consistently at all engine loads with no particular dependence on magnetic field strength.

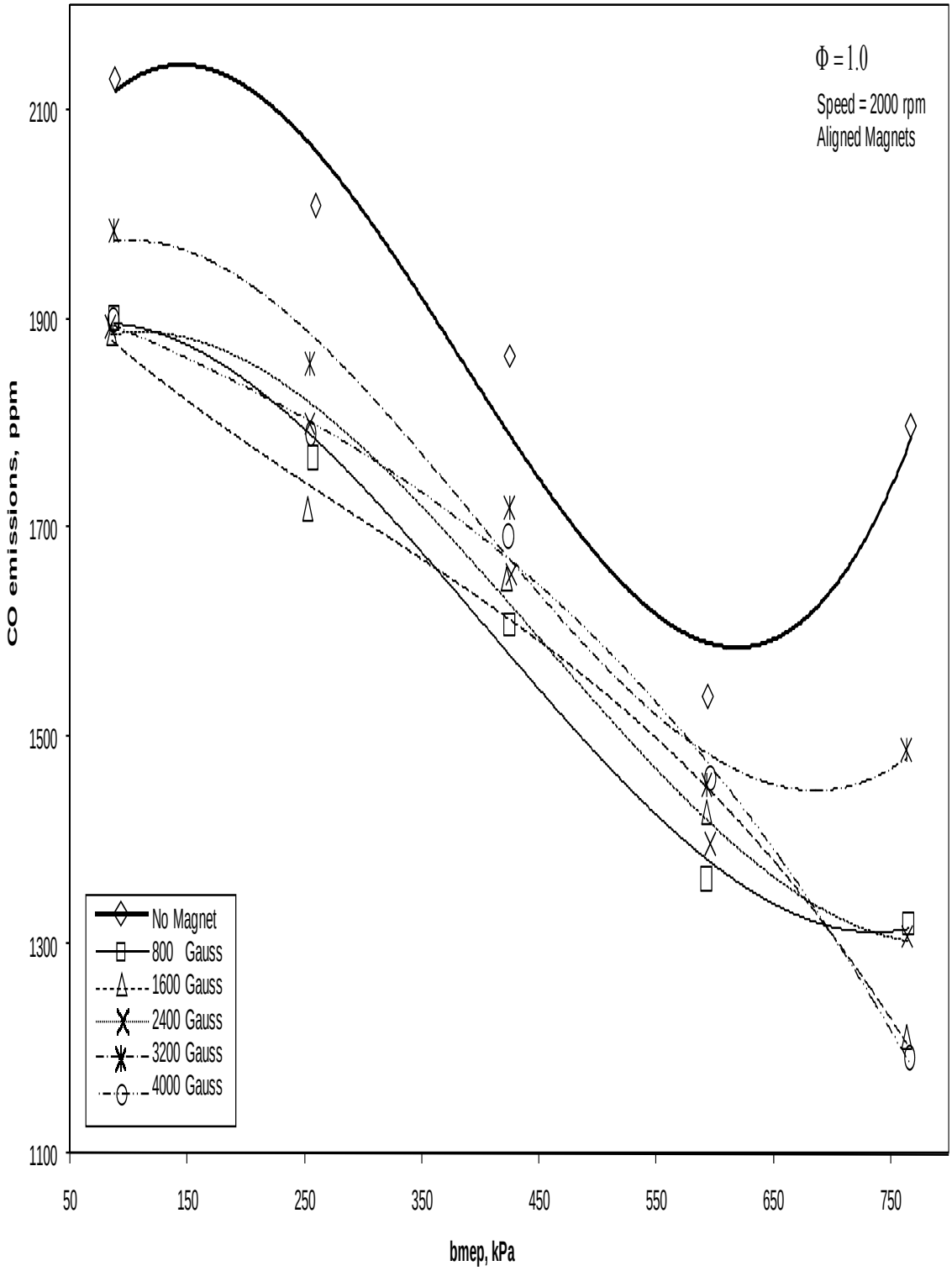

Figure 5-8: Magnetic strength effect on CO at constant speed of 2000 rpm

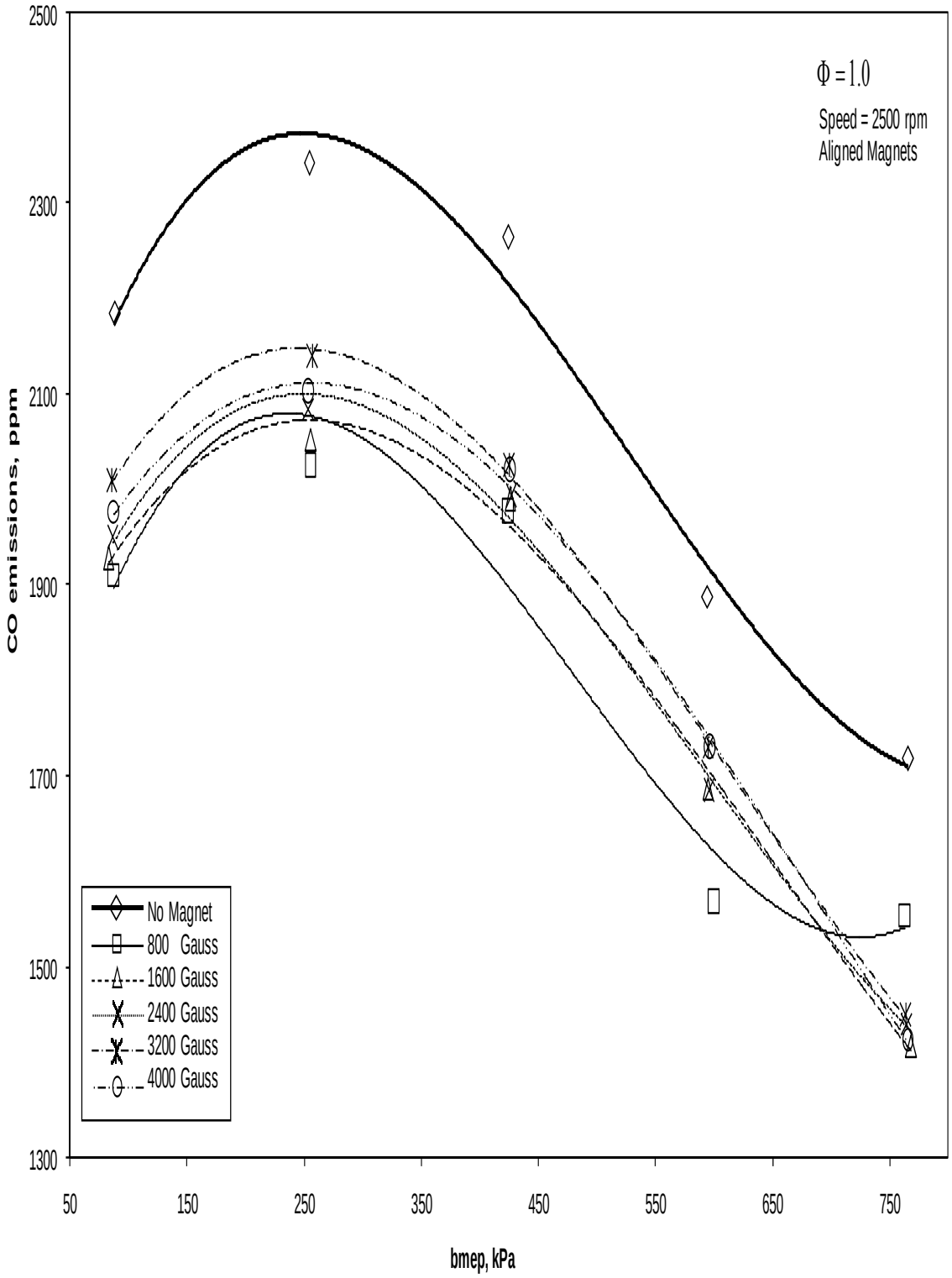

Figure 5-9: Magnetic strength effect on CO at constant speed of 2500 rpm

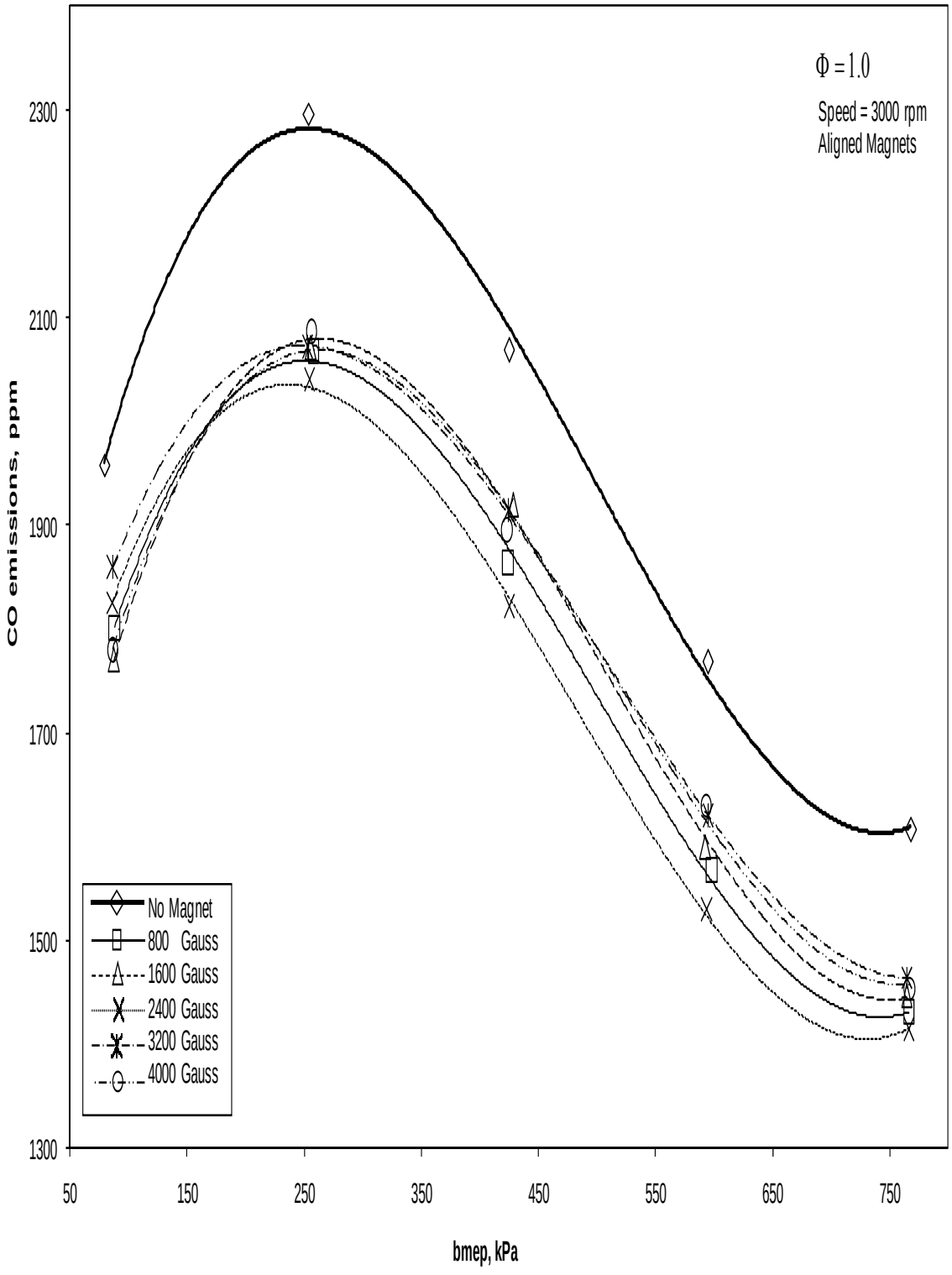

Figure 5-10: Magnetic strength effect on CO at constant speed of 3000 rpm

5.2 Magnetic Field Configuration Effect

5.2.1 Constant Load Simulation

The variation of the CO emissions against varying engine speeds at a constant load of 20 Nm and constant magnetic field strength of 4000 Gauss with three different magnetic field configurations is shown in Figure 5-11. Before starting the magnetic field effect, the CO emissions show a mixed trend. Initially, the CO emissions decrease with increasing engine speed, settling down at a near constant value for engine speeds of 1500 to 2500 rpm and then again slightly decreasing with a further rise in the engine speed to 3000 rpm. The CO emissions vary from a maximum of 3000 ppm to a minimum of 1900 ppm. With the application of the magnetic field, a marked decrease in the emissions is observed at all engine speeds and more noticeably at 1000 rpm. The curves follow the zero magnetic field curve trend for almost all engine speeds. Also, in this region no effect difference is observed in the different magnetic field strength configurations. However, for the lower range of the engine speed, less than 1500 rpm, different magnetic configurations show different trends, with the least emissions taking place for the 'Repulsion' configuration. The reduction reaches 48% with the 'Repulsion' configuration at 1000 rpm compared to 23% reduction with the 'Attraction' configuration. In addition, the 'Spiral' configuration acts somewhat in between at this lowest speed with a reduction of 40% in CO emission.

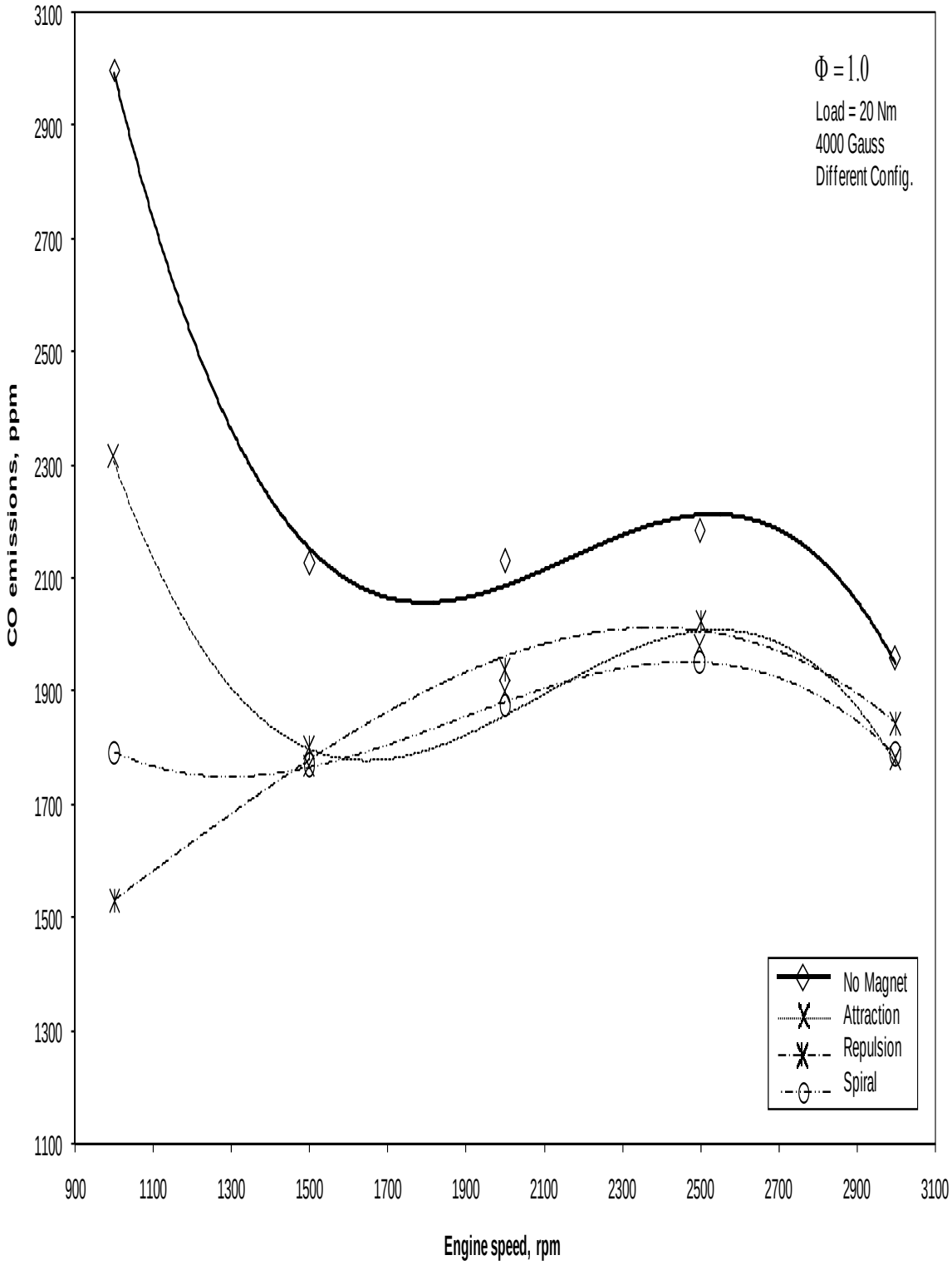

Figure 5-11: Magnetic configuration effect on CO at constant load of 20 Nm

Figure 5-12 shows the relationship between the same variables at an increased load to 60 Nm. It is noted that now the behaviour of the CO emission curves is totally changed. The curves now start from a low value of CO emissions at the lowest engine speed, and they increase monotonically with increasing engine speed. However, a maximum emission value of 2350 ppm is reached at around the highest engine speed. This is in marked contrast to the previous figure, where the CO emissions decreased with increasing engine speed. In general, the overall CO emissions decrease by comparison with the previous load settings at all engine speeds. With the application of the magnetic field, a considerable decrease of 10% in the CO emissions occurs at engine speeds higher than 2000 rpm, but this change is less pronounced at lower speeds. All magnetic field configurations show similar behaviour with no preference.

Figure 5-13 shows the effect of a further increase in the load to a value of 100 Nm. The behaviour of all curves is essentially the same as that in the previous figure, with a slight decrease in the overall CO emissions at all engine speeds. The reduction continues to be around 10% at higher engine speeds.

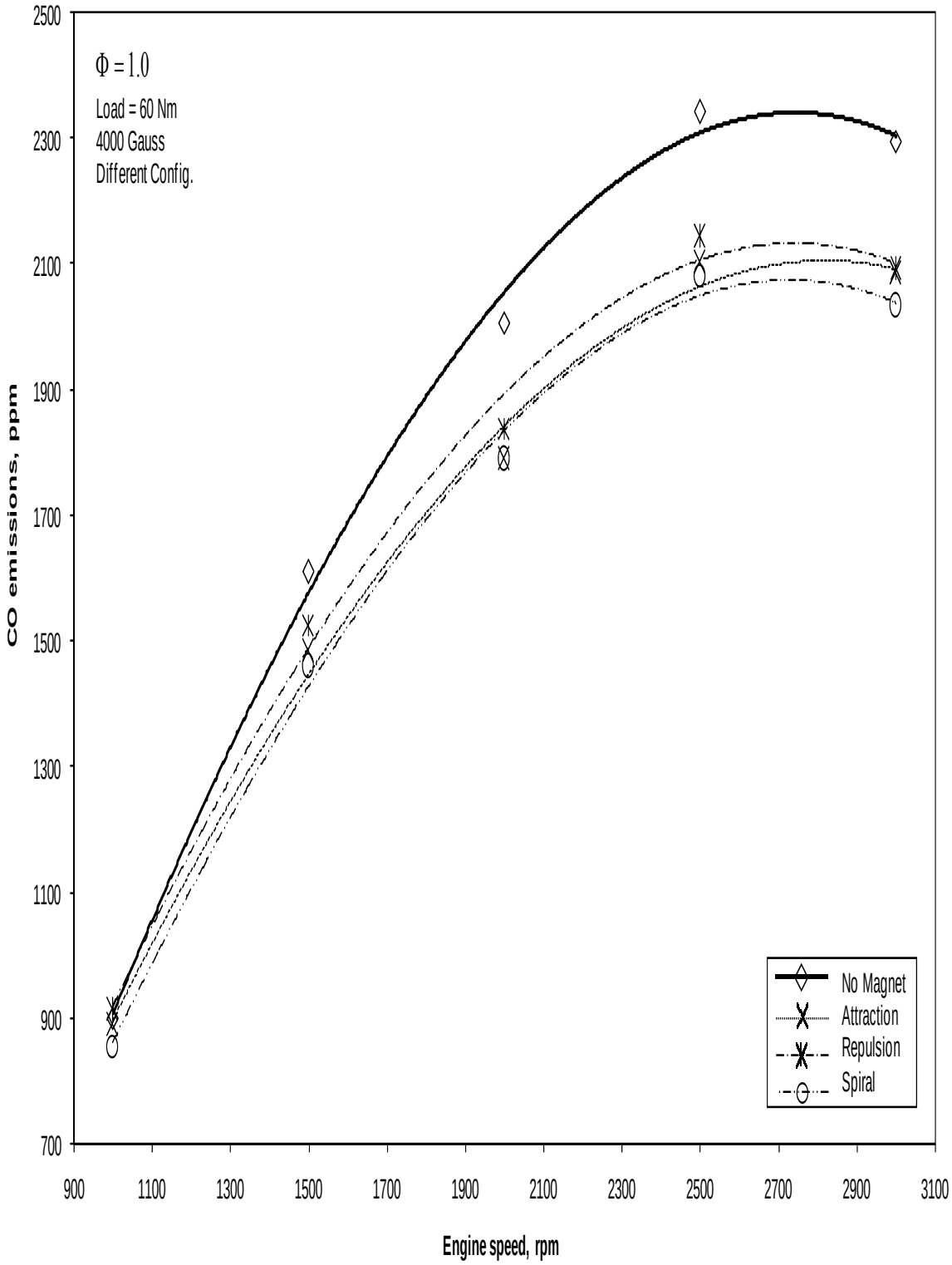

Figure 5-12: Magnetic configuration effect on CO at constant load of 60 Nm

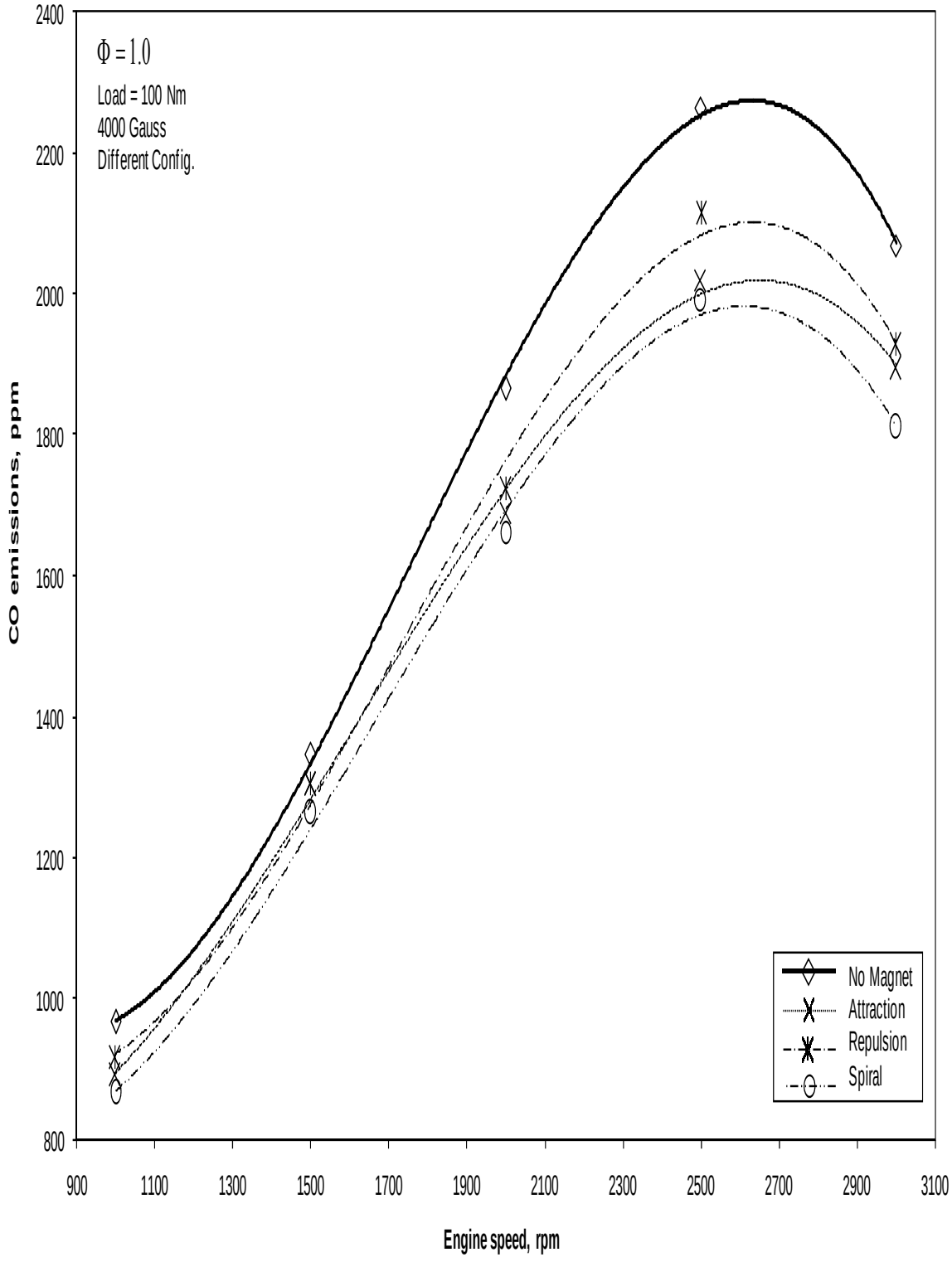

Figure 5-13: Magnetic configuration effect on CO at constant load of 100 Nm

Further increase in the load to 140 Nm, depicted in Figure 5-14, shows a change in the relation between the CO emissions and the engine speed, reverting back to what was observed at the lowest load of 20 Nm. The CO emissions have a high value of 1800 ppm at the lowest engine speed, but they decrease initially with increasing engine speed to 1200 ppm. Then, they increase to a maximum of 2000 ppm to end at the same starting level of 1800 ppm at the maximum speed. Above 1500 rpm, there is an overall decrease in the emissions at all engine speeds as compared to the data in the previous figure. All the configurations show the same behaviour after the application of the magnetic field, resulting in a decrease in the emissions at most engine speeds. Below 1500 rpm and above 2000 rpm, again the application of the magnetic field induces a considerable decrease of 12% in the emissions, with different configurations showing slightly different levels of effect. These behaviours of the curves are comparable to the behaviour shown at 20 Nm of load. The maximum reduction reaches 38% at the lowest engine speed with a slightly less favourable effect from the ‘Spiral’ configuration.

Figure 5-15 shows the effect of a further increase in the load to 180 Nm. For speeds above 1500 rpm the emissions remain more or less constant at around 1750 ppm, while they increase rapidly for speeds below 1500 rpm to a value of 3500 ppm. With the application of the magnetic field, a marked decrease in the CO emissions occurs at all engine speeds. The different magnetic configurations have no noticeable effect above 1500 rpm, but they show a favourable discrepancy below 1500 rpm for the ‘Repulsion’ and ‘Attraction’ configurations with a maximum reduction of 48%. This behaviour is somewhat similar to the 20 Nm load, as depicted in Figure 5-11.

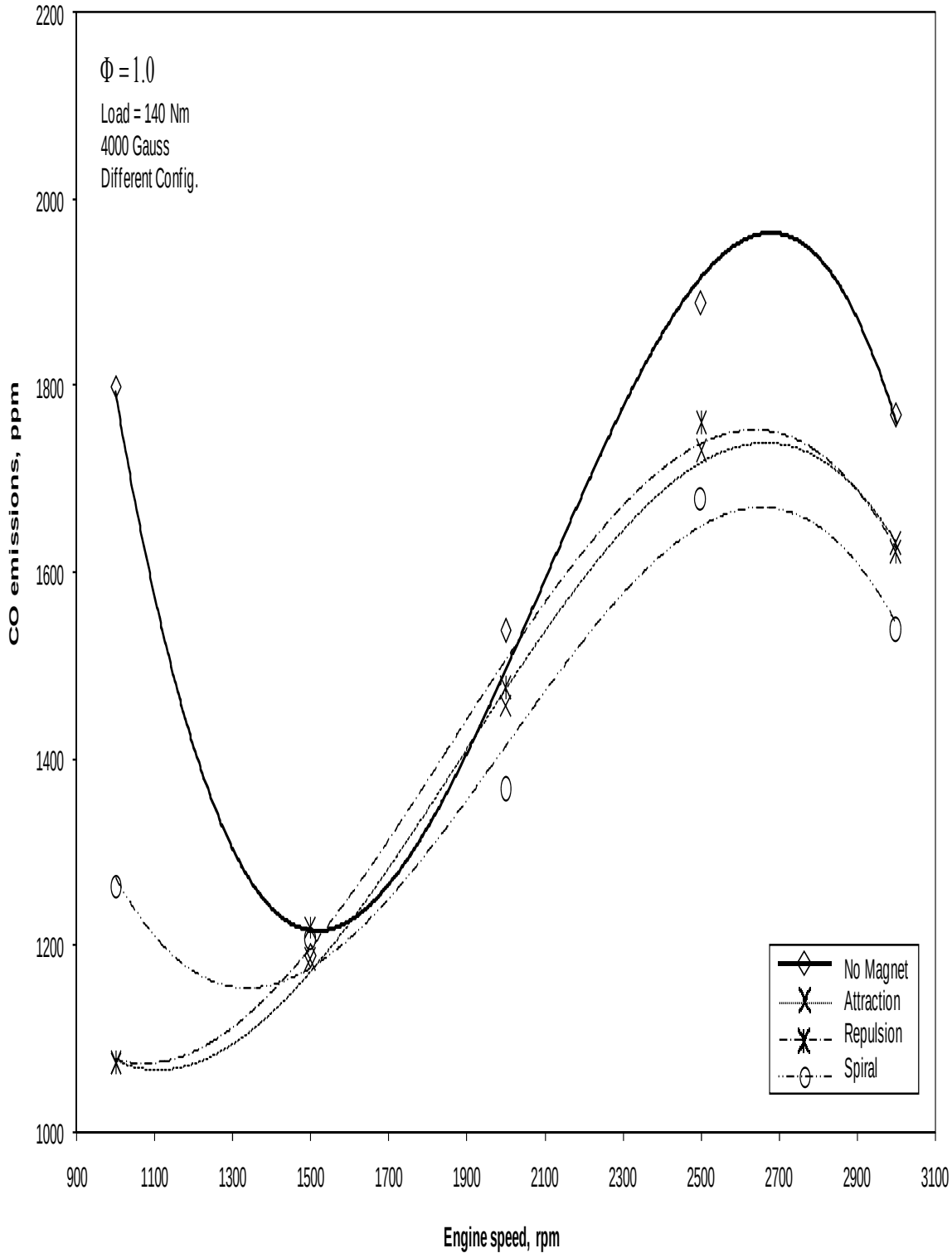

Figure 5-14: Magnetic configuration effect on CO at constant load of 140 Nm

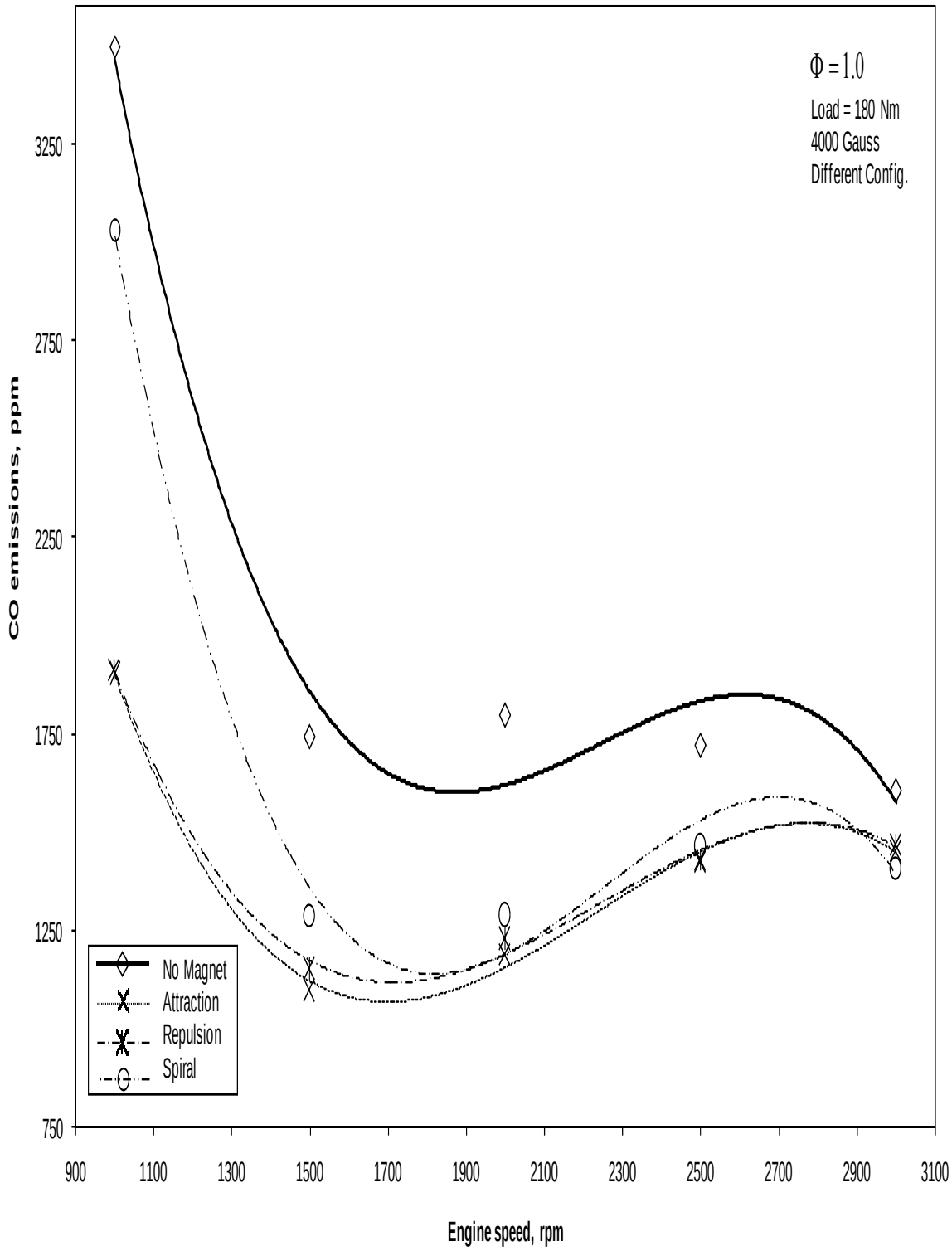

Figure 5-15: Magnetic configuration effect on CO at constant load of 180 Nm

5.2.2 Constant Speed Simulation

The variation of the engine CO emissions against different loads at a constant speed of 1000 rpm and constant magnetic field strength of 4000 Gauss with three different magnetic field configurations is shown in Figure 5-16. With the magnetic field turned off, the CO emission initially decreases with rising engine load until it reaches a minimum of 700 ppm at an engine load of around 350 kPa. Then, the emission increases monotonically to around 3500 ppm at the highest engine load. The shape of the emissions curve resembles a parabola. As the magnetic field is turned on, the CO emission decreases substantially by 48% at both ends of the load spectrum. This magnetic field effect is more pronounced for the 'Attraction' and 'Repulsion' configurations than for the 'Spiral' configuration. However, the minimum value of the CO emissions remains nearly the same and also occurs at around the same engine load. This indicates a somewhat restricted effect of the magnetic field at that engine load of 350 kPa.

Figure 5-17 shows the variation in the same variables at a constant engine speed of 1500 rpm. With no magnetic field, the CO emission is observed to go down substantially near the lowest and the highest values of engine load in comparison with the previous lower engine speed setting. However, for moderate values of engine load, the CO emission goes drastically higher with the minimum now at around 1200 ppm occurring at nearly 500 kPa of engine load. As the magnetic field is turned on, the CO emissions again go down around the extreme values of the engine load, and the minimum CO emission remains approximately the same. The reduction varies between 15% and 30% at the lowest and highest load respectively. Moreover, it can be observed that now there is less discrepancy between the 'Spiral' magnetic configuration and the other two magnetic configurations at

most engine loads. Overall, the shape of all the curves is qualitatively the same in both previous figures.

Figure 5-18 shows a further increase in engine speed which is now set to 2000 rpm. It is observed, without magnetic field effect, that the maximum value of the CO emission has gone down slightly and the minimum value has gone up dramatically. In this regard, the CO emission variation is trying to become 'flatter' with increasing engine speed. On the other hand, the overall shape of the curve is now changed, where the minimum value of the CO emission has moved further right and occurs at a higher engine load of around 600 kPa and the curve now has a point of inflection at an engine load of 500 kPa, which was not observed in the previous two figures. When the magnetic field is turned on, the CO emissions at all engine loads goes down, and there is little effect in changing the magnetic field configuration. It is also noted that the minimum CO emission goes down by 30% once the magnetic field is applied at the highest engine load of 750 kPa while a reduction level of 10% remains constant at most other engine loads.

Figure 5-19 and Figure 5-20 show the effect of a further increase in the engine speed, now set to 2500 and 3000 rpm respectively. With no magnetic field, a considerable rise in CO emission is observed for the first half of the engine loads. When the magnetic field is turned on, the CO emission goes down consistently by 15% for most values of engine loads. In addition, there is less variation between the emission curves corresponding to different magnetic configurations.

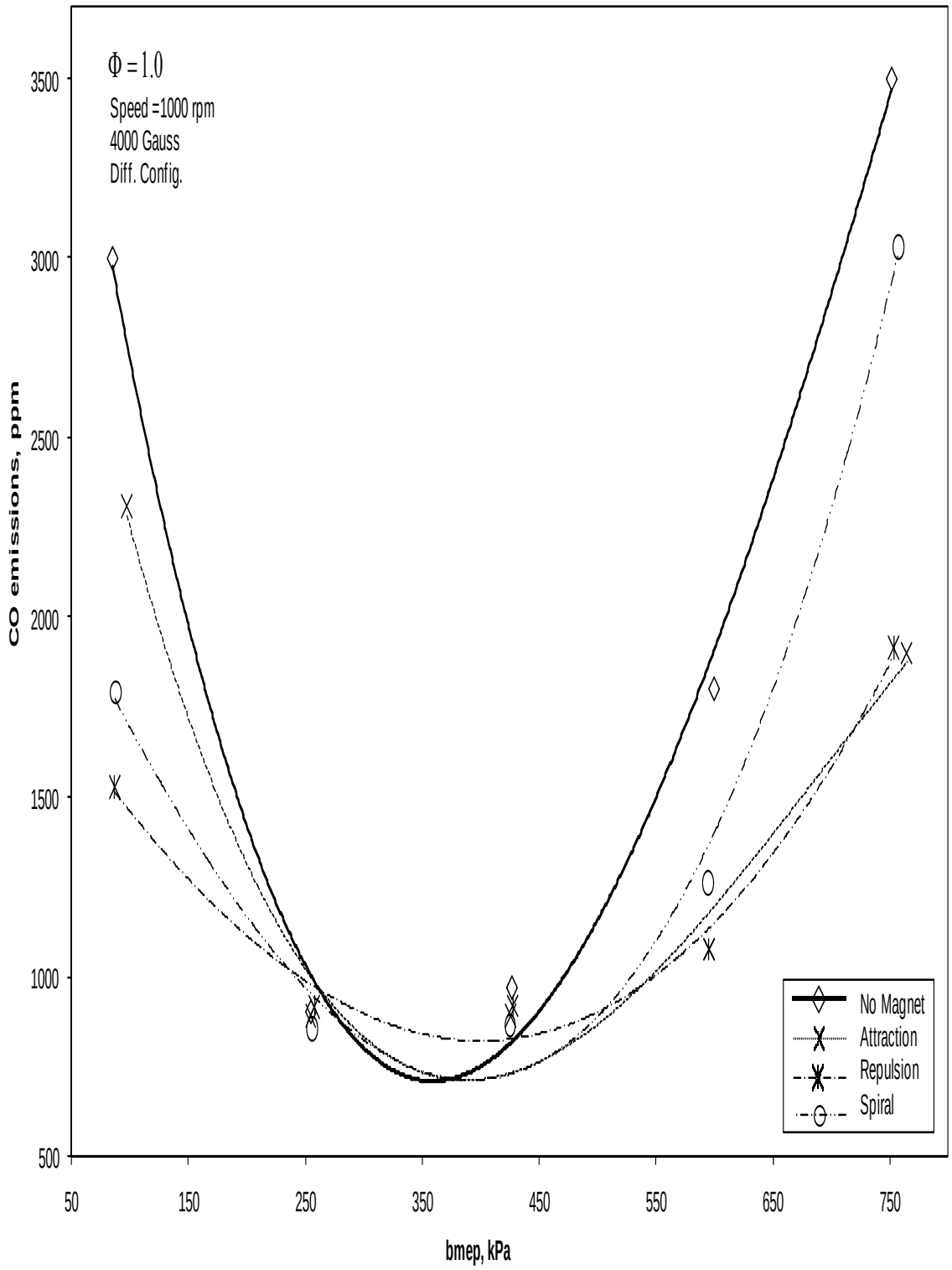

Figure 5-16: Magnetic configuration effect on CO at constant speed of 1000 rpm

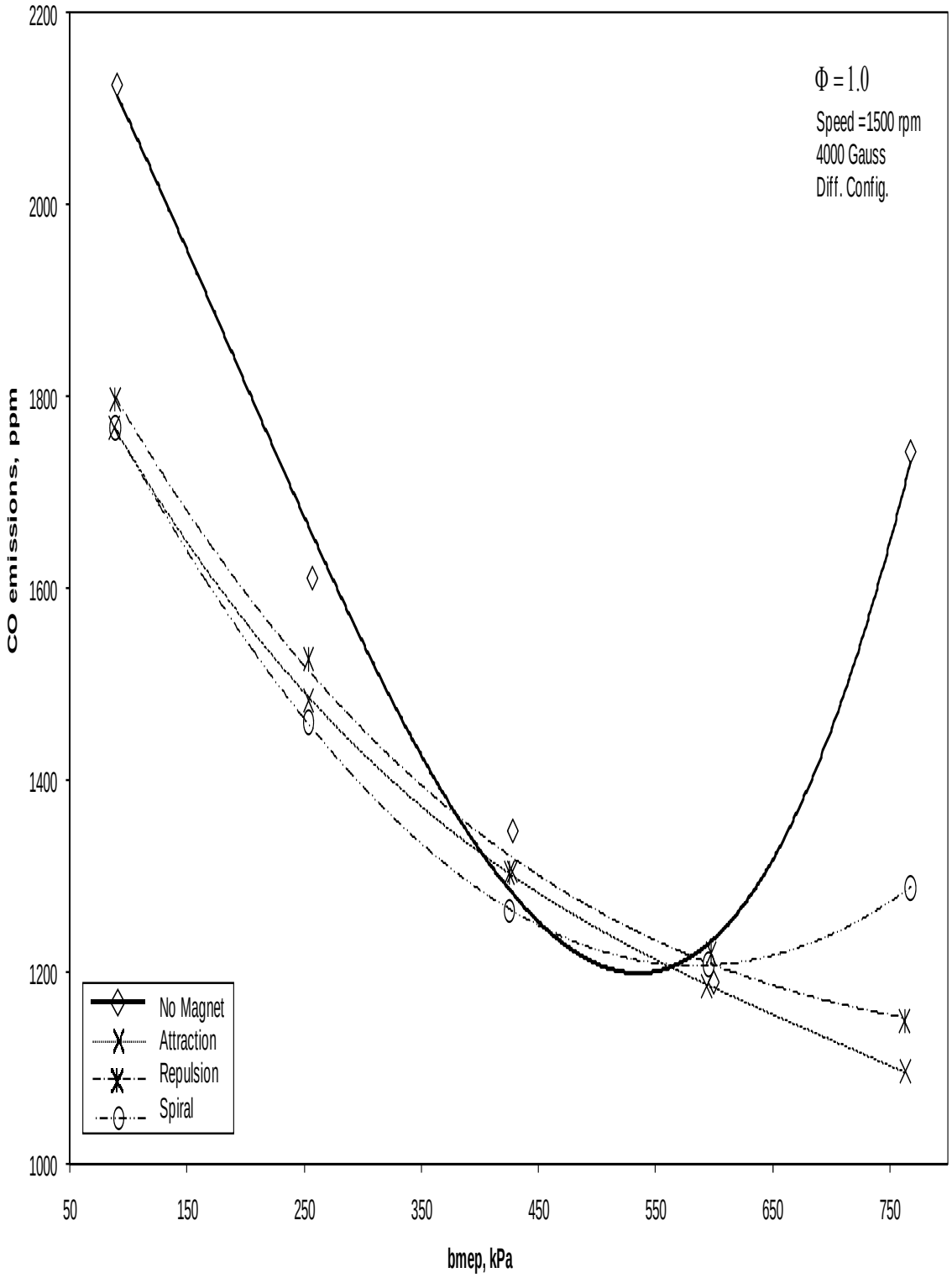

Figure 5-17: Magnetic configuration effect on CO at constant speed of 1500 rpm

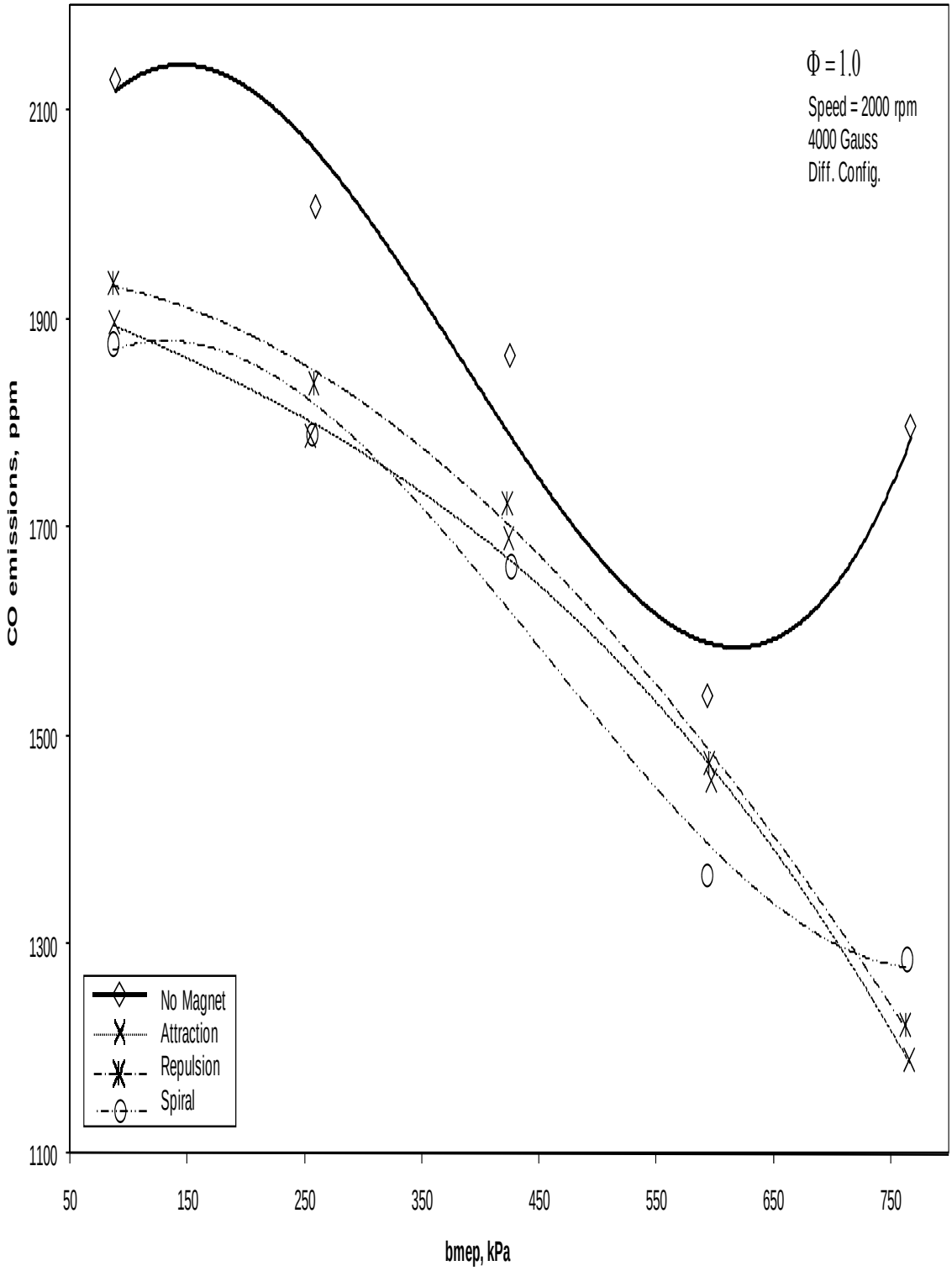

Figure 5-18: Magnetic configuration effect on CO at constant speed of 2000 rpm

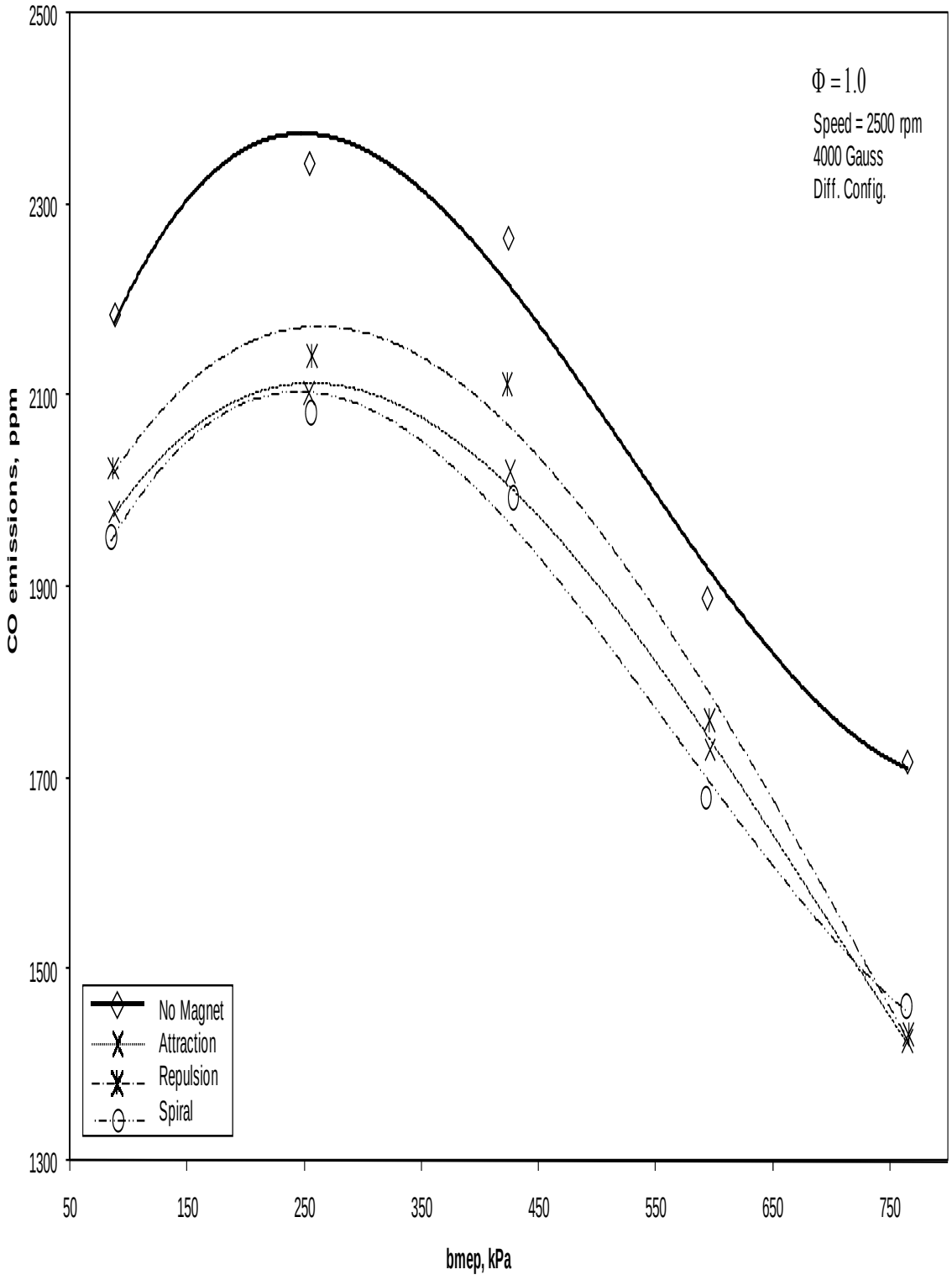

Figure 5-19: Magnetic configuration effect on CO at constant speed of 2500 rpm

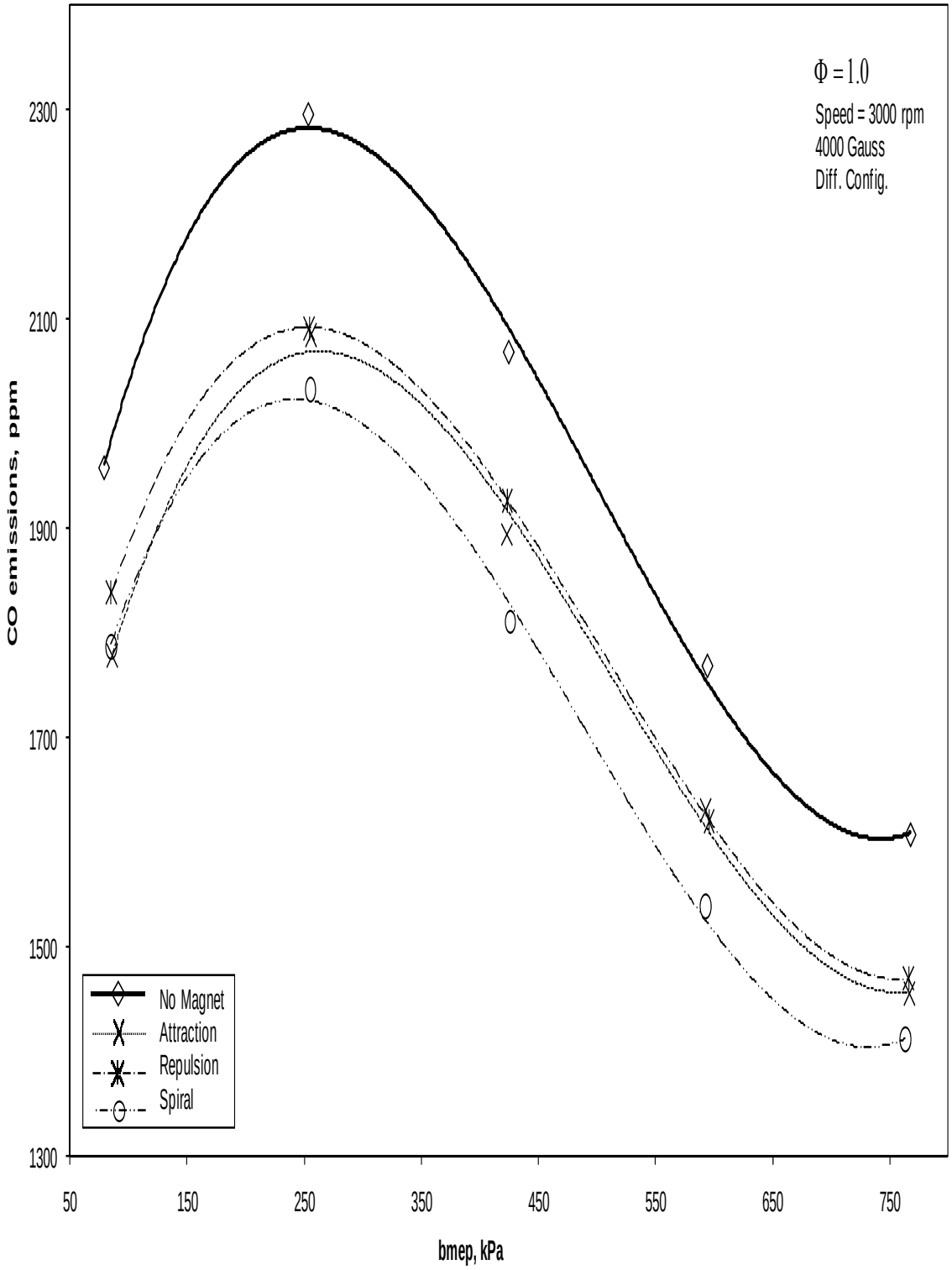

Figure 5-20: Magnetic configuration effect on CO at constant speed of 3000 rpm

CHAPTER 6

6 NITROGEN OXIDES EMISSIONS (NOx)

6.1 Magnetic Field Strength Effect

6.1.1 Constant Load Simulation

The variation of NOx emissions in ppm against varying speeds at a constant load of 20 Nm and different aligned magnetic field strength in 'Attraction' configuration is shown in Figure 6-1. Before the magnetic field is applied, the NOx emissions increase almost linearly to a maximum of 600 ppm with increasing engine speed up to 2500 rpm, before they start to decrease again. Application of the magnetic field shows little unfavourable deviation from the base curve for field strength of 800 Gauss, especially for engine speeds higher than 2000 rpm. An increase to 1600 Gauss, however, starts to show a marked decrease of 15% in the emissions level at higher engine speeds. A further increase to 2400 Gauss now shows a clear decrease by 35% in the emissions level at the lowest engine speed. Stronger field strength of 3200 Gauss shows a slight decrease from the previous magnetic strength. However, as the field strength is increased to 4000 Gauss, the emissions once again rise and show no significant change from the base curve at virtually all engine speeds. This shows that the intermediate values of the field strengths improve the performance of NOx emissions at almost all engine speeds. Moreover, it is to be noted that almost all the curves exhibit the same qualitative behaviour.

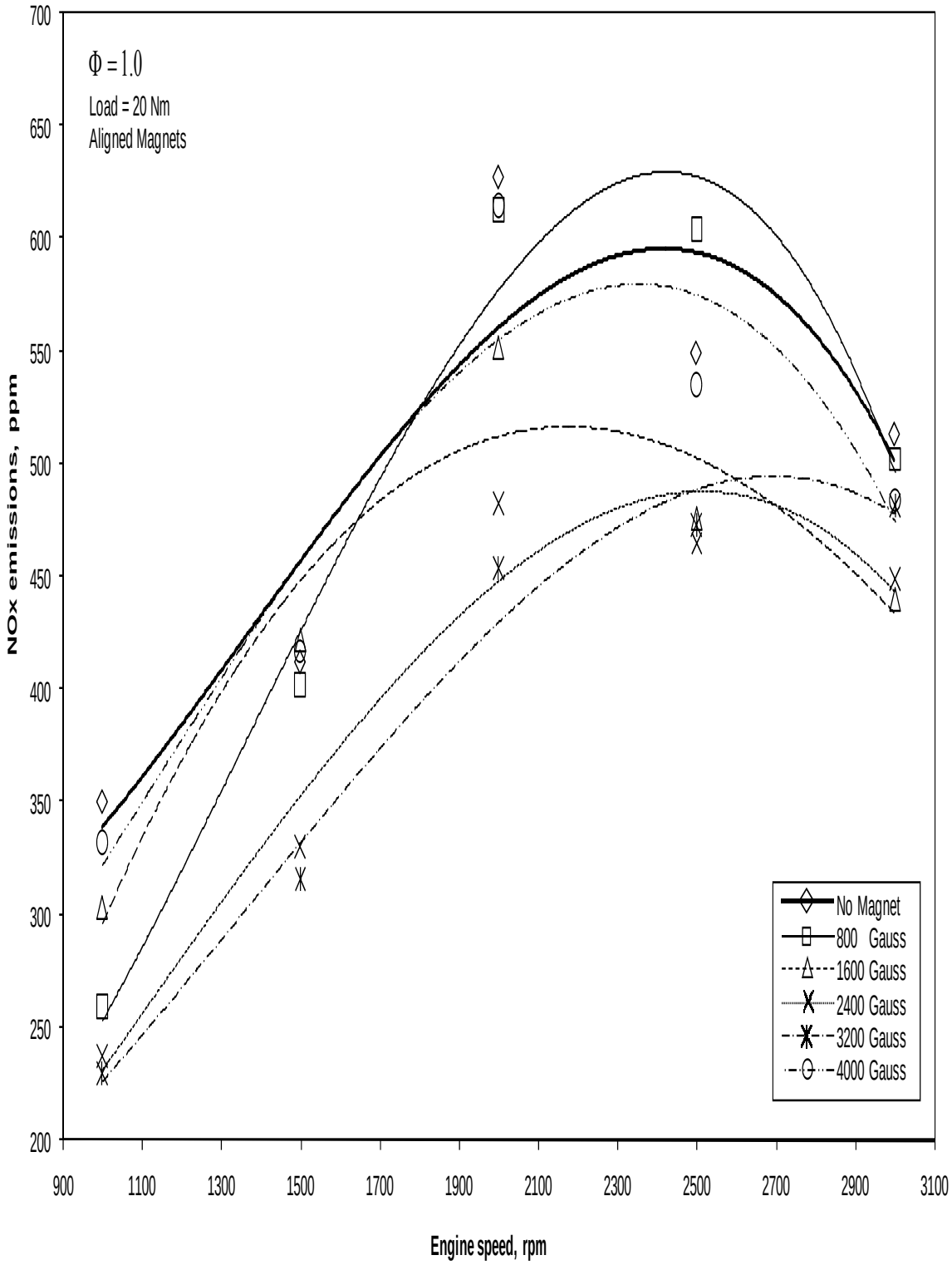

Figure 6-1: Magnetic strength effect on NOx at constant load of 20 Nm

With a load increase to 60 Nm, a marked change in the qualitative behaviour of the curves is observed, as portrayed in Figure 6-2. The NOx emissions practically stabilize around a constant value of 950 ppm after 1500 rpm, before which the emissions decay rapidly from 1450 ppm at 1000 rpm. Application of the magnetic field of 800 Gauss shows a slight detriment in the NOx emission performance after 1500 rpm. An increase to 1600 Gauss shows an appreciable decrease of 10% in the emissions level at higher engine speeds. Further increase to 2400 and 3200 Gauss field strengths show a clear decrease in the emissions level by 20% at almost all engine speeds. This is the same result as observed in the previous load setting. At field strength of 4000 Gauss, deterioration is observed at almost all engine speeds compared to the previous field strength settings, but the decrease in the emissions level from the bases values is still appreciable. All the curves exhibit more or less the same trend across the entire engine speed interval. Moreover, it is to be noticed that the overall NOx emissions increase considerably at all engine speeds compared to the previous load setting.

At a load of 100 Nm, the qualitative behaviour of the base curve tends to be decreasing more linearly as represented in Figure 6-3. Here, the NOx emissions decrease steeply from 2500 ppm with increasing engine load, reaching a minimum of 1500 ppm. Again, it can be seen that there is a considerable increase in the emissions level at all engine speeds compared to the previous load setting. Application of the magnetic field shows no appreciable deviation from the base curve, except a decrease by 15% at the lowest engine speed for the intermediate magnetic field strengths of 2400 and 3200 Gauss. This shows that increasing the load nullifies to some extent the effect of the magnetic field.

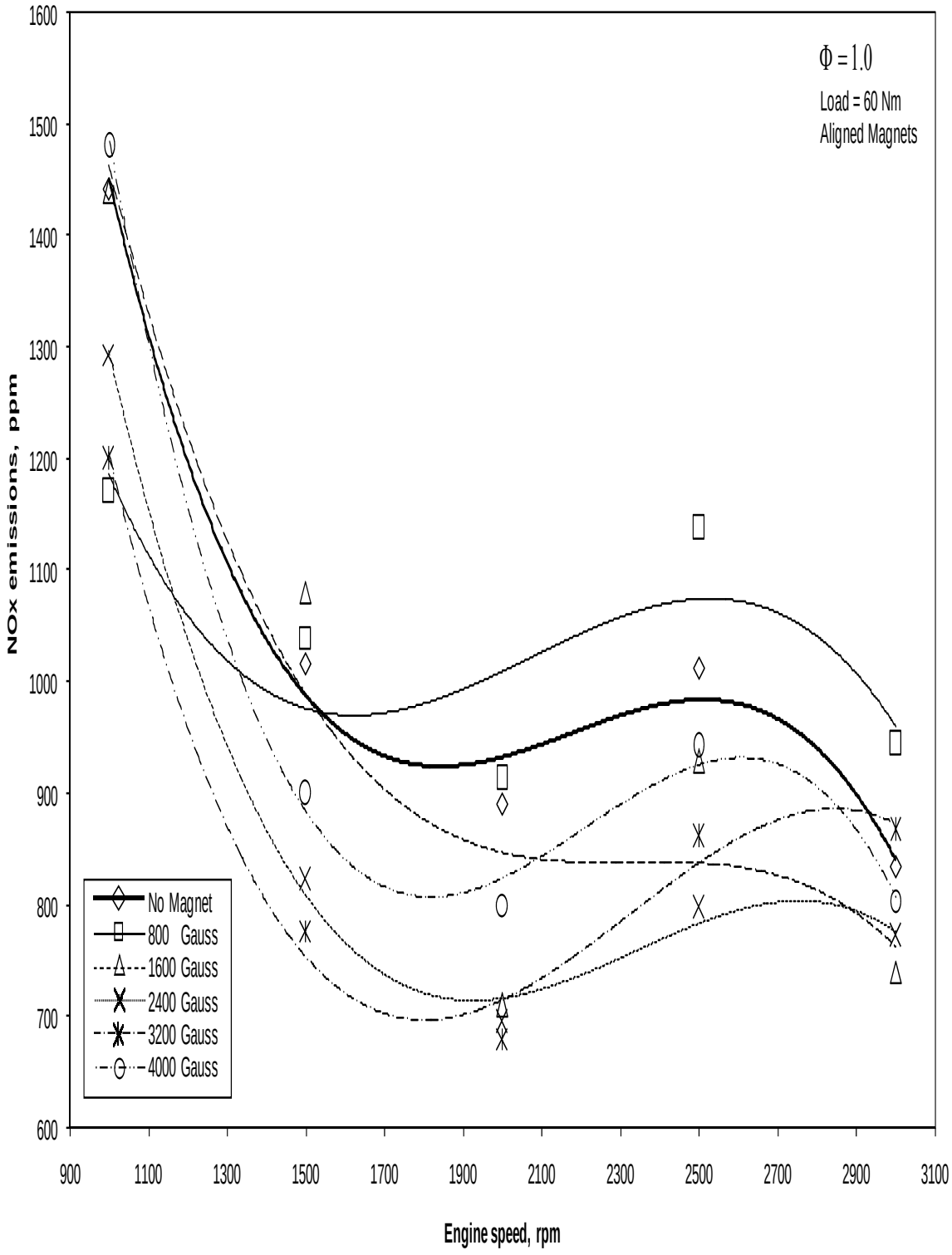

Figure 6-2: Magnetic strength effect on NOx at constant load of 60 Nm

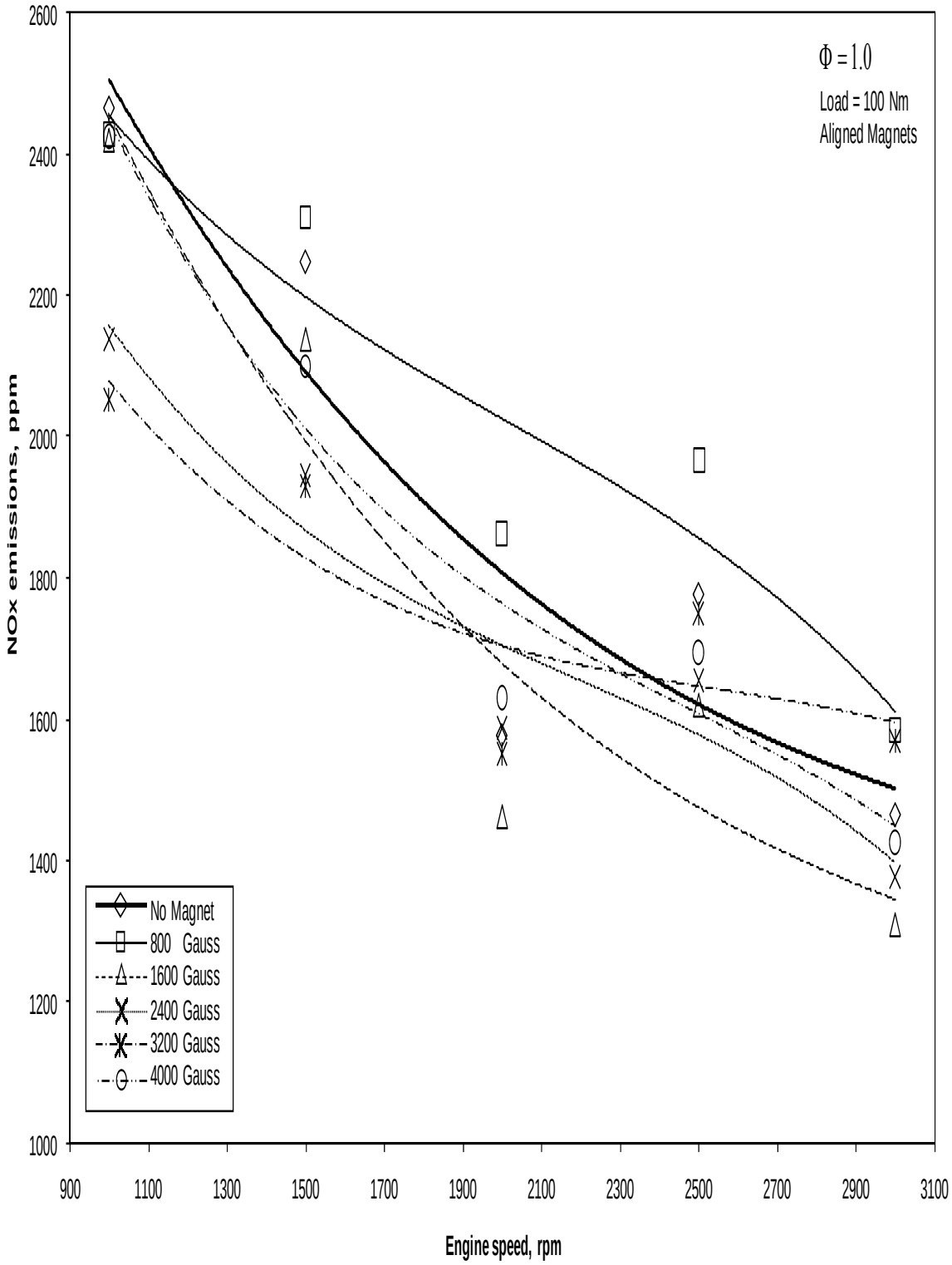

Figure 6-3: Magnetic strength effect on NOx at constant load of 100 Nm

Figure 6-4 shows the relationship between the same variables at a higher constant load of 140 where the behaviour of the curve changes again to remain decreasing monotonically as a function of engine speed. Application of the magnetic field initially increases the emissions level slightly at field strength of 800 Gauss. On the other hand, a slight decrease by 6% in the emissions level is observed for a field strength 1600 Gauss at higher engine speeds, which is analogous to the behaviour in the early load settings. In contrast, field strengths of 2400 and 3200 Gauss show an appreciable decrease of 12% at lower engine speeds similar to previous load settings. Finally, the emissions level remains virtually unchanged when 4000 Gauss is applied at essentially all engine speeds.

The above observations also exhibit a strong effect of load on the effectiveness of the magnetic field. Figure 6-5 portrays a relationship between the same variables at a constant load of 180 Nm, where the qualitative behaviour and different magnetic field strengths mimic the previous figure to a certain extent. However, the 800 Gauss field strength shows little improvement over the base curve. The overall NOx emissions continue to increase with increasing loads.

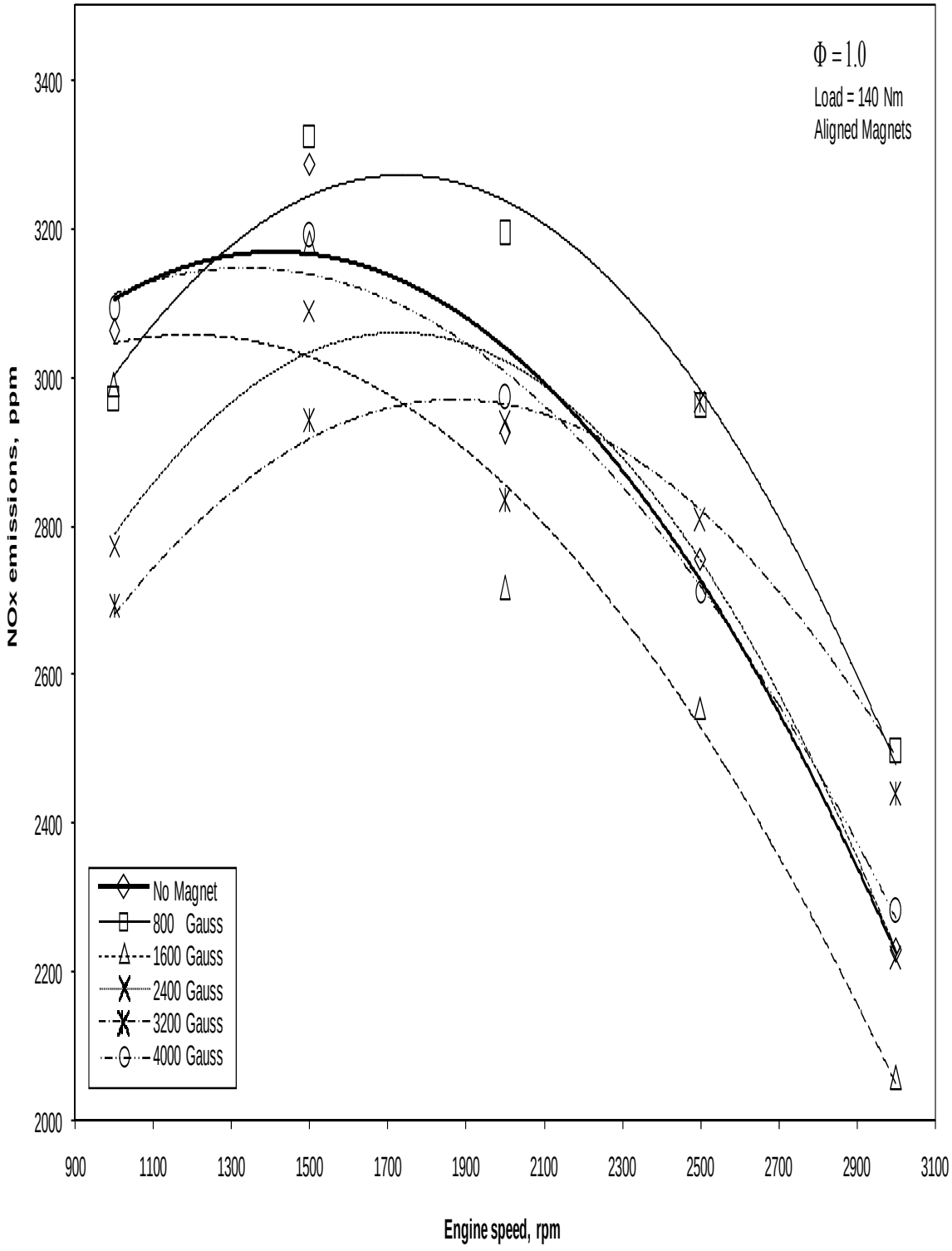

Figure 6-4: Magnetic strength effect on NOx at constant load of 140 Nm

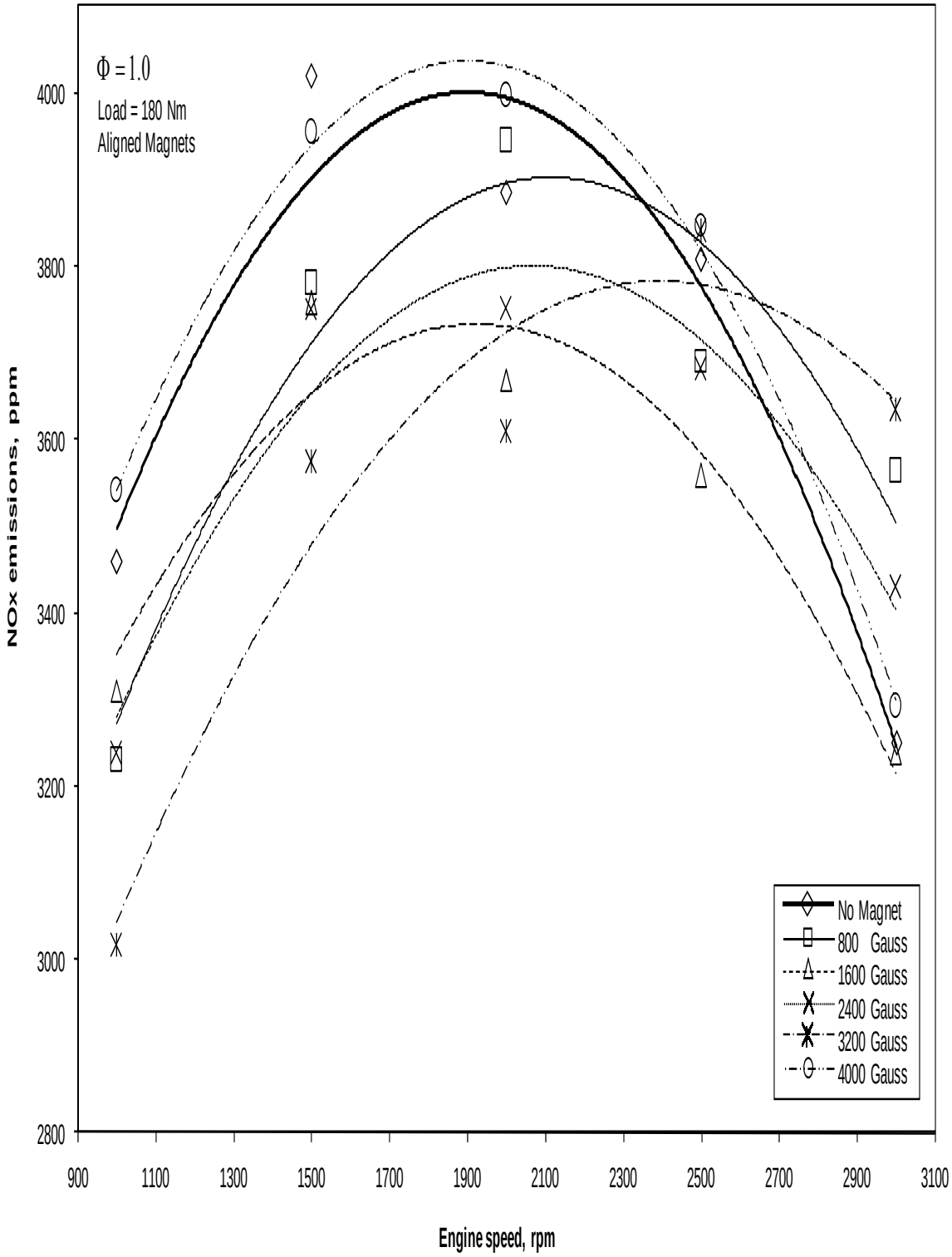

Figure 6-5: Magnetic strength effect on NOx at constant load of 180 Nm

6.1.2 Constant Speed Simulation

The variation of the NOx emissions against engine loads at a constant engine speed of 1000 rpm and different aligned magnetic field strengths in 'Attraction' configuration is shown in Figure 6-6. Generally, the NOx emissions conform to a crude linear relation with increasing engine loads. The rate of increase of NOx emissions is high at low engine loads, but then they decrease continuously. When the magnetic field is turned on, an appreciable reduction of 15% in the NOx emissions is observed only for magnetic field strengths of 2400 and 3200 Gauss, especially at higher engine loads.

As the engine speed is increased to 1500 rpm, as depicted in Figure 6-7, it is observed that the overall NOx emissions increase slightly at almost all engine loads to become more linear. Similarly, when the magnetic field is applied, a lower reduction of 10% is observed only for 2400 and 3200 Gauss values, especially for higher engine loads.

Further increase in the engine speed to 2000 rpm, as shown in Figure 6-8, shows no noticeable change in the maximum and minimum NOx values. However, the qualitative behaviour of the curve changes, and now it has a point of inflection at about 600 kPa of engine load. The application of the magnetic field reduces the NOx emissions by 10% at most engine loads.

Figure 6-9 and Figure 6-10 show the effect of a further increase in engine speed to 2500 and 3000 rpm respectively. It is observed that there is a slight decrease in the NOx production at a majority of engine loads with each rise in engine speed. In addition, the effect of a magnetic field is seen to be diminishing at 2500 and 3000 rpm as compared to an engine speed of 2000 rpm.

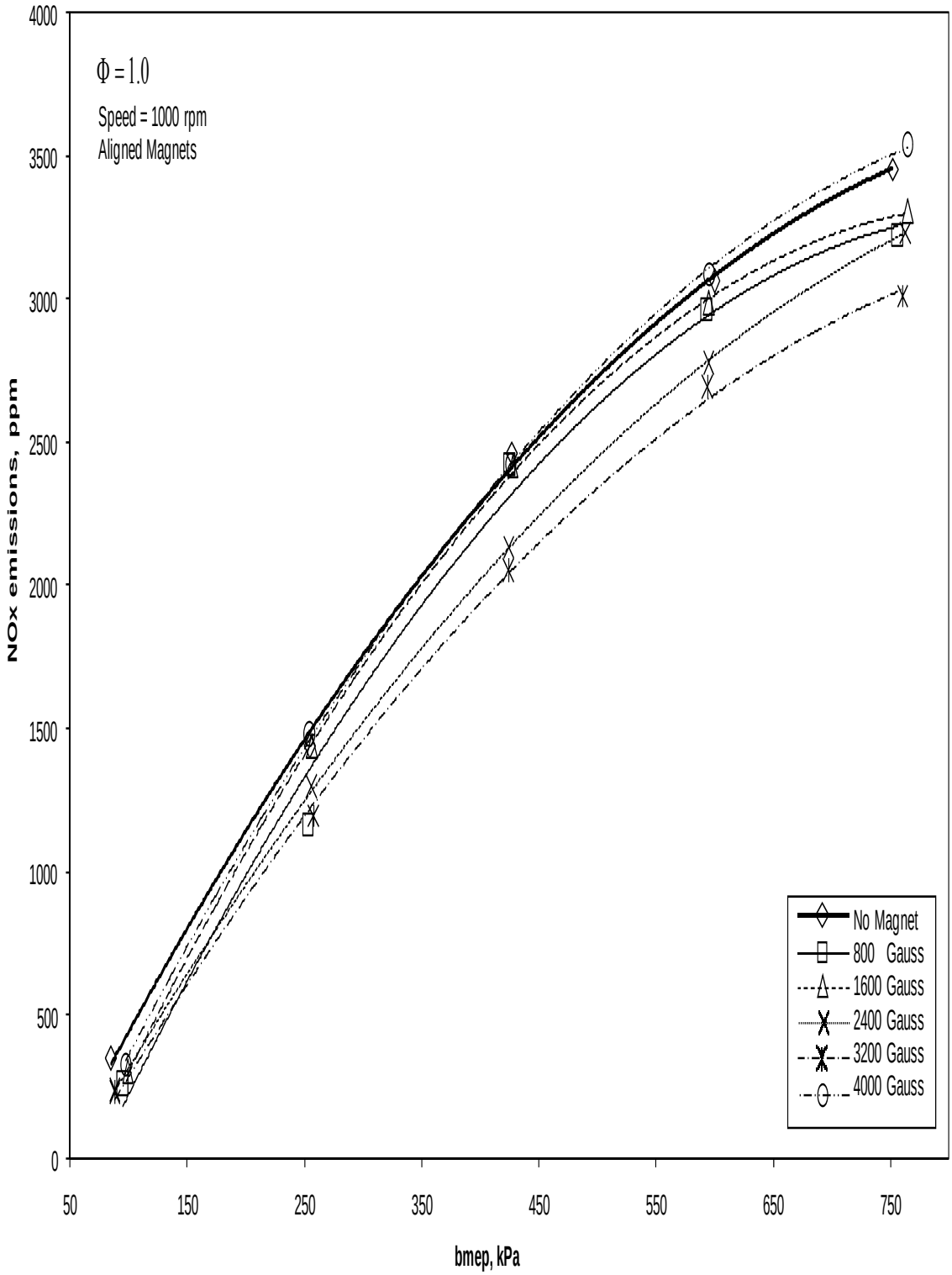

Figure 6-6: Magnetic strength effect on NOx at constant speed of 1000 rpm

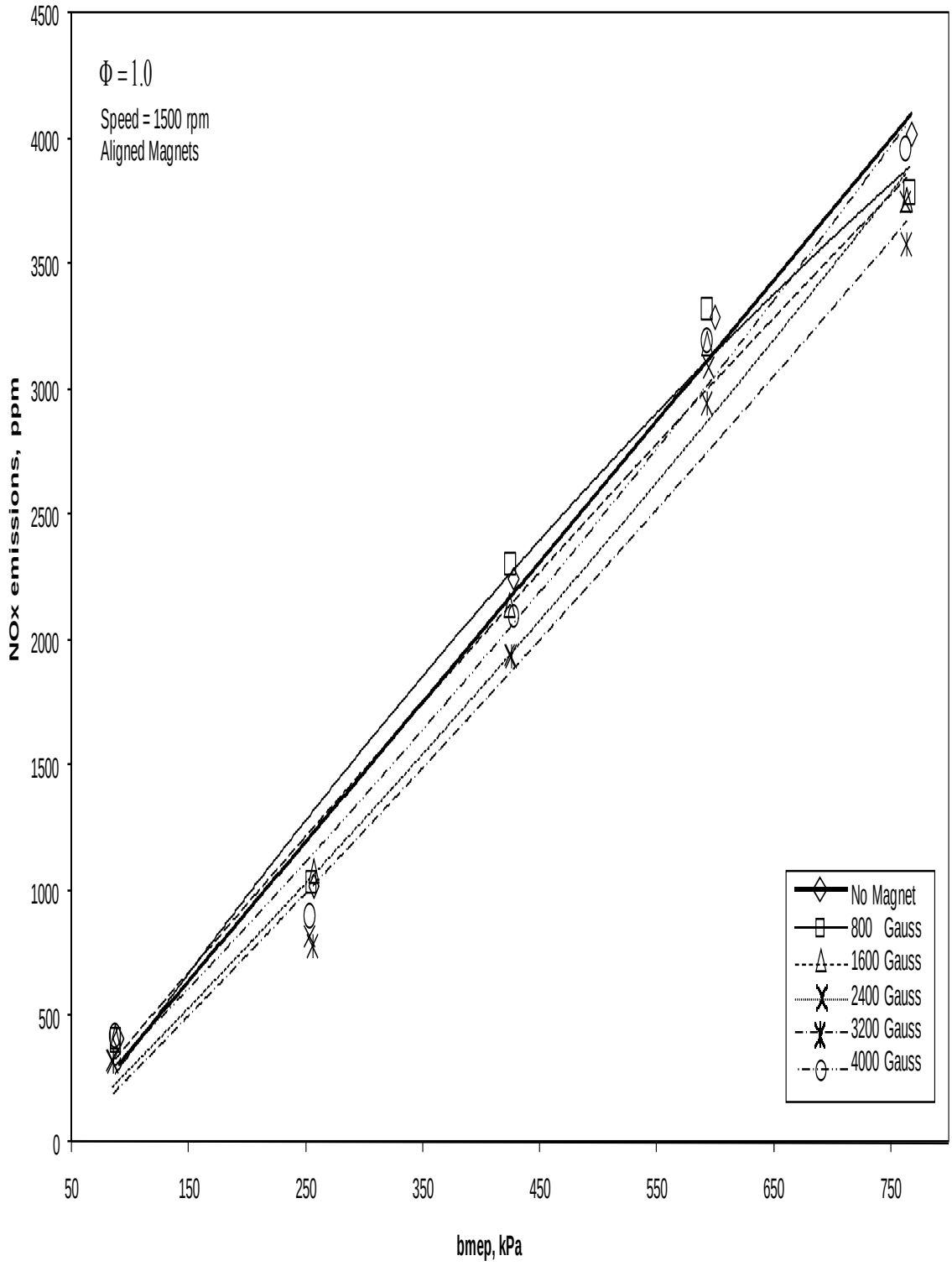

Figure 6-7: Magnetic strength effect on NOx at constant speed of 1500 rpm

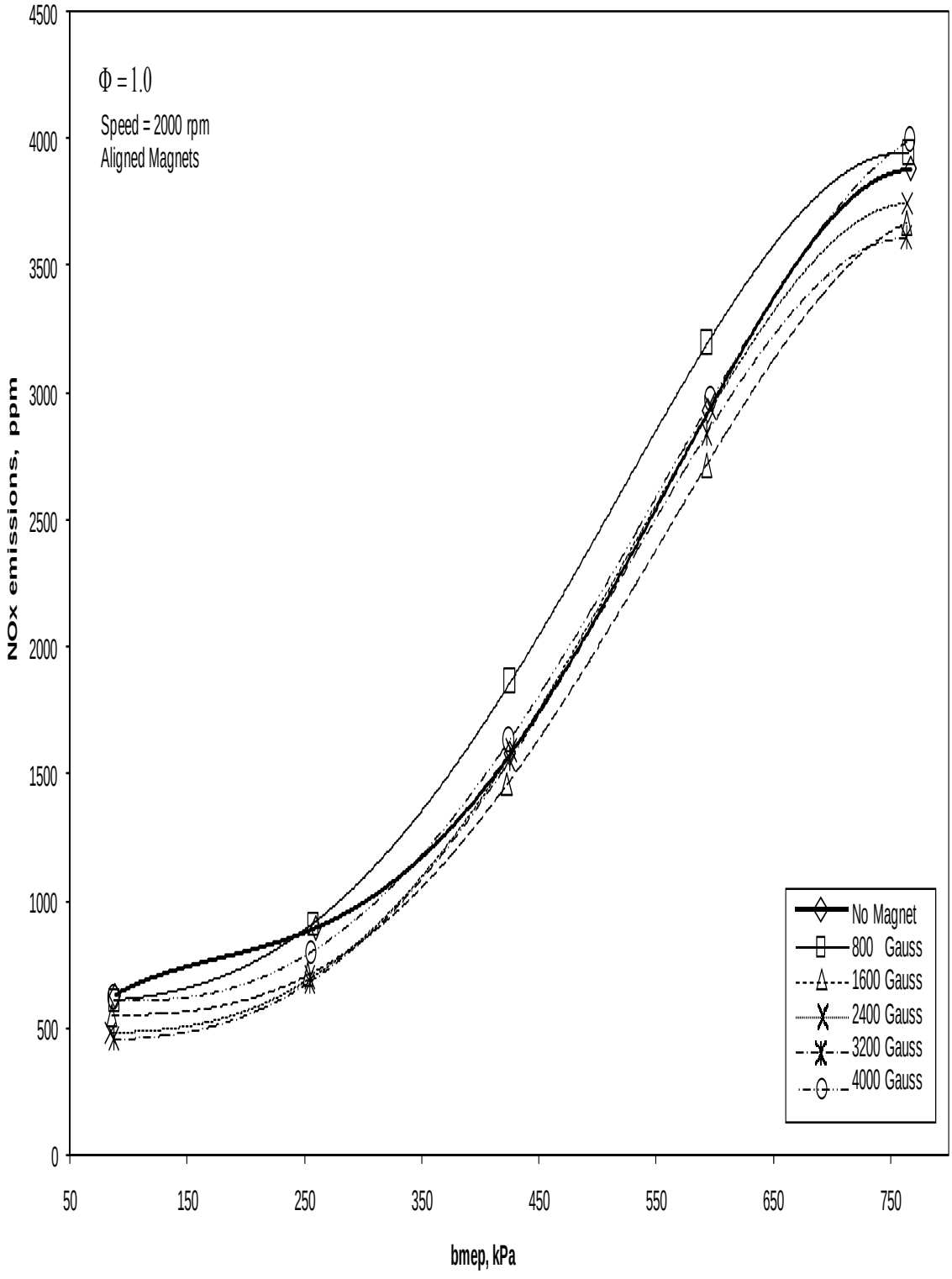

Figure 6-8: Magnetic strength effect on NOx at constant speed of 2000 rpm

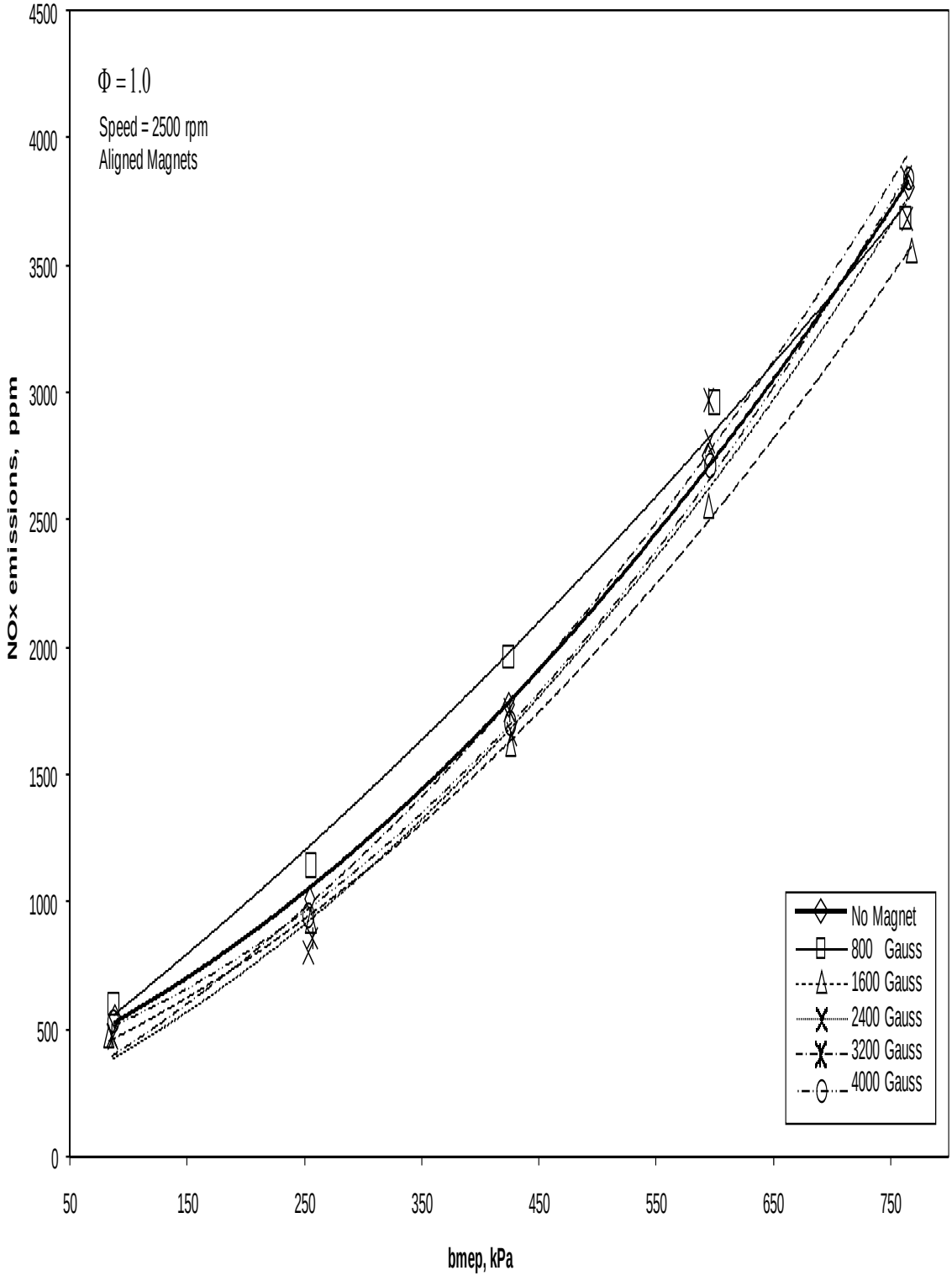

Figure 6-9: Magnetic strength effect on NOx at constant speed of 2500 rpm

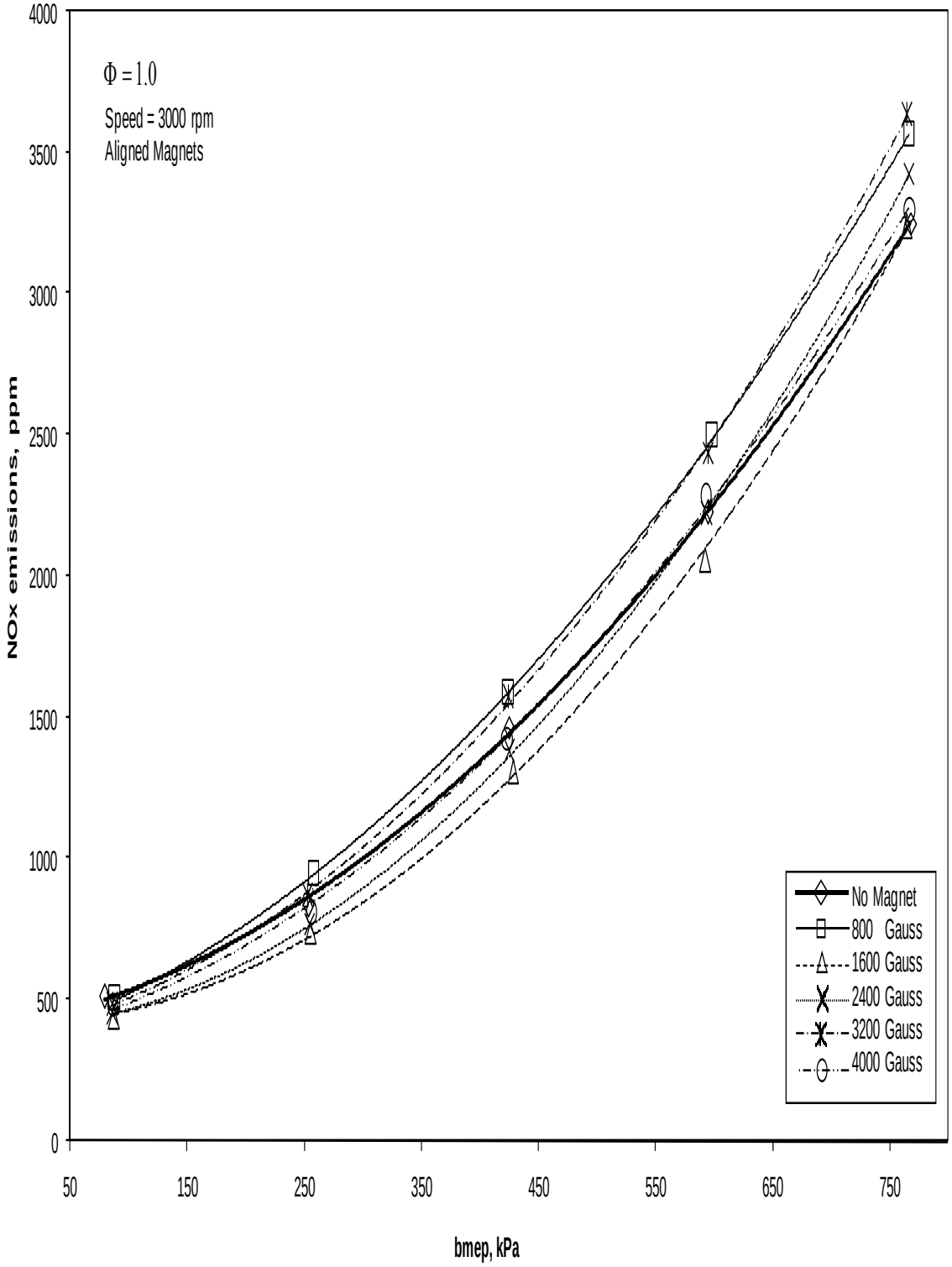

Figure 6-10: Magnetic strength effect on NOx at constant speed of 3000 rpm

6.2 Magnetic Field Configuration Effect

6.2.1 Constant Load Simulation

The variation of the NOx emissions in ppm against varying engine speeds at a constant load of 20 Nm and constant magnetic field strength of 4000 Gauss with three different magnetic field configurations is shown in Figure 6-11. With the magnetic field turned off, the NOx emissions increase with increasing engine speed to a maximum of 600 ppm at around 2500 rpm. With the introduction of the magnetic field, a reduction in the NOx emissions is observed at almost all engine speeds with the 'Spiral' configuration performing marginally better, while the 'Attraction' configuration produces no significant change as observed in lower magnetic field strengths. The maximum emission reduction of 35% with the 'Spiral' configuration occurs at the lowest engine speed of 1000 rpm.

Figure 6-12 shows the previous relationship at a higher constant load of 60 Nm. With zero magnetic field strength, the behaviour of the curve changes, where the NOx emissions decrease with increasing engine speed starting from the highest value of 1450 ppm to the lowest value of 800 ppm. For most parts, the emissions level settles down at around 950 ppm. The application of the magnetic field again demonstrates a decrease in the emissions at almost all engine loads. Less difference is now found in the different magnetic field configurations. However, the 'Spiral' configuration still gives the best performance with a reduction by 20% at the intermediate engine speeds. It is to be noted that in general the overall NOx emissions increase considerably at all engine speeds at this particular load.

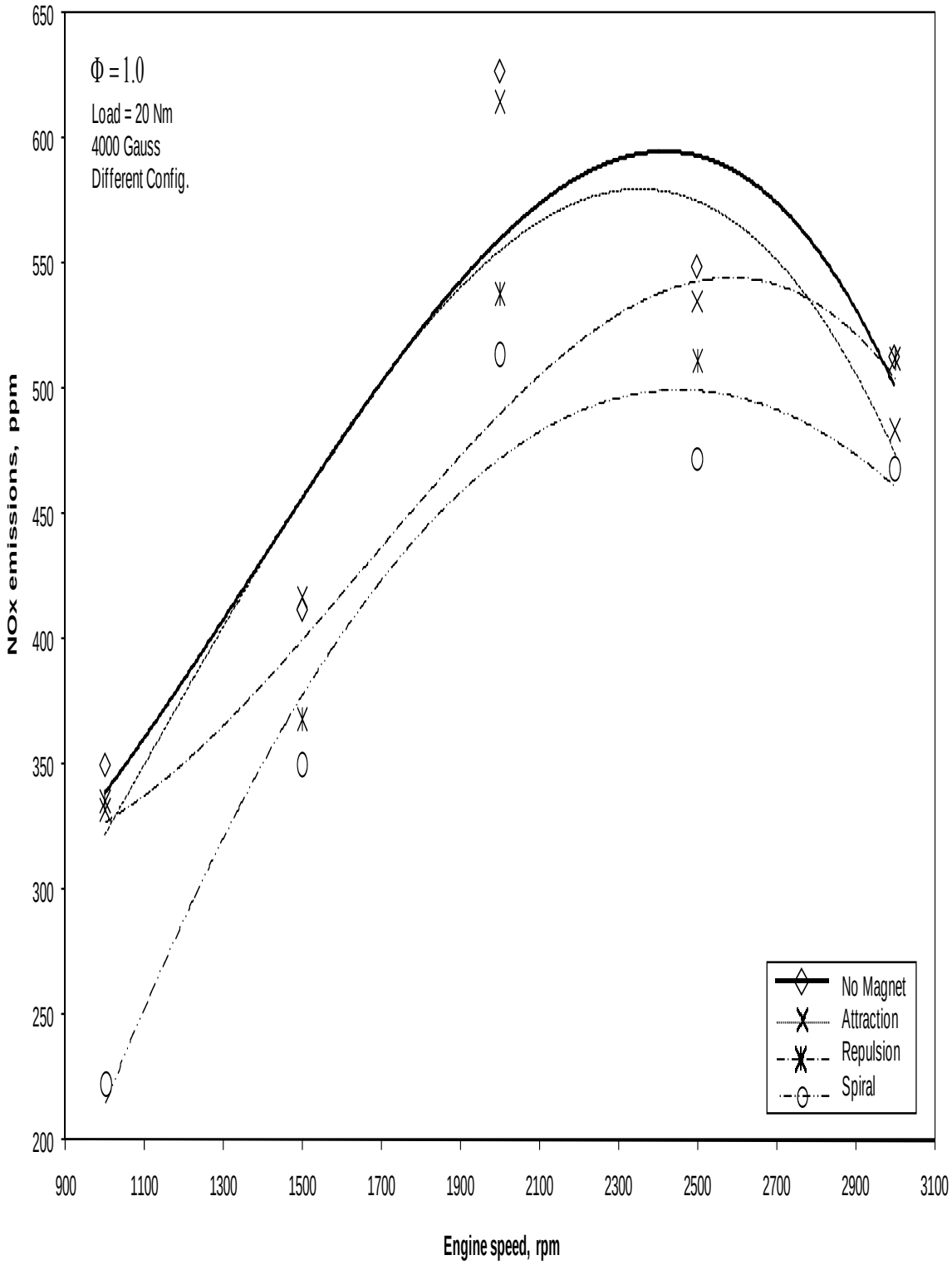

Figure 6-11: Magnetic configuration effect on NOx at constant load of 20 Nm

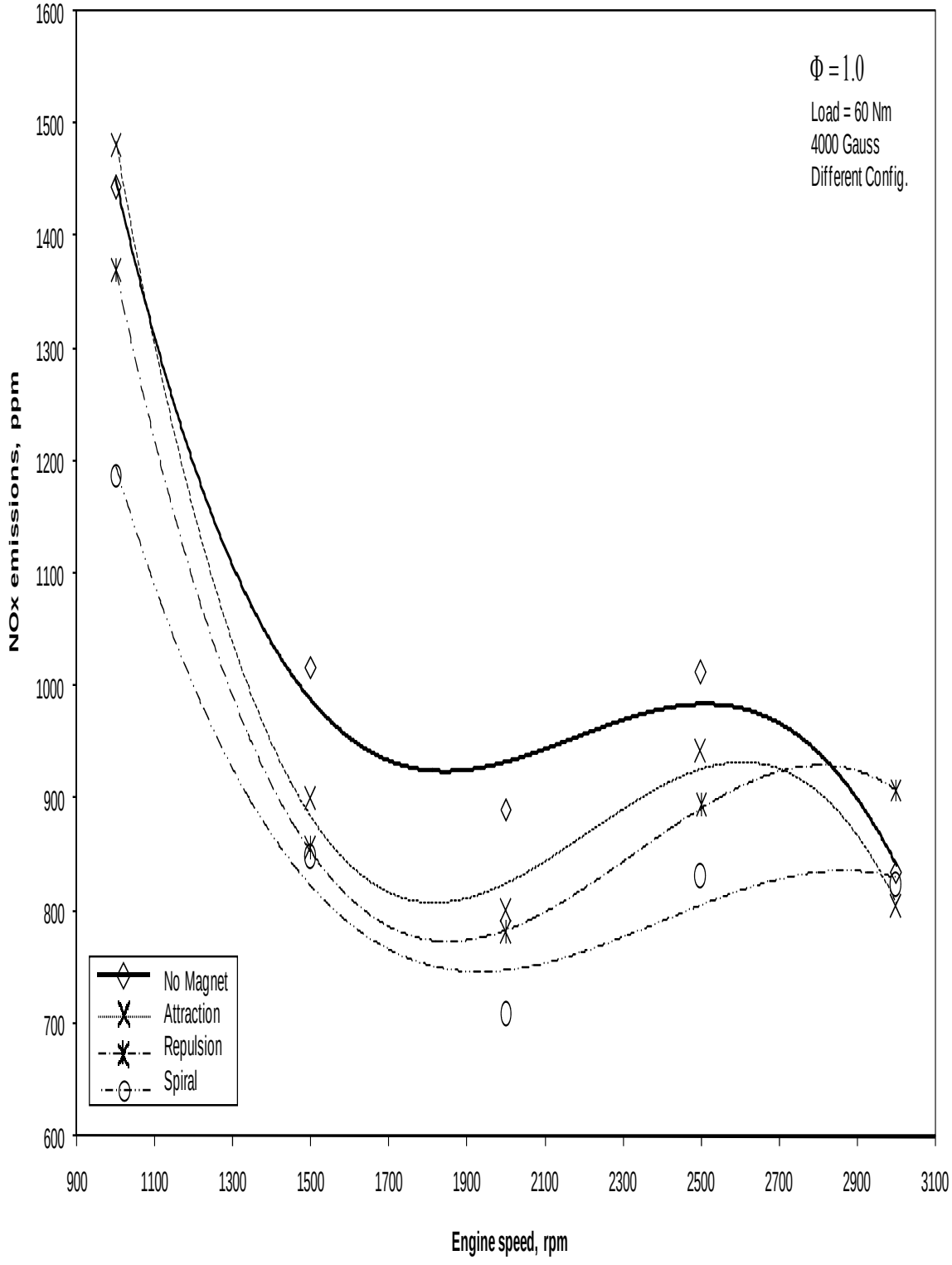

Figure 6-12: Magnetic configuration effect on NOx at constant load of 60 Nm

Figure 6-13 shows the relationship among the same variables at a load of 100 Nm. The trend is the reverse of that seen in Figure 6-11 where the emissions decrease with increasing speed from 2500 ppm to a minimum of 1500 ppm. Overall, the emissions again increase considerably as compared to those at the previous load value. Application of the magnetic field now shows no overall appreciable decrease in the emissions for any magnetic configuration at most engine speeds. On the other hand, the 'Spiral' configuration continues to give the best performance at the lowest engine speed of 1000 rpm with a reduction in emissions by 15%.

Effects of further increase in the load value to 140 Nm are depicted in Figure 6-14. The NOx emissions decrease monotonically with increasing engine speeds starting from the highest value of around 3100 ppm, which is an overall sharp increase in the emissions level compared to the previous load. Application of the magnetic field has little or no effect on the emissions at most engine speeds with any magnetic field configuration. On the other hand, the 'Spiral' configuration continues to give the best performance at the lowest engine speed of 1000 rpm with a reduction in emissions by 10%.

Reaching the maximum tested load of 180 Nm again a sharp increase in the overall emissions level is observed at all engine speeds, as shown in Figure 6-15. Now, the trend is analogous to a conic section with a maximum value of 4000 ppm at around 1800 rpm. The introduction of the magnetic field is seen to affect the emissions level to some extent for the 'Spiral' configuration only at engine speeds lower than 2500 rpm. The maximum emission reduction reaches 8% at the lowest engine speed of 1000 rpm.

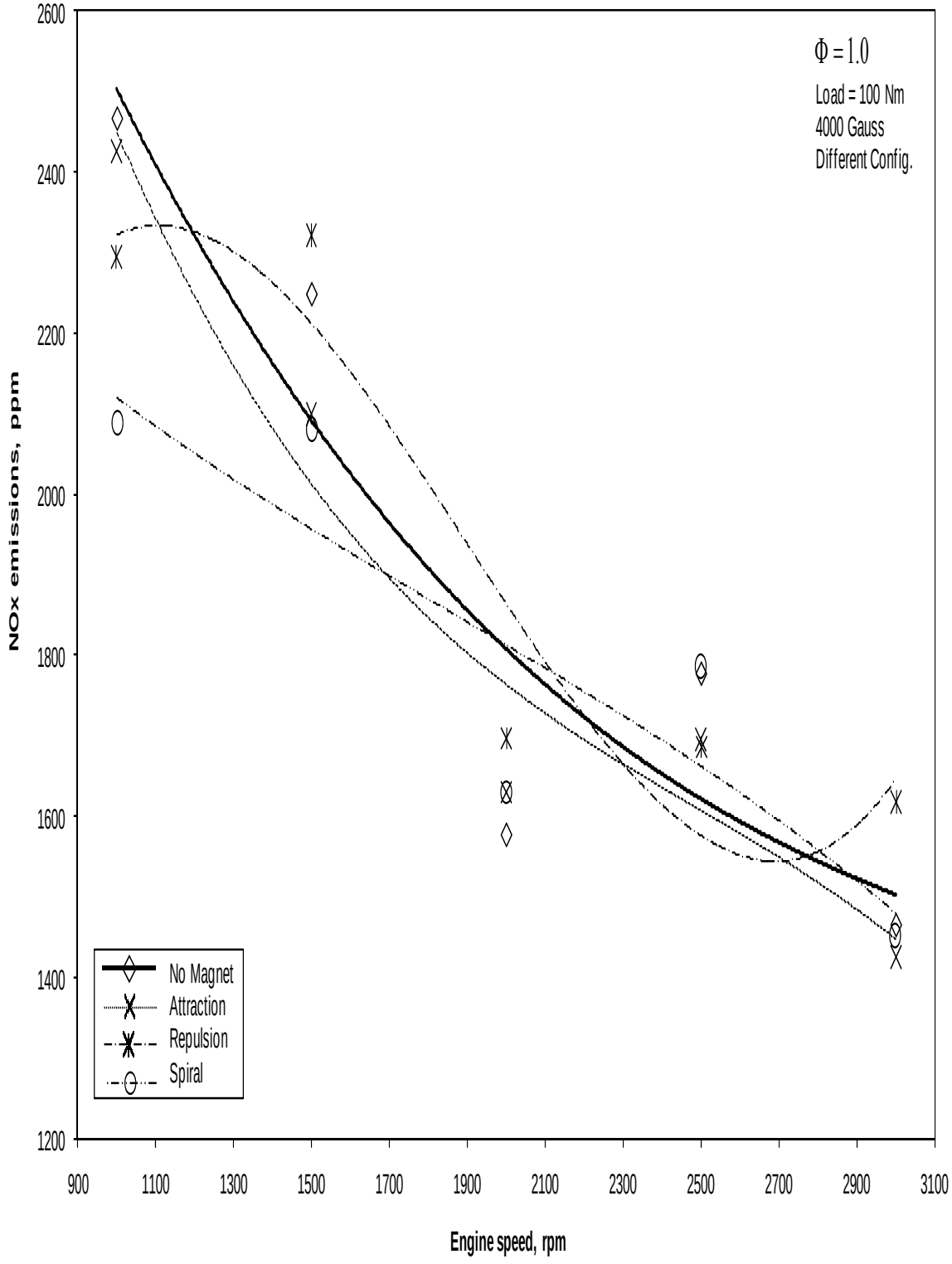

Figure 6-13: Magnetic configuration effect on NOx at constant load of 100 Nm

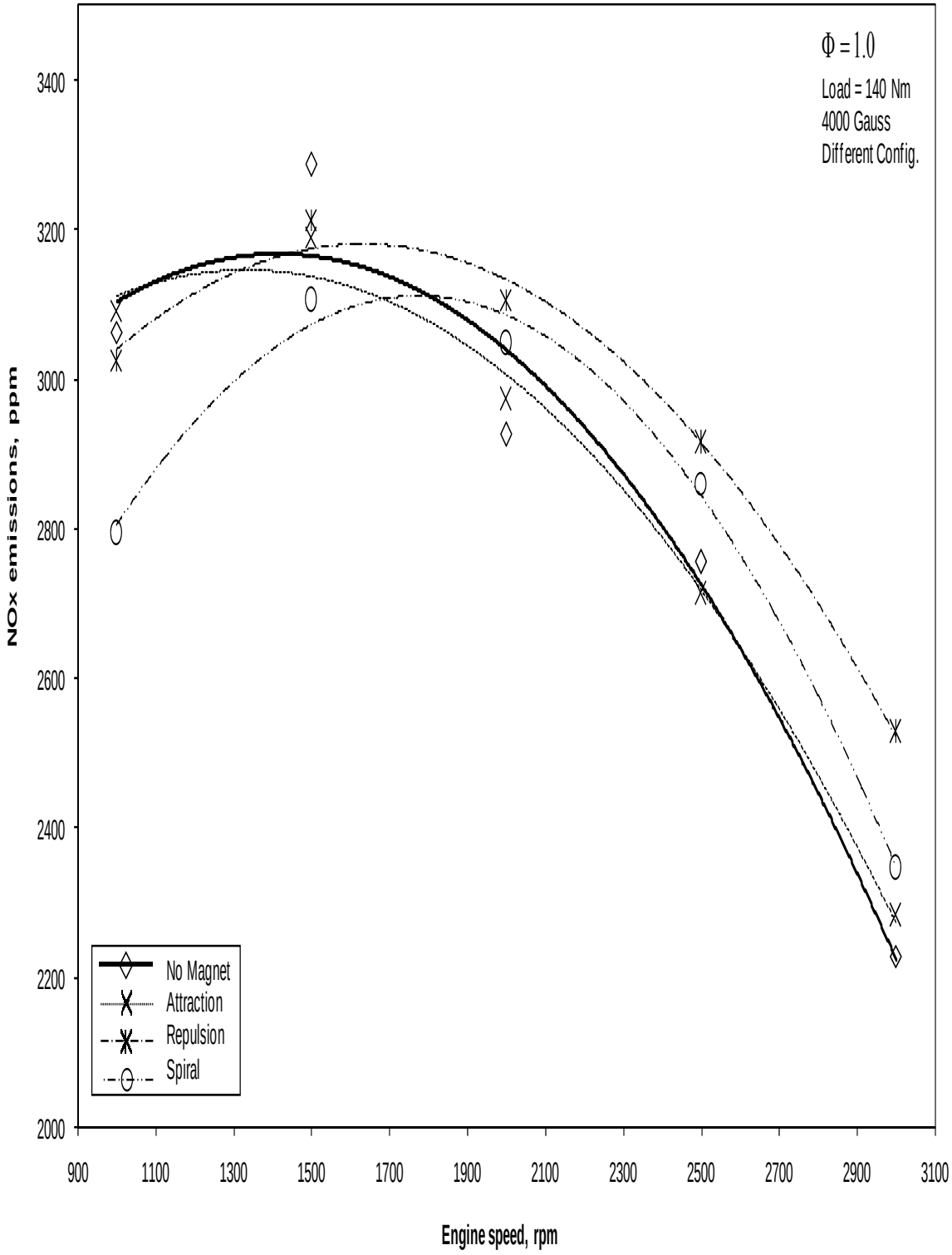

Figure 6-14: Magnetic configuration effect on NOx at constant load of 140 Nm

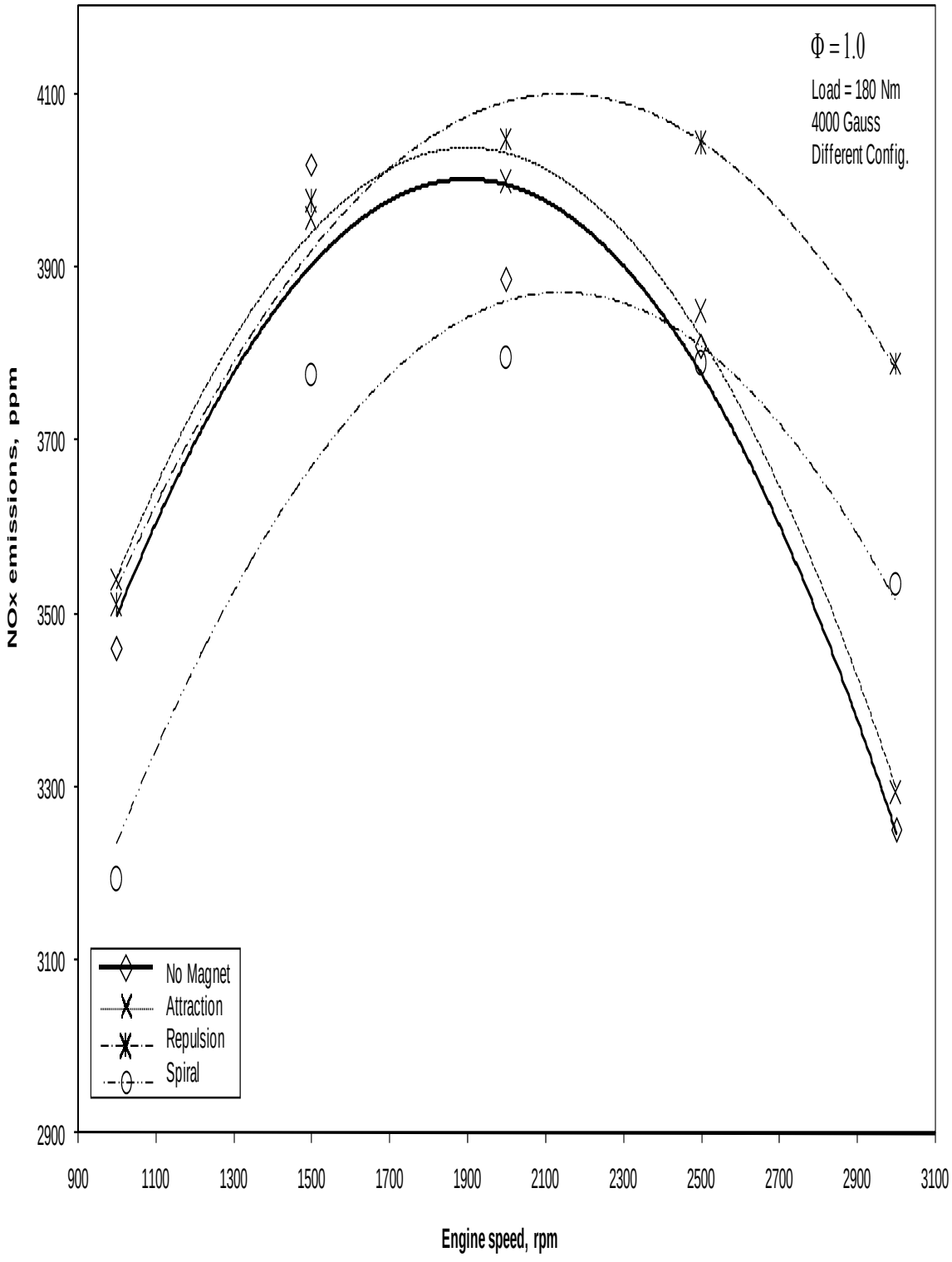

Figure 6-15: Magnetic configuration effect on NOx at constant load of 180 Nm

6.2.2 Constant Speed Simulation

The variation of the NOx emissions against different engine loads at a constant speed of 1000 rpm and constant magnetic field strength of 4000 Gauss with three different magnetic field configurations is shown in Figure 6-16. With no magnetic field effect, the NOx emission increases steadily with increasing engine loads, where the curve crudely follows a straight line. When the magnetic field is turned on, a slight effect is observed on the NOx emissions, except the 'Spiral' magnetic configuration, which has a better effect at all engine loads with an average reduction by 10% at most engine loads.

Figure 6-17 shows the variation in the same variables but at an increased engine speed of 1500 rpm. The NOx emissions are observed to follow a linear variation with increasing engine load. However, the overall NOx emissions increase slightly at all engine loads. In this case, the effect of the magnetic field is even less pronounced, with the 'Spiral' configuration acting slightly better at most engine loads.

Figure 6-18, Figure 6-19, and Figure 6-20 show the NOx emissions against engine load at 2000, 2500, and 3000 rpm respectively. The curves still follow a crudely near-linear behaviour similar to Figure 6-16. In addition, the magnetic field application in all its configurations again fails to produce a substantially different effect.

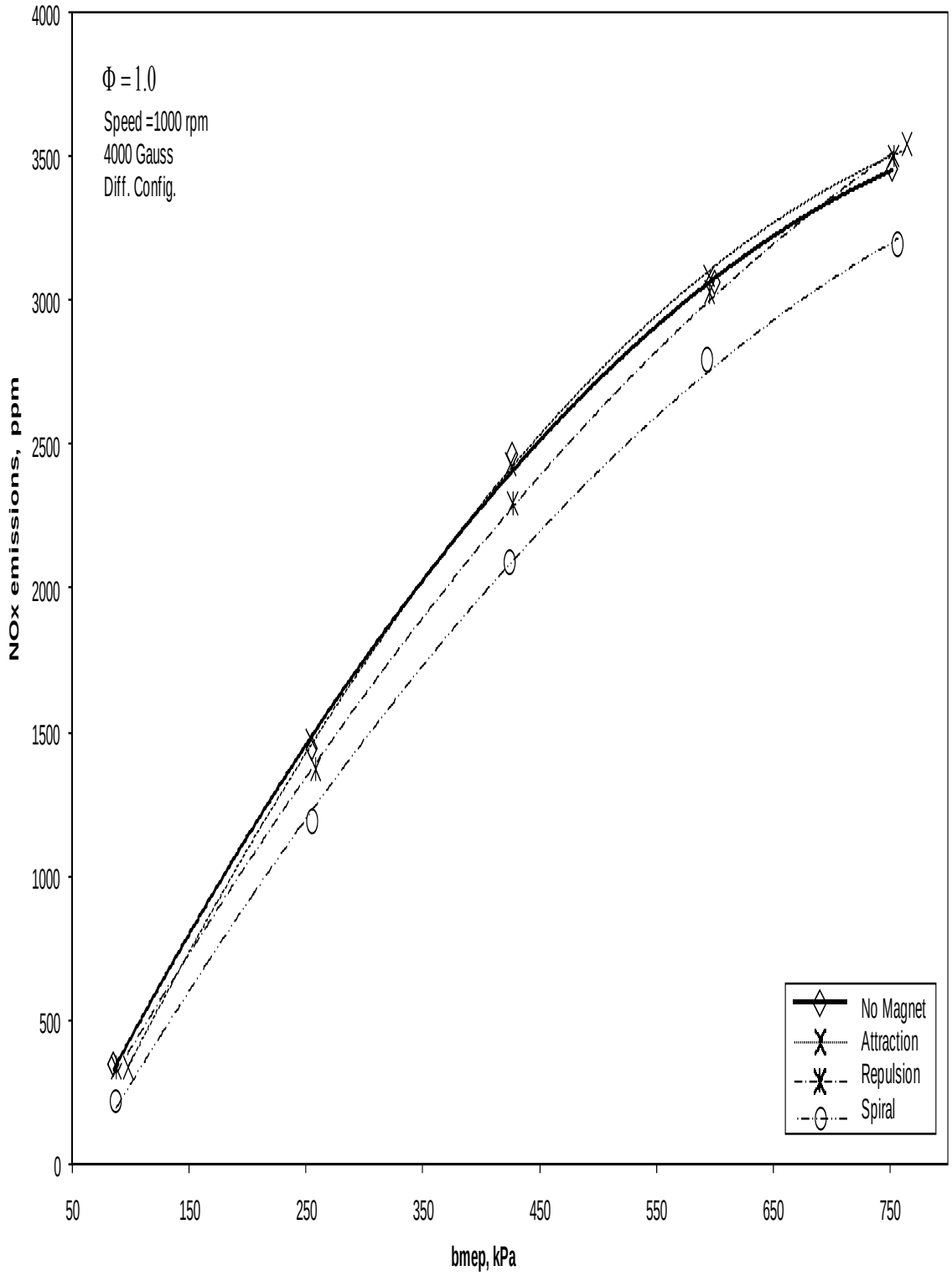

Figure 6-16: Magnetic configuration effect on NOx at constant speed of 1000 rpm

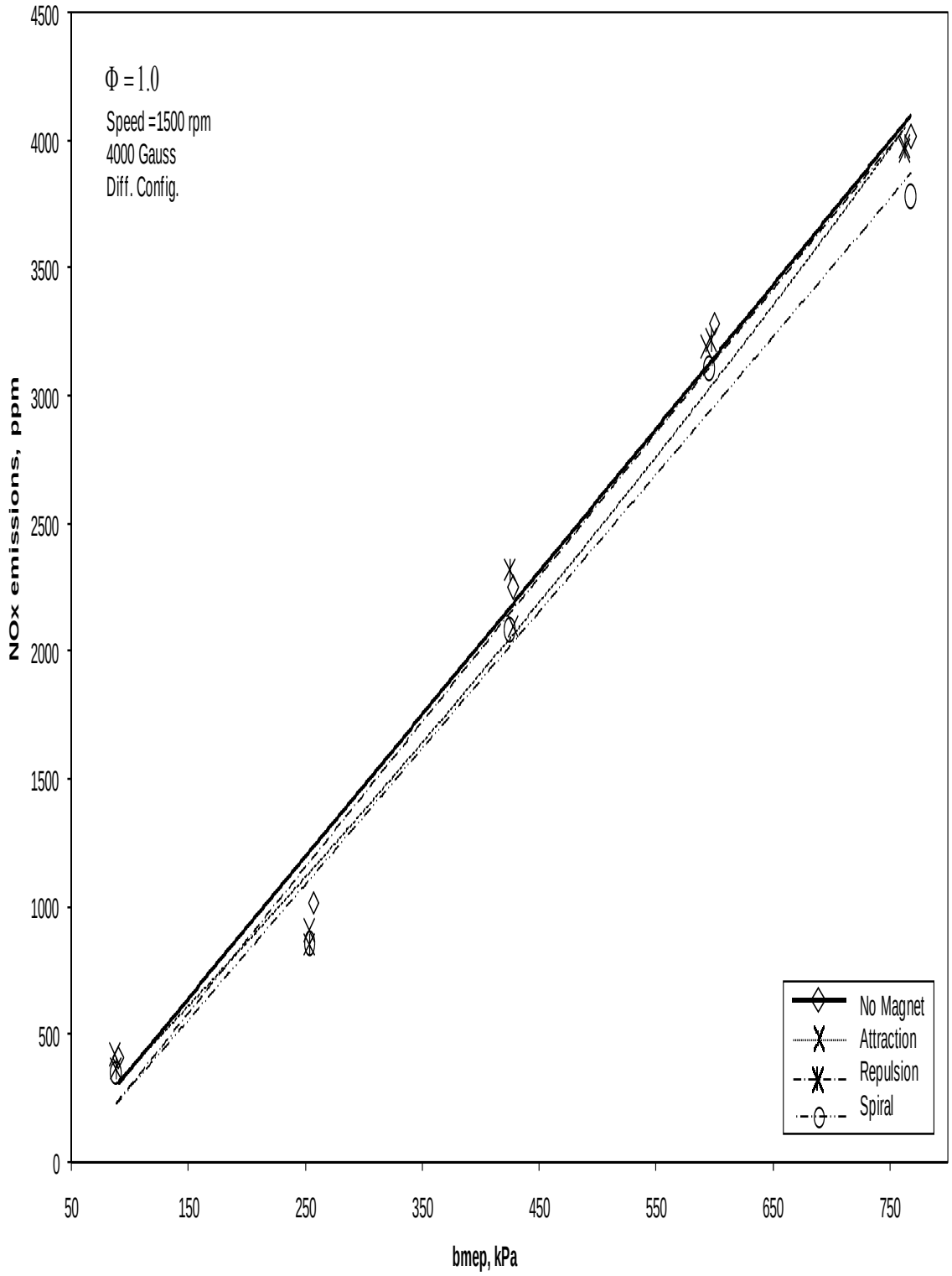

Figure 6-17: Magnetic configuration effect on NOx at constant speed of 1500 rpm

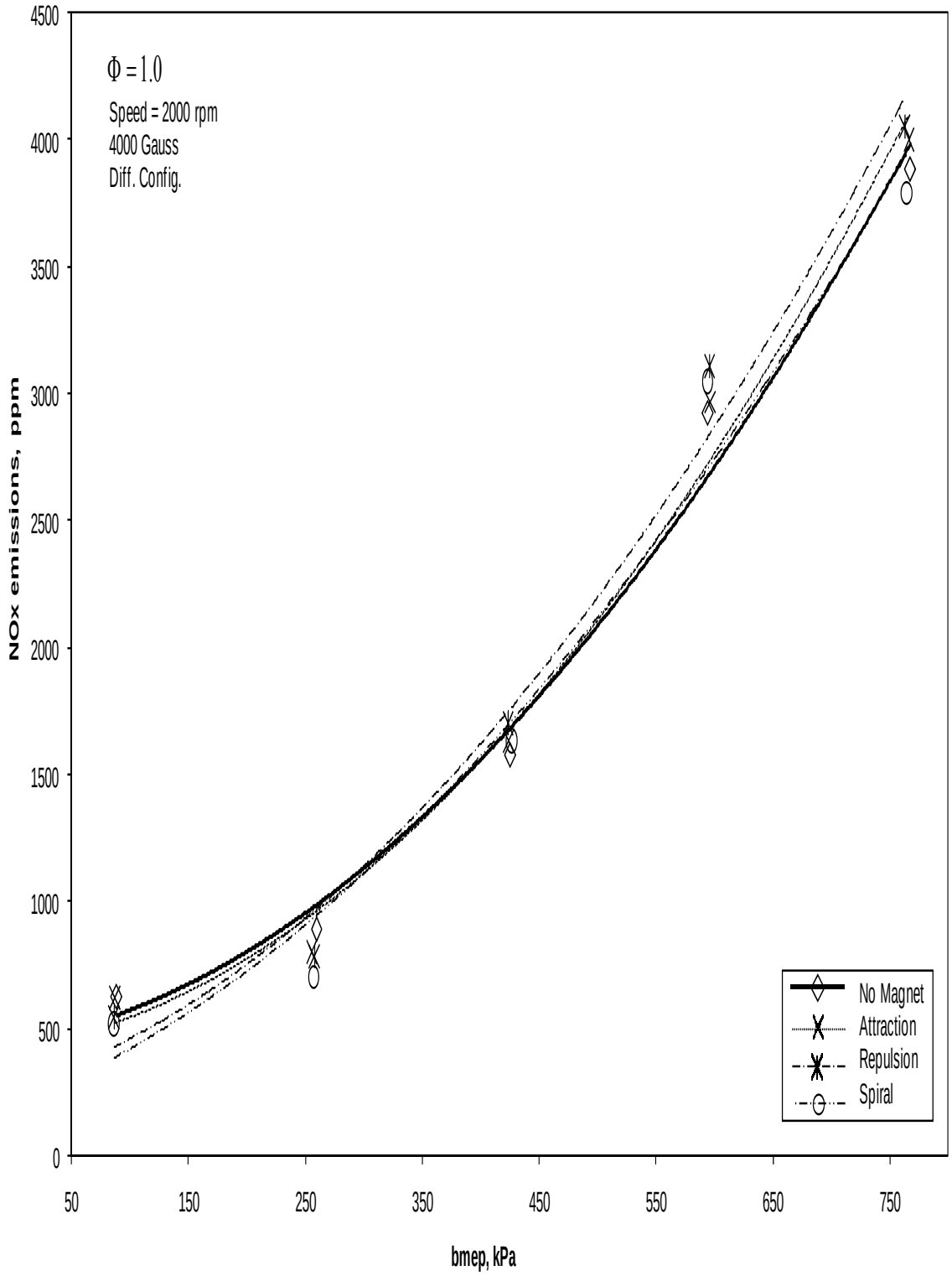

Figure 6-18: Magnetic configuration effect on NOx at constant speed of 2000 rpm

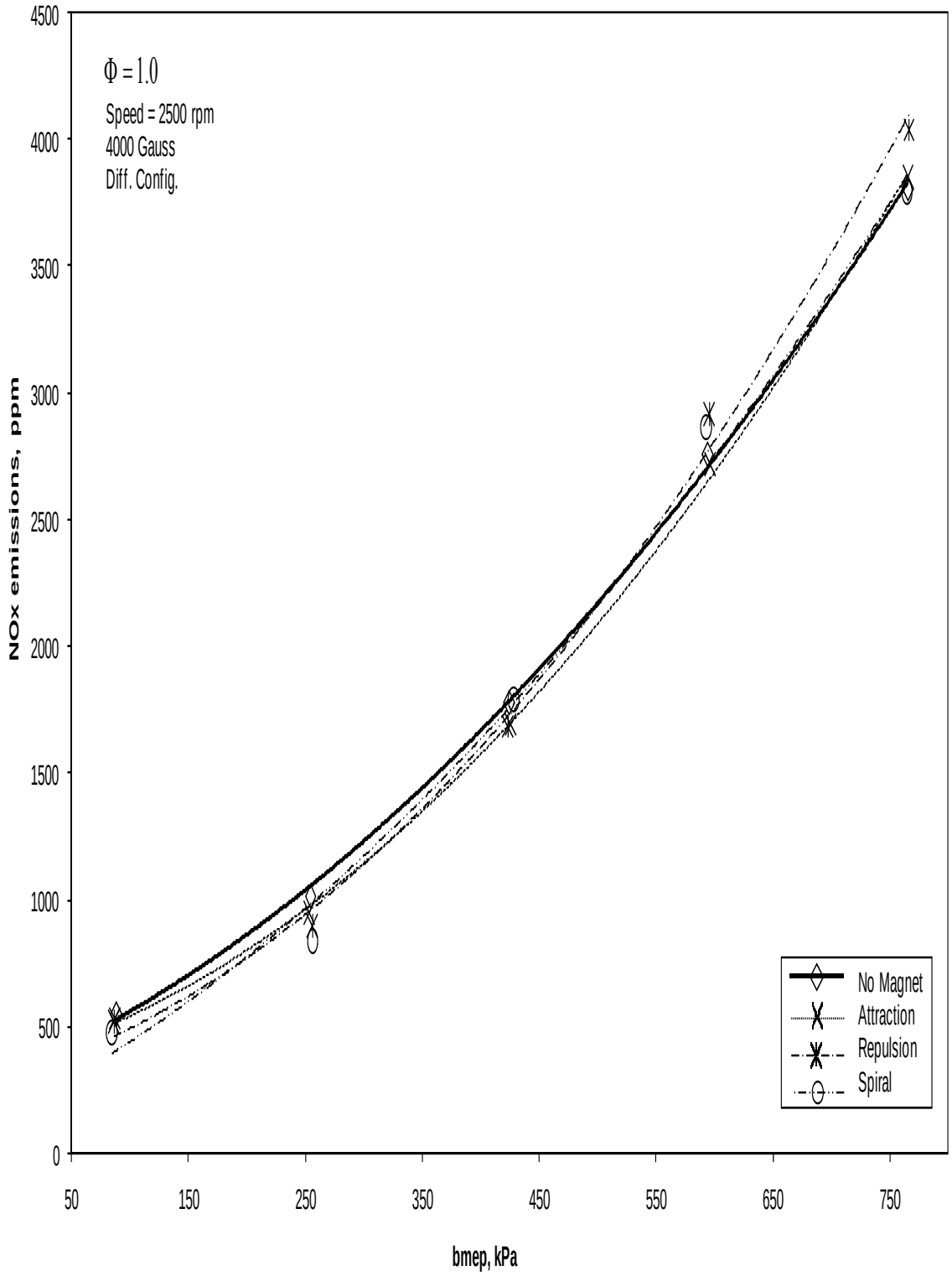

Figure 6-19: Magnetic configuration effect on NOx at constant speed of 2500 rpm

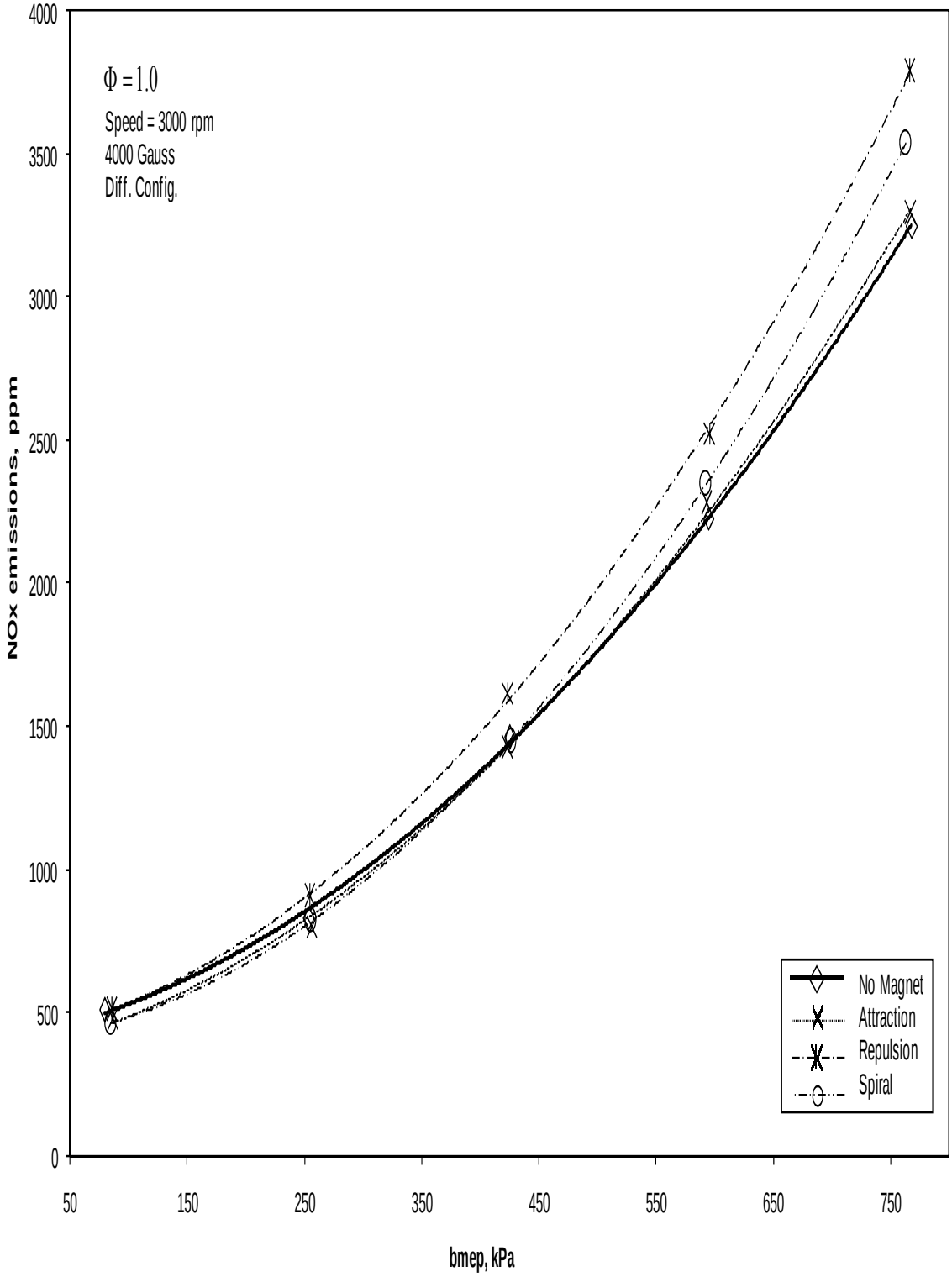

Figure 6-20: Magnetic configuration effect on NOx at constant speed of 3000 rpm

CHAPTER 7

7 HYDROCARBONS EMISSIONS (HC)

7.1 Magnetic Field Strength Effect

7.1.1 Constant Load Simulation

The variation of HC emissions in vol% against varying speeds at a constant load of 20 Nm and different aligned magnetic field strength in 'Attraction' configuration is shown in Figure 7-1. For zero magnetic field strength, the HC emissions initially decrease in a nonlinear fashion with increasing engine speed, but they follow a linear relationship with a small slope after 1500 rpm. The difference between the maximum (0.32 vol%) and the minimum (0.15 vol%) emissions level is around 50%. With the application of the magnetic field, a general decrease by 10% in the emissions level is observed over virtually all engine speeds for all field strengths. For engine speeds higher than 2000 rpm not much difference in effect is observed for different field strengths. On the other hand, below this speed the curves corresponding to different field strengths begin to diverge significantly. The maximum reduction in emissions reaches 30% at the lowest engine speed of 1000 rpm with the magnetic field strength of 3200 Gauss. All the curves follow the same trend across the speed scale. There is an observed dependence on the magnetic field strength at the lowest engine speed in relation to the NOx emission reduction.

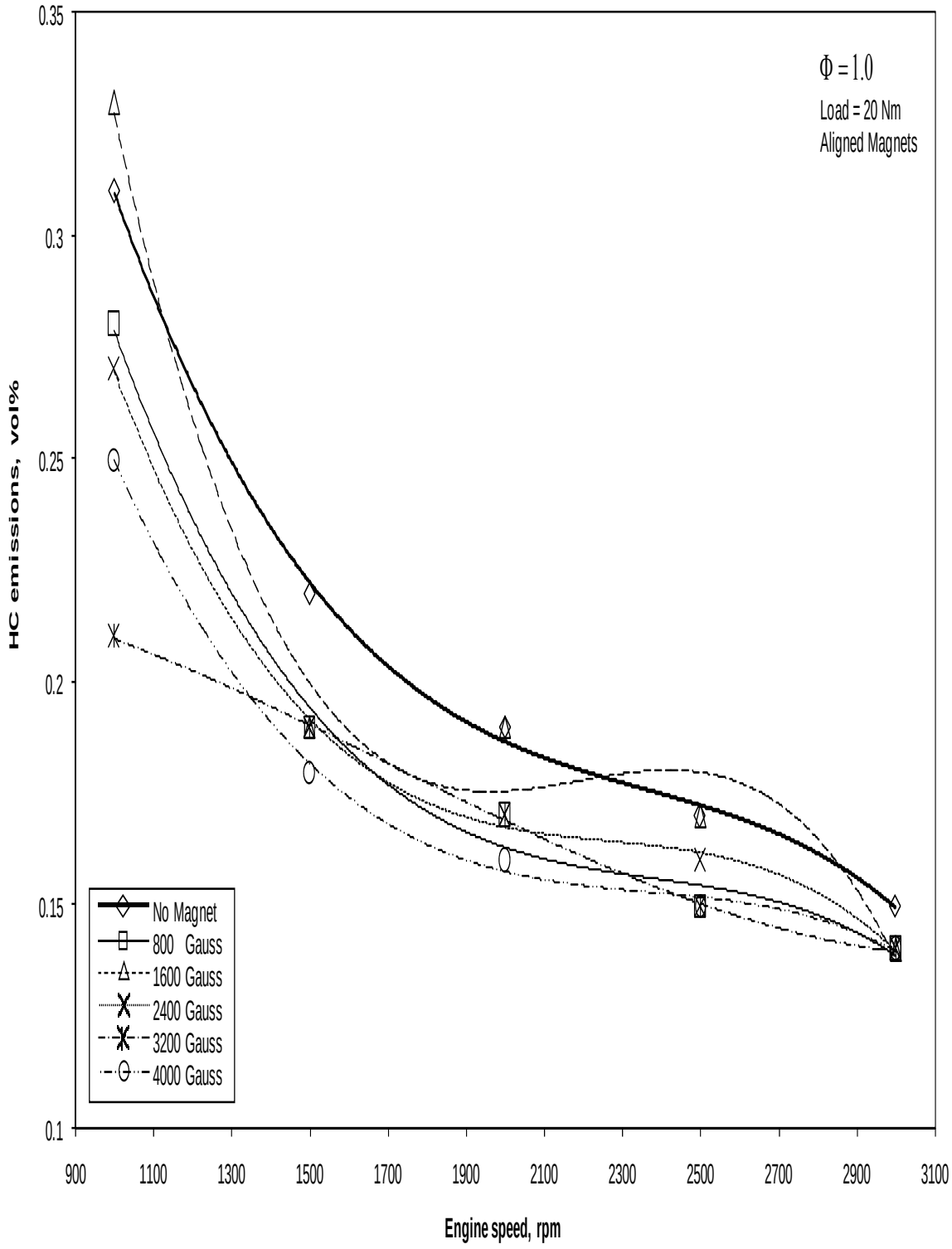

Figure 7-1: Magnetic strength effect on HC at constant load of 20 Nm

Increasing the load to 60 Nm, as portrayed in Figure 7-2, produces an almost linear curve with a negligible slope for the zero magnetic strength. The overall HC emissions go down for most engine speeds. Application of the magnetic field produces a considerable decrease by an average 15% in the emissions level, especially with field strengths of 800, 3200, and 4000 Gauss. However, at field strength of 1600 and 2400 Gauss, a similar appreciable decrease is seen at lower speeds only.

Figure 7-3 shows the changes corresponding to a load increase to 100 Nm, where the curve is quite flat, suggesting a constant emission level at all engine speeds. Application of the magnetic field produces a constant average decrease by 10% in emissions level at all engine speeds. For higher field strengths except 1600 Gauss, the emission levels decreases further by 15% with the best result obtained for the strongest magnetic field.

At a load of 140 Nm, as shown in Figure 7-4, a tendency to return to the behaviour exhibited at 20 Nm load in Figure 7-1 is observed. Application of the magnetic field produces a considerable decrease by 15% in the emissions level, more obvious at the strongest field strength.

Finally, Figure 7-5 depicts the HC emissions level dependency on engine speed at the highest load of 180 Nm, where the overall emissions level goes up considerably compared to the previous load setting. The qualitative behaviour of the curves continues to match the 20 Nm load in Figure 7-1. The emissions level tends to stabilize at 0.16 vol% after 1500 rpm, before which it decreases nonlinearly from 0.26 vol%. Application of the magnetic field produces no significant improvement for almost all field strengths and engine speeds, except the 4000 Gauss strength with very little consistent decrease.

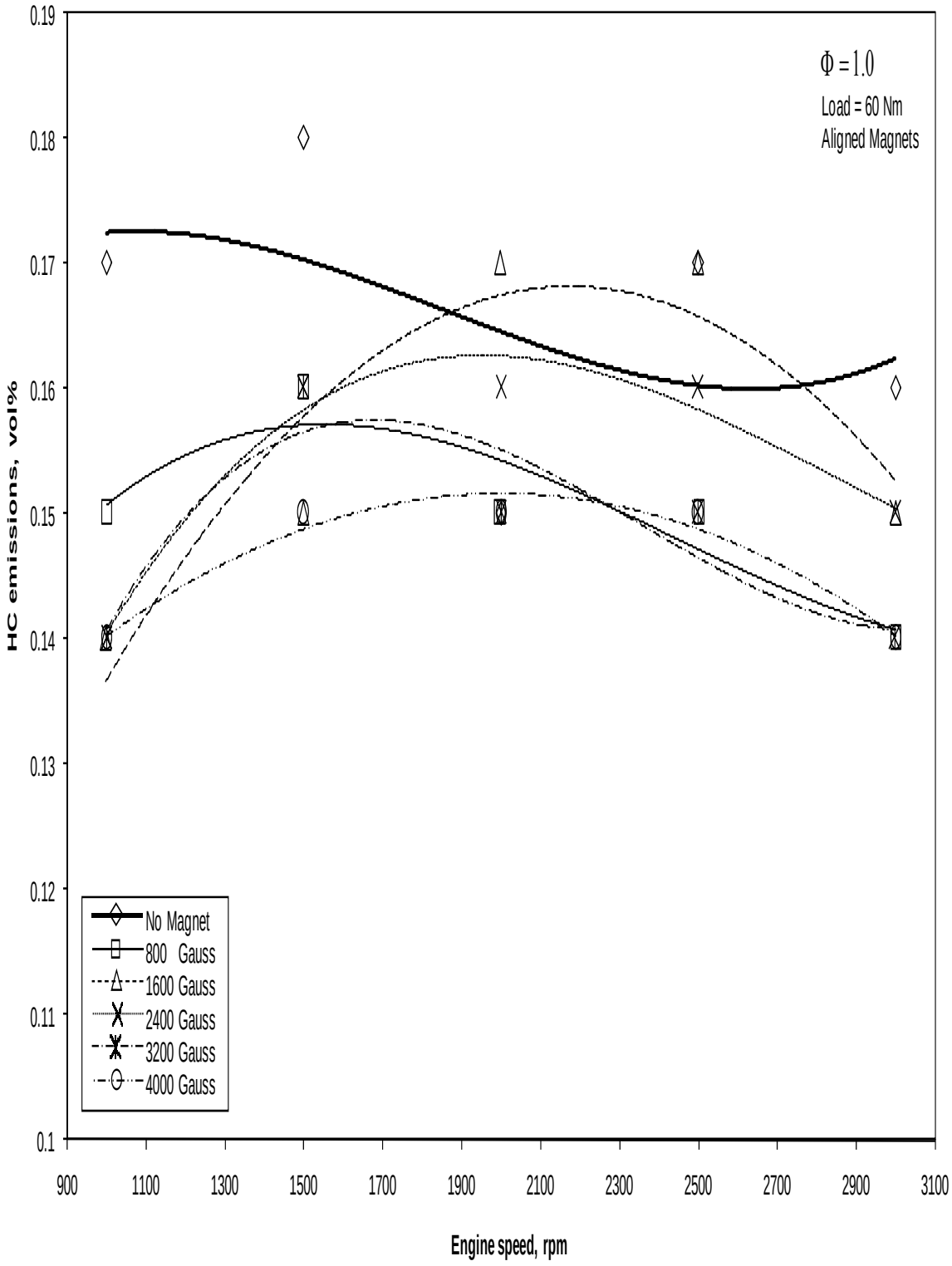

Figure 7-2: Magnetic strength effect on HC at constant load of 60 Nm

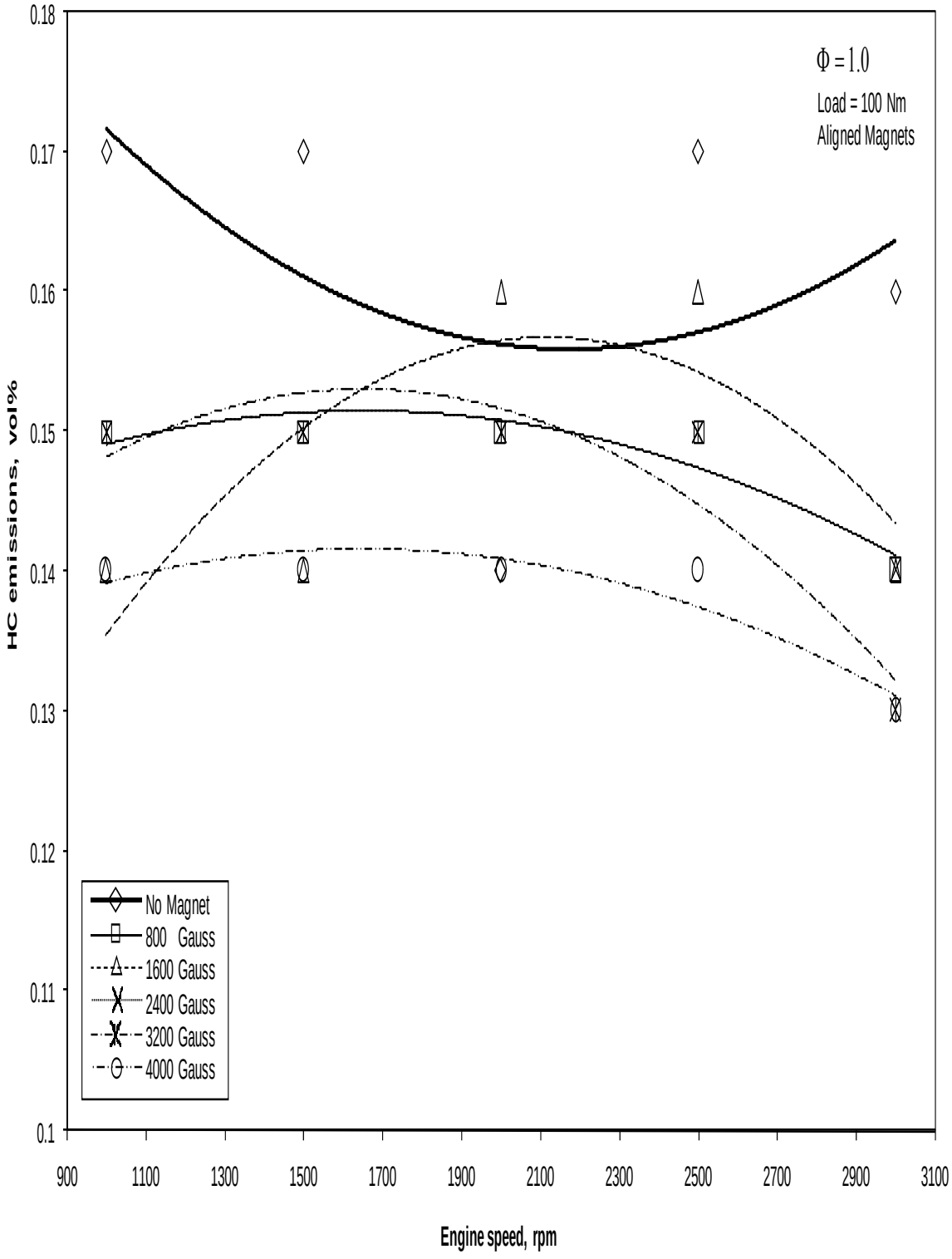

Figure 7-3: Magnetic strength effect on HC at constant load of 100 Nm

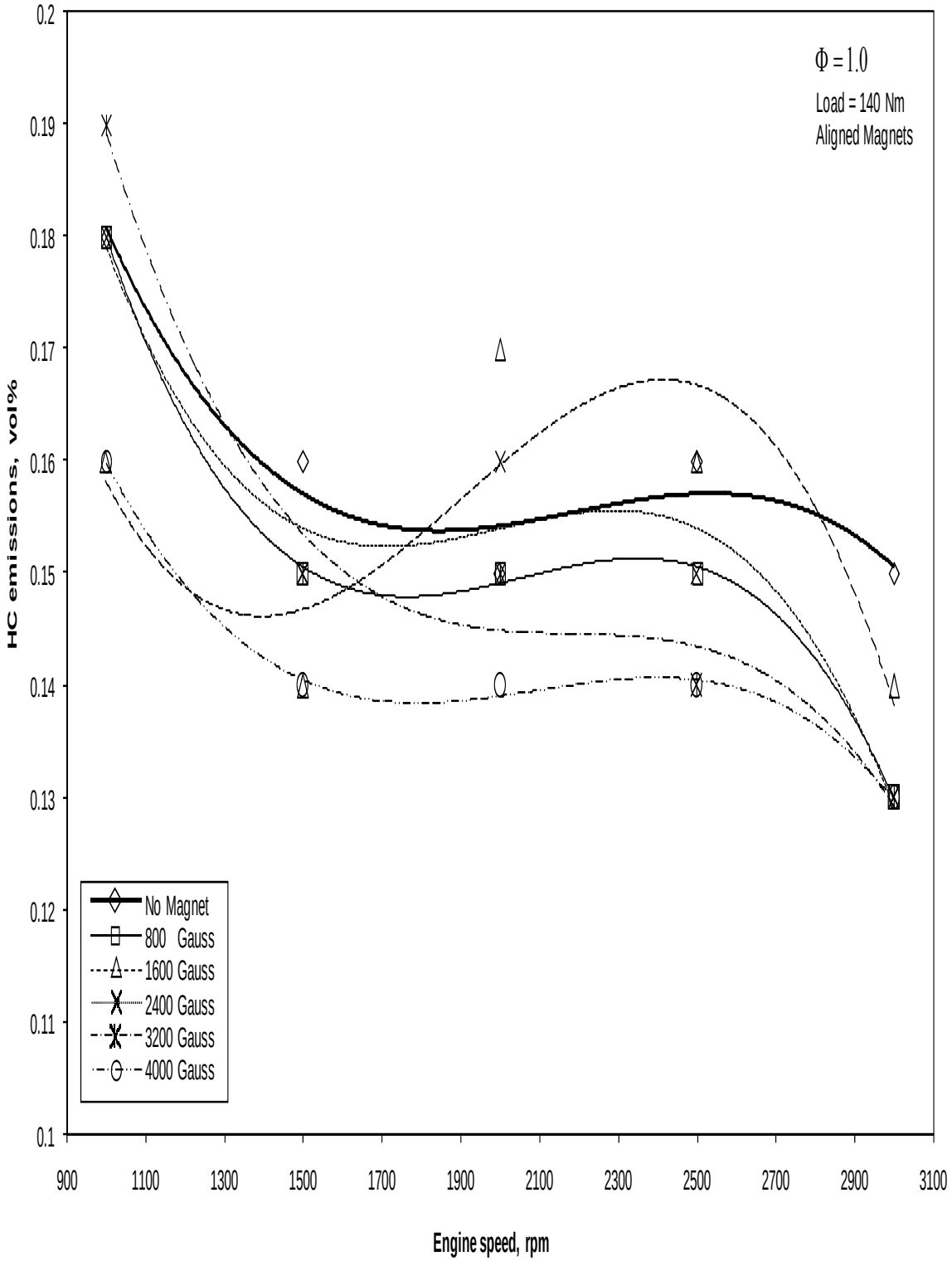

Figure 7-4: Magnetic strength effect on HC at constant load of 140 Nm

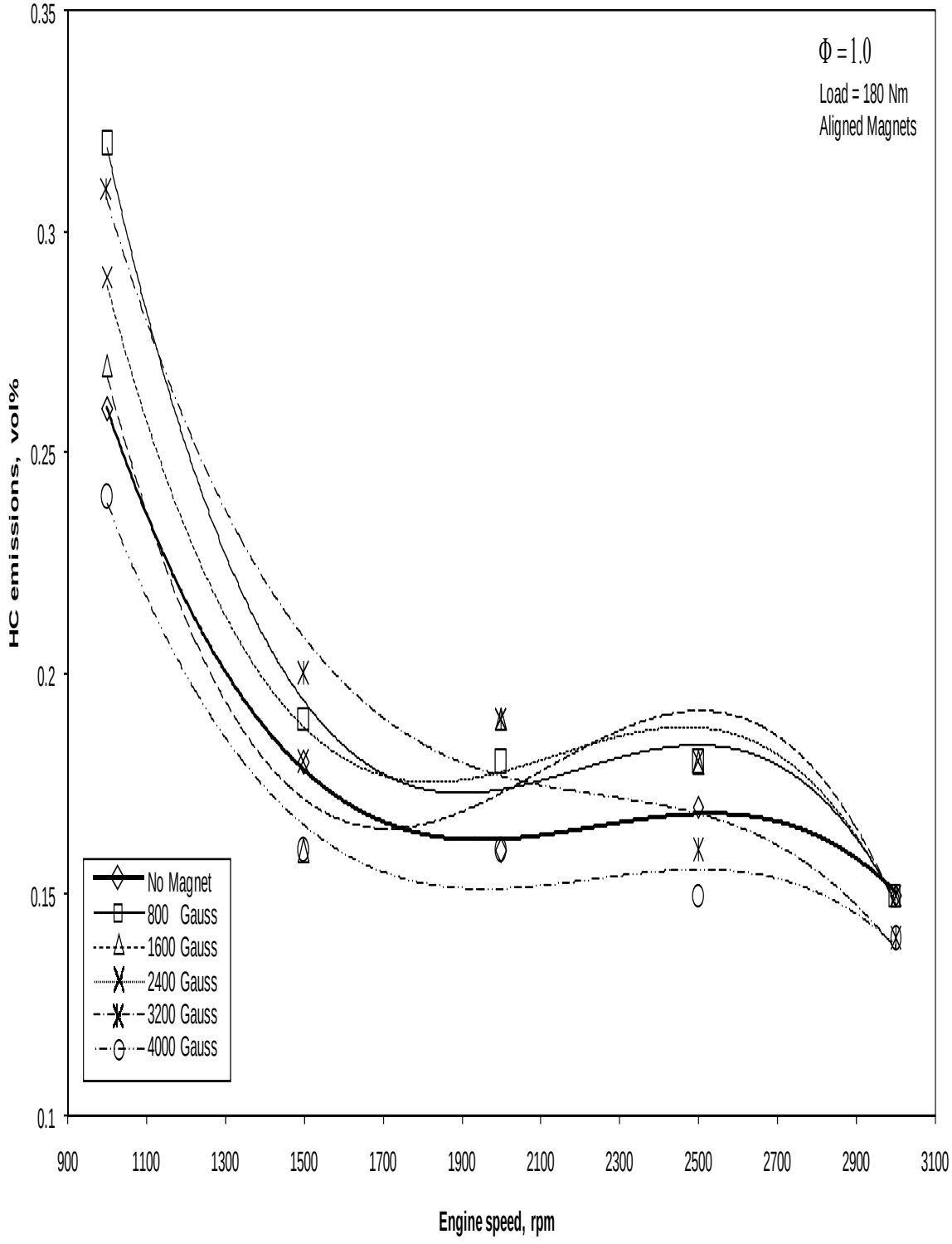

Figure 7-5: Magnetic strength effect on HC at constant load of 180 Nm

7.1.2 Constant Speed Simulation

The variation of HC emissions against increasing engine load at 1000 rpm and different aligned magnetic field strengths in 'Attraction' configuration is shown in Figure 7-6. With the magnetic field turned off, it is observed that the HC emissions decrease from 0.31 vol% with increasing engine load to a minimum of 0.15 vol% at 400 kPa. After that, the HC emissions increase and reach a final value of approximately 0.25 vol%. The overall shape of the curve approximates a parabola. When the magnetic field is turned on, it is observed that at low engine loads most magnetic strengths show a remarkable decrease by 30% in the HC emissions. As the engine load is increased toward the extreme end of the engine load range, the HC emissions show inversely a rise under the magnetic field effect except at the highest strength of 4000 Gauss. It is seen that the strongest magnetic field gives reduced HC emissions at all engine loads.

Figure 7-7 shows the same relationship but at a higher constant engine speed of 1500 rpm. It is seen that, without a magnetic field, the maximum value of the HC emissions decreases and the minimum value increases. However, it is observed that all magnetic field strengths produce an appreciable 15% reduction in HC emissions at most engine loads. The dependence of the HC emission reduction on the magnetic field strength seems to be insignificant except at the highest end of the engine load range. Overall, the 1600 and 4000 Gauss magnetic field strengths perform consistently the best at all engine loads.

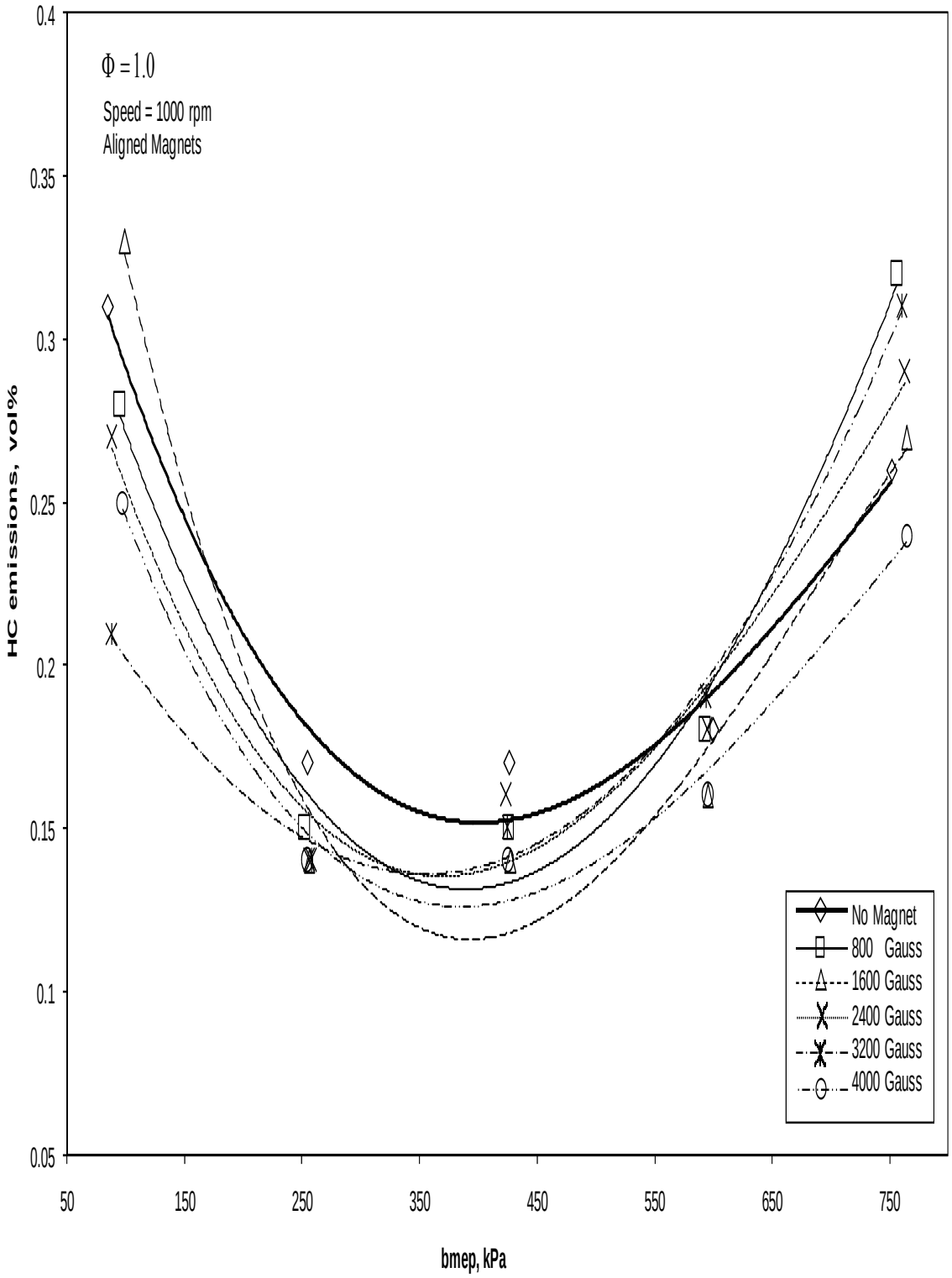

Figure 7-6: Magnetic strength effect on HC at constant speed of 1000 rpm

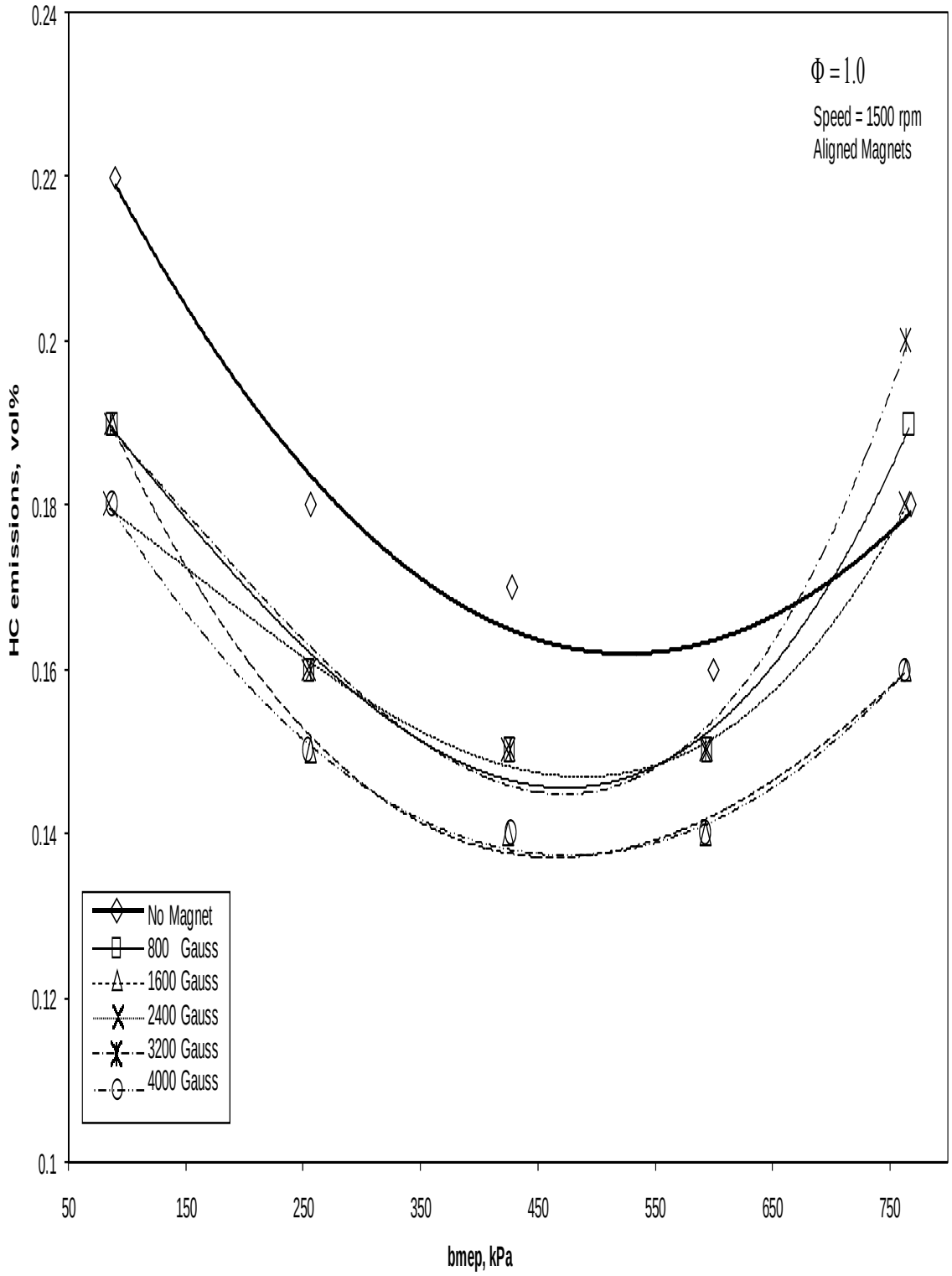

Figure 7-7: Magnetic strength effect on HC at constant speed of 1500 rpm

Figure 7-8 shows the same relationship but at a higher constant speed of 2000 rpm. Here, it is observed that the qualitative behaviour of the zero magnetic field curve remains the same with a slight overall reduction in HC emissions. However, this trend is not followed by the curves depicting the effect of the magnetic field. At almost all engine loads, all the magnetic field strengths show an increase in HC emissions, except the highest field strength which does not show a significant reduction either.

Figure 7-9 and Figure 7-10 show the effects of increasing engine speeds to 2500 and 3000 rpm respectively. The previous trend of the zero magnetic field curve is back to flatten itself at a mean value near 0.16 vol%. Now, the application of the magnetic field shows a significant consistent average reduction by 15% in HC emissions at almost all engine loads, with a further reduction in HC emissions generally with increasing magnetic field strengths.

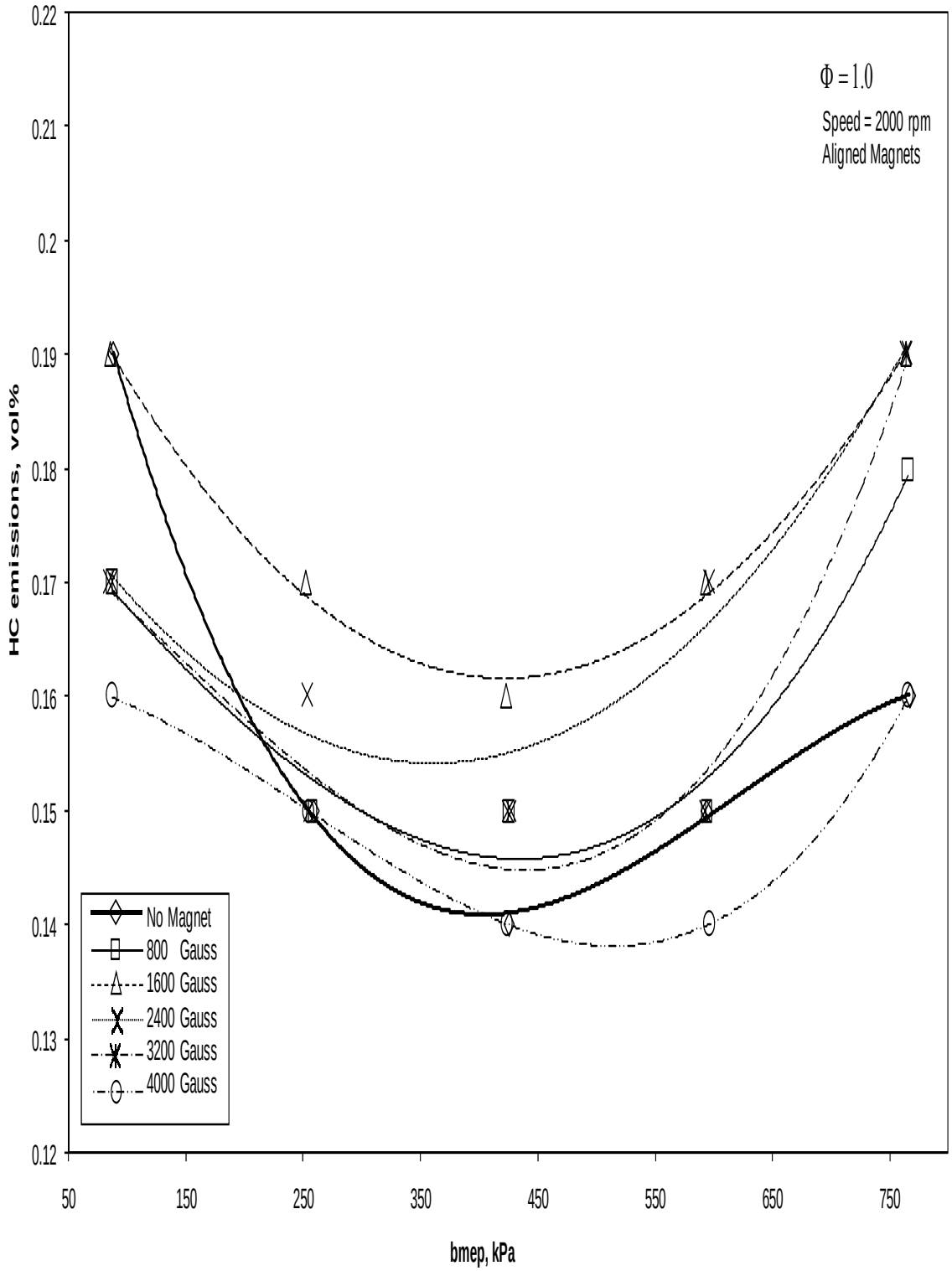

Figure 7-8: Magnetic strength effect on HC at constant speed of 2000 rpm

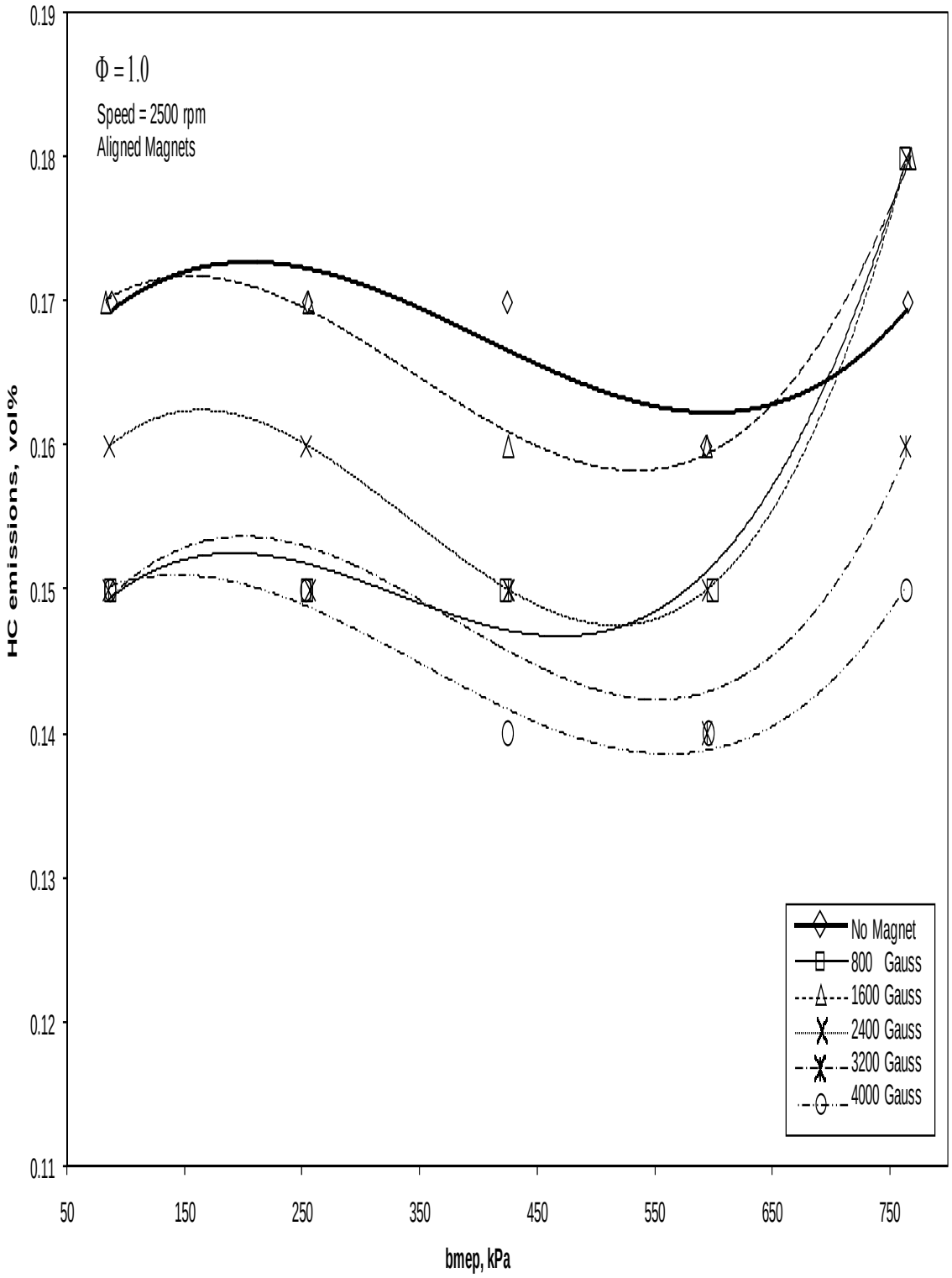

Figure 7-9: Magnetic strength effect on HC at constant speed of 2500 rpm

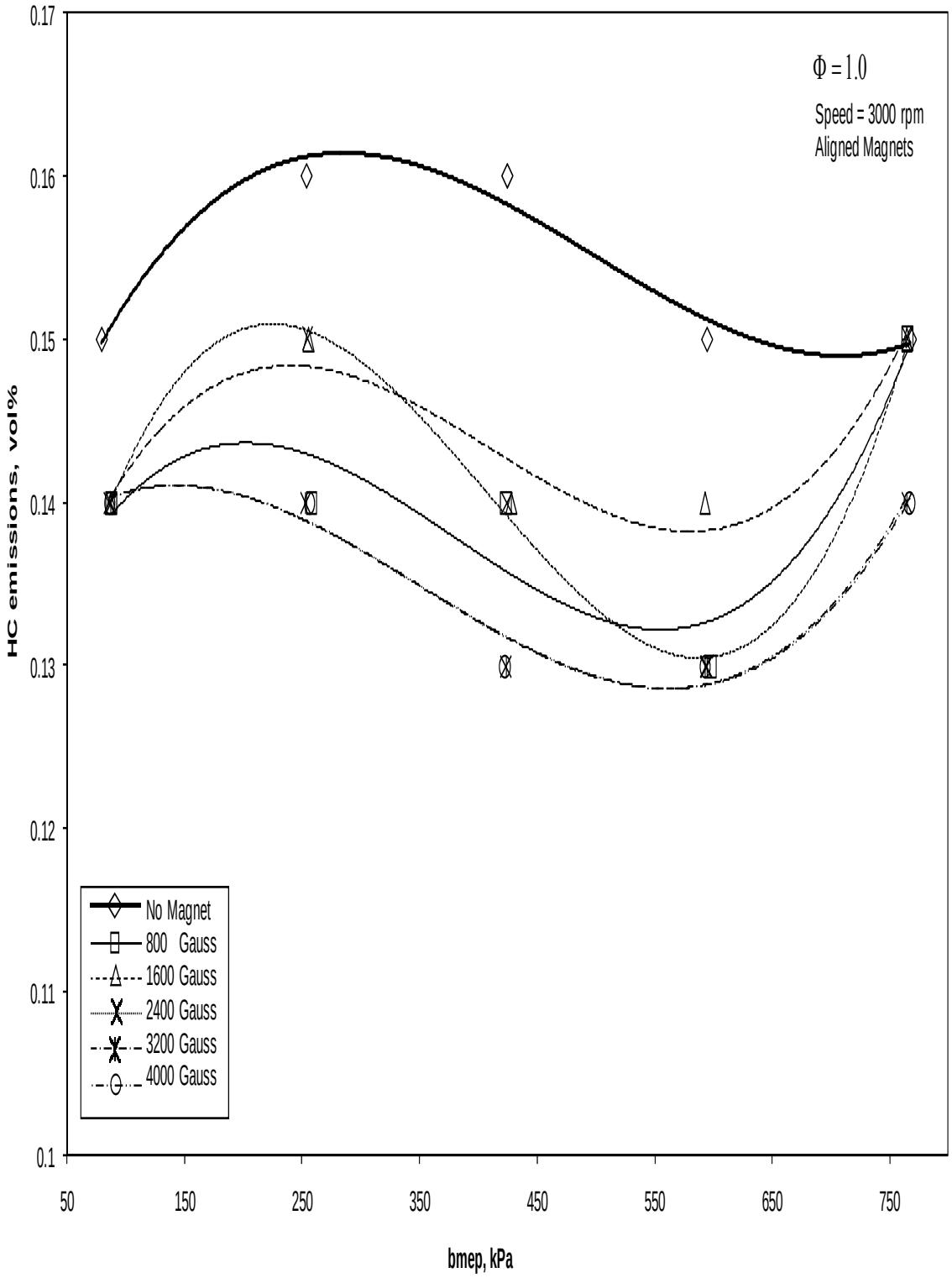

Figure 7-10: Magnetic strength effect on HC at constant speed of 3000 rpm

7.2 Magnetic Field Configuration Effect

7.2.1 Constant Load Simulation

The variation of the HC emissions in vol% against varying engine speeds at a constant load of 20 Nm and constant magnetic field strength of 4000 Gauss with three different magnetic field configurations is shown in Figure 7-11. With zero magnetic field strength, the HC emissions decrease monotonically with increasing engine speed. Initially, the decrease in the emissions level is sharp, but then it becomes gradual at higher values of the independent variable. Application of the magnetic field induces an average 20% reduction in the emissions level at virtually all values of the engine speed. However, there is a slightly less desirable effect observed with the 'Repulsion' configuration since it increases in comparison with the other two configurations.

When the load is increased to 60 Nm, as depicted in Figure 7-12, an overall reduction by almost half the volume in the emissions level is detected at all engine speeds. Also, the difference in the highest and lowest emission levels is small, so that the variation with engine speed is less meaningful. Rather, a linear relationship between the HC emissions and engine speed is a more appropriate description. The application of the magnetic field generally produces an average 15% reduction in the emissions level at almost all engine speeds, except the 'Repulsion' configuration.

Figure 7-13 shows the relationship between the same variables at a load of 100 Nm where the general tendency of the curves to become flatter continues to be apparent. The application of the magnetic field produces a similar appreciable 15% decrease in the emissions level, where the 'Attraction' and 'Spiral configuration seems to perform the best, while the 'Repulsion' configuration continues to give unfavourable results.

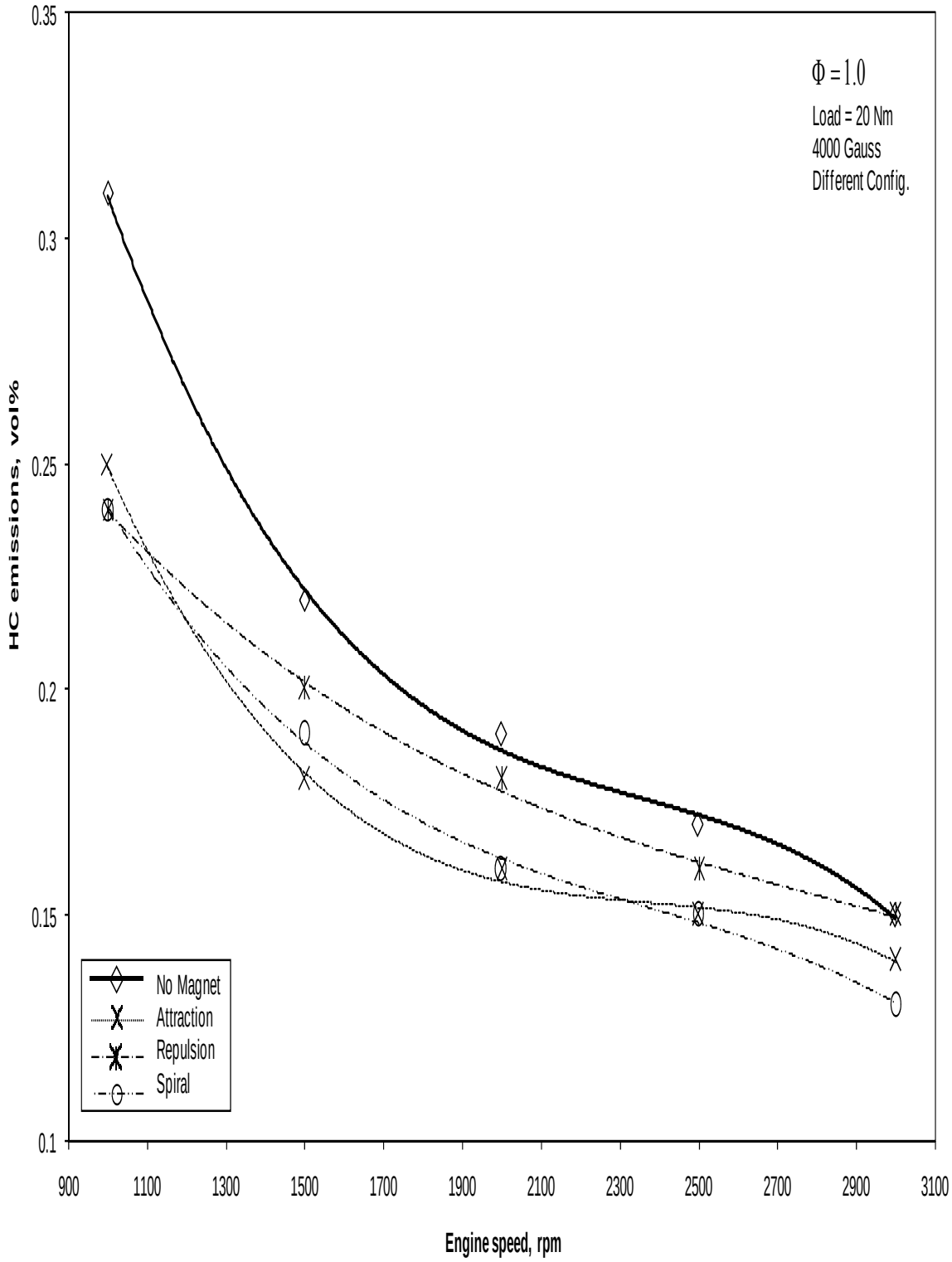

Figure 7-11: Magnetic configuration effect on HC at constant load of 20 Nm

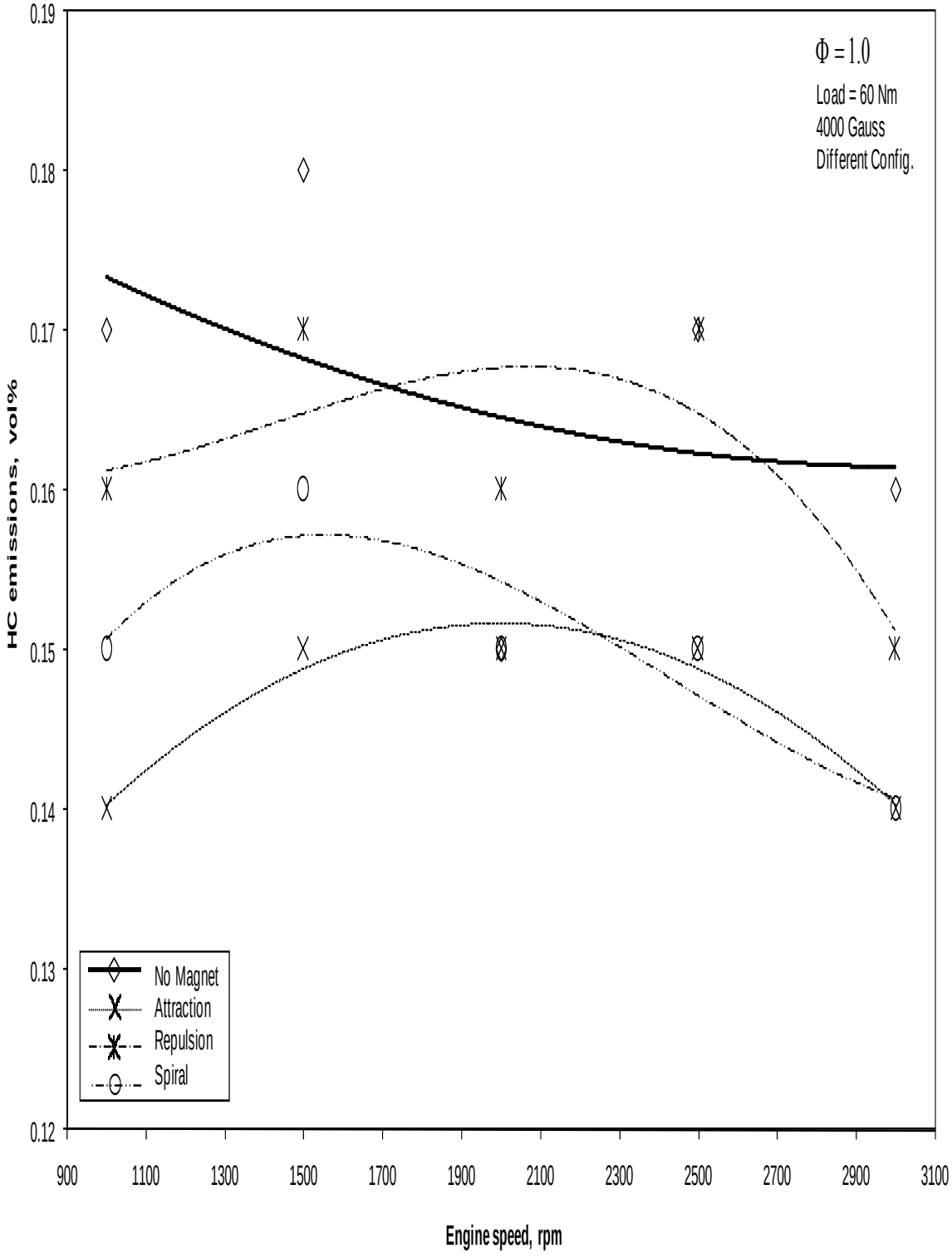

Figure 7-12: Magnetic configuration effect on HC at constant load of 60 Nm

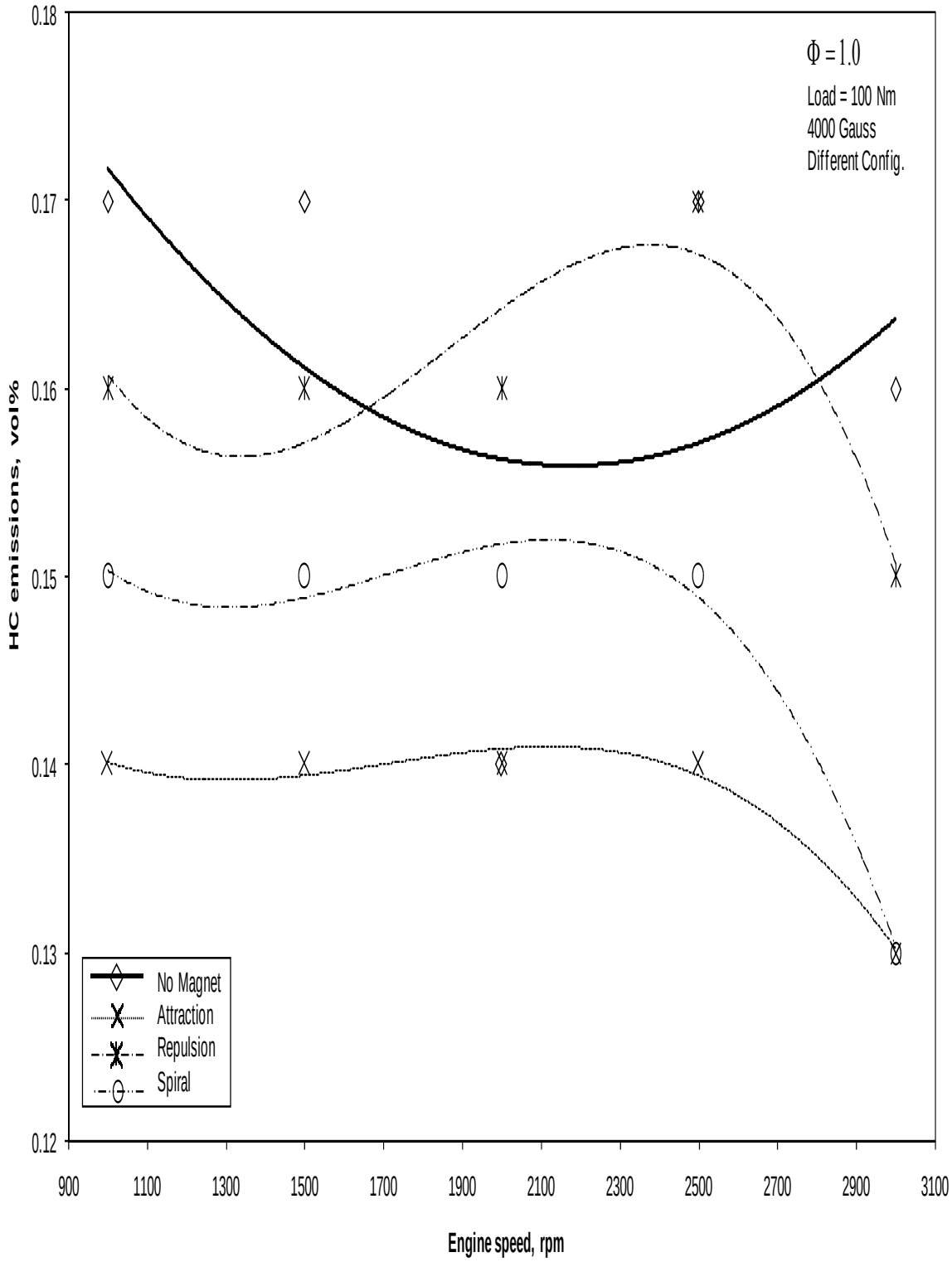

Figure 7-13: Magnetic configuration effect on HC at constant load of 100 Nm

Figure 7-14 shows the variation in the HC emissions level against engine speed at a load of 140 Nm. It is observed that a slight increase in the emissions occurs at the lower range of the engine speed but the emissions tend to decrease at almost all other speeds. The curve may still be considered as tending towards a constant value, although, a linear relationship with a very small slope may be a better description. The application of the magnetic field again produces a 15% decrease in the emissions at all engine speeds. However, this continues to be true only for the 'Attraction' and 'Spiral' configurations since the 'Repulsion' configuration continues to produce unfavourable results. The curves corresponding to the application of the magnetic field follow the same trend as that of the zero magnetic field strength.

Further increase in the load to 180 Nm, as shown in Figure 7-15, demonstrates a general increase in the HC emissions level, which is considerably greater at the lower engine speeds. The curve is almost horizontal at around 0.17 vol% for most of the speed range, but around 0.27 vol% for the lowest speed of 1000 rpm to be The application of the magnetic field now produces an almost vanishing effect for all magnetic configurations where all the curves essentially follow the same trend.

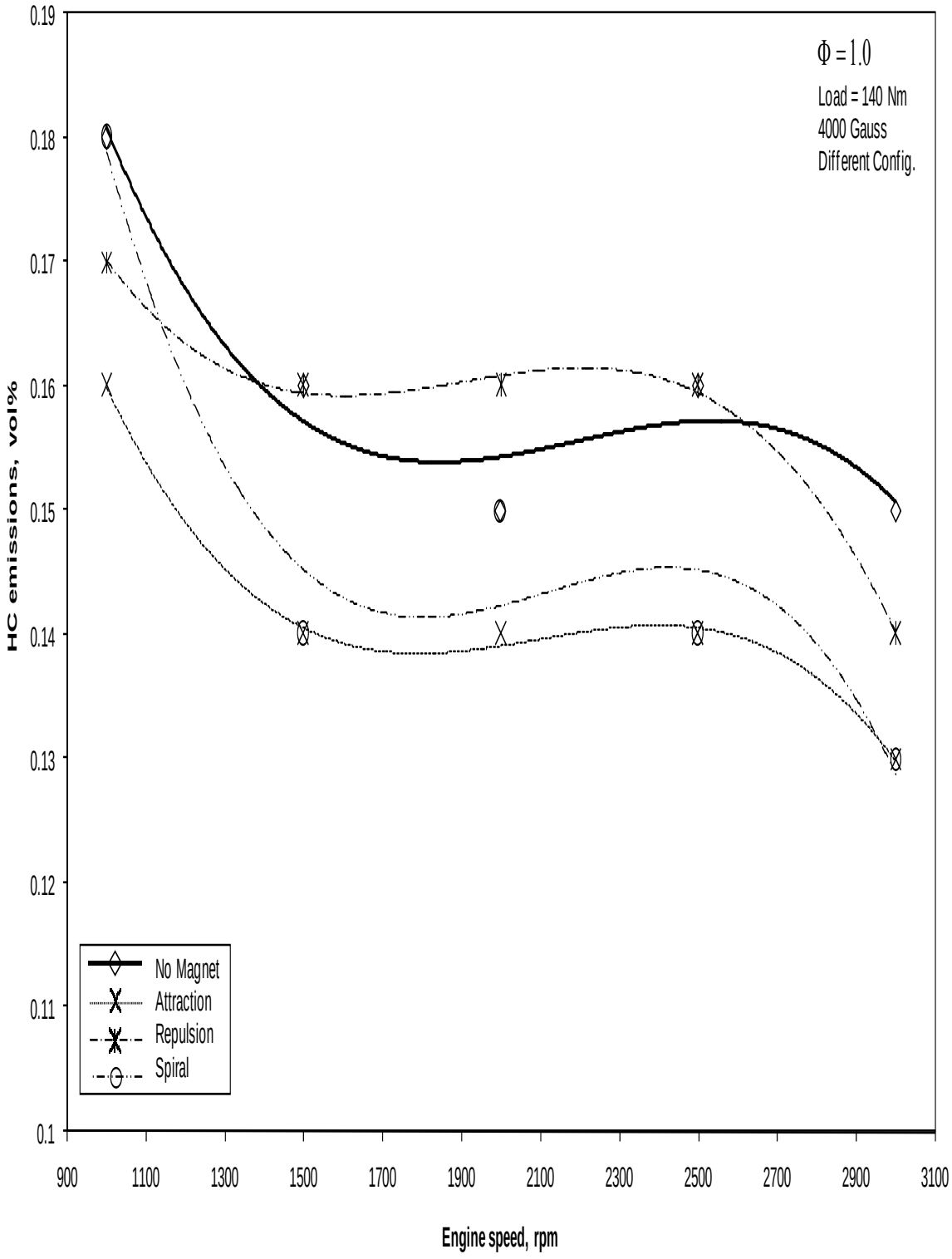

Figure 7-14: Magnetic configuration effect on HC at constant load of 140 Nm

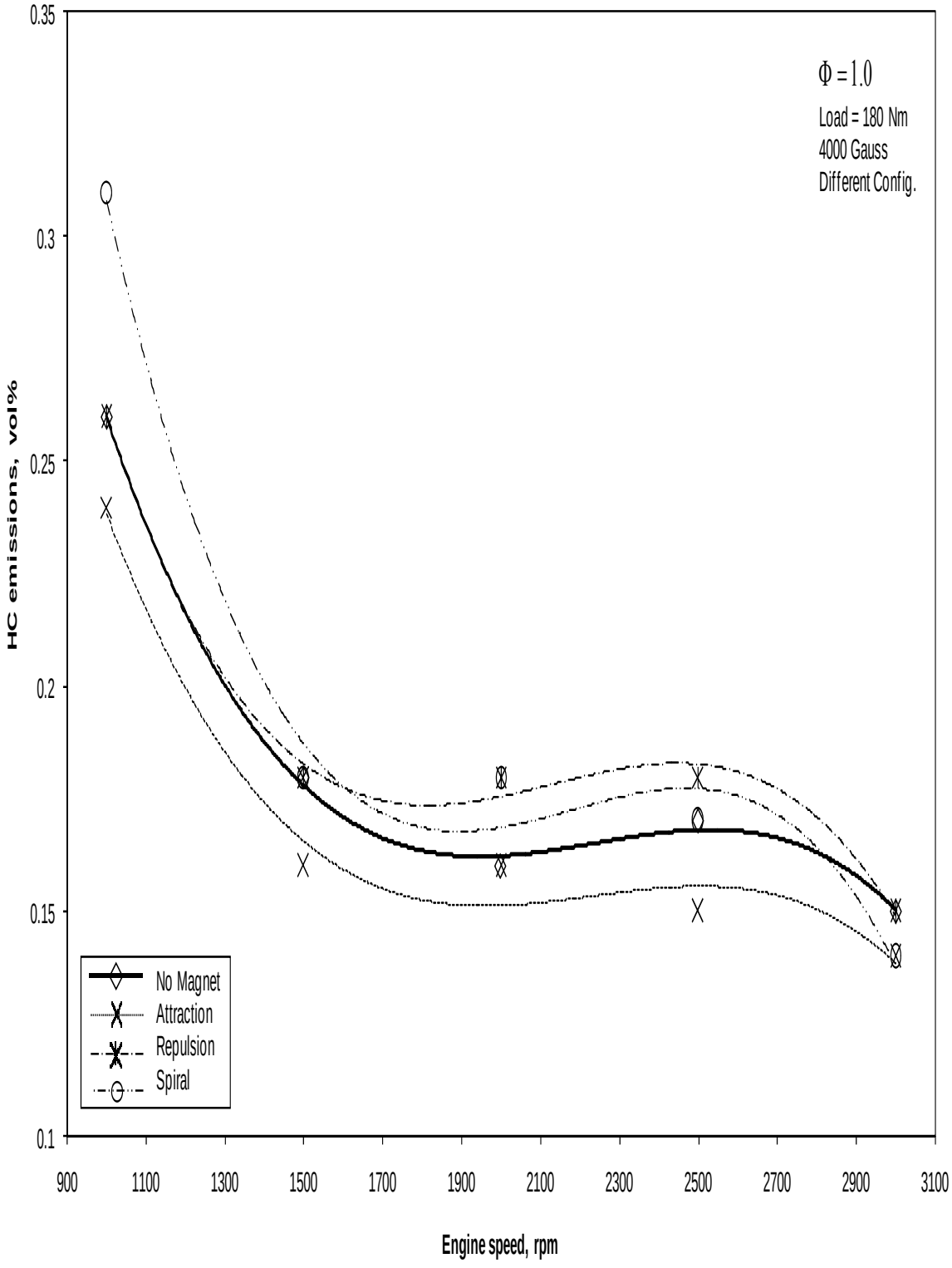

Figure 7-15: Magnetic configuration effect on HC at constant load of 180 Nm

7.2.2 Constant Speed Simulation

The variation of HC emissions against different engine loads at a constant speed of 1000 rpm and constant magnetic field strength of 4000 Gauss with three different magnetic field configurations is shown in Figure 7-16. With no magnetic field effect, the HC emission decreases with increasing engine load, to a minimum of nearly 0.15 vol% at about 400 kPa of engine load. After that, the HC emission increases to a final value of approximately 0.25 vol%. The overall shape of the curve approximates a parabola. As the magnetic field is turned on, a substantial decrease by 20% in HC emissions occurs at the lowest engine loads. The favourable reduction effect becomes less noticeable as the engine load increases. The different magnetic field configurations exhibit varying behaviours, where the 'Spiral' configuration shows a sudden increase in HC emissions at the highest engine load, and the 'Attraction' configuration shows a consistent reduction at all engine loads. Overall, the application of a magnetic field reduces the HC emissions at almost all engine loads, but with varying degrees at different magnetic field configurations.

Figure 7-17 shows the relationship between the same variables but at an increased engine speed of 1500 rpm. With no magnetic field, the maximum value of the HC emissions decreases significantly, whereas the minimum value increases noticeably. This shows a reduced sensitivity of HC emissions variation at this engine speed while varying the engine loads. Application of a magnetic field again reduces the HC emissions by 20% at almost all engine loads with slight varying degrees depending on the magnetic field configuration. However, the 'Attraction' configuration continues to give the best improvement which remains consistent at all engine loads.

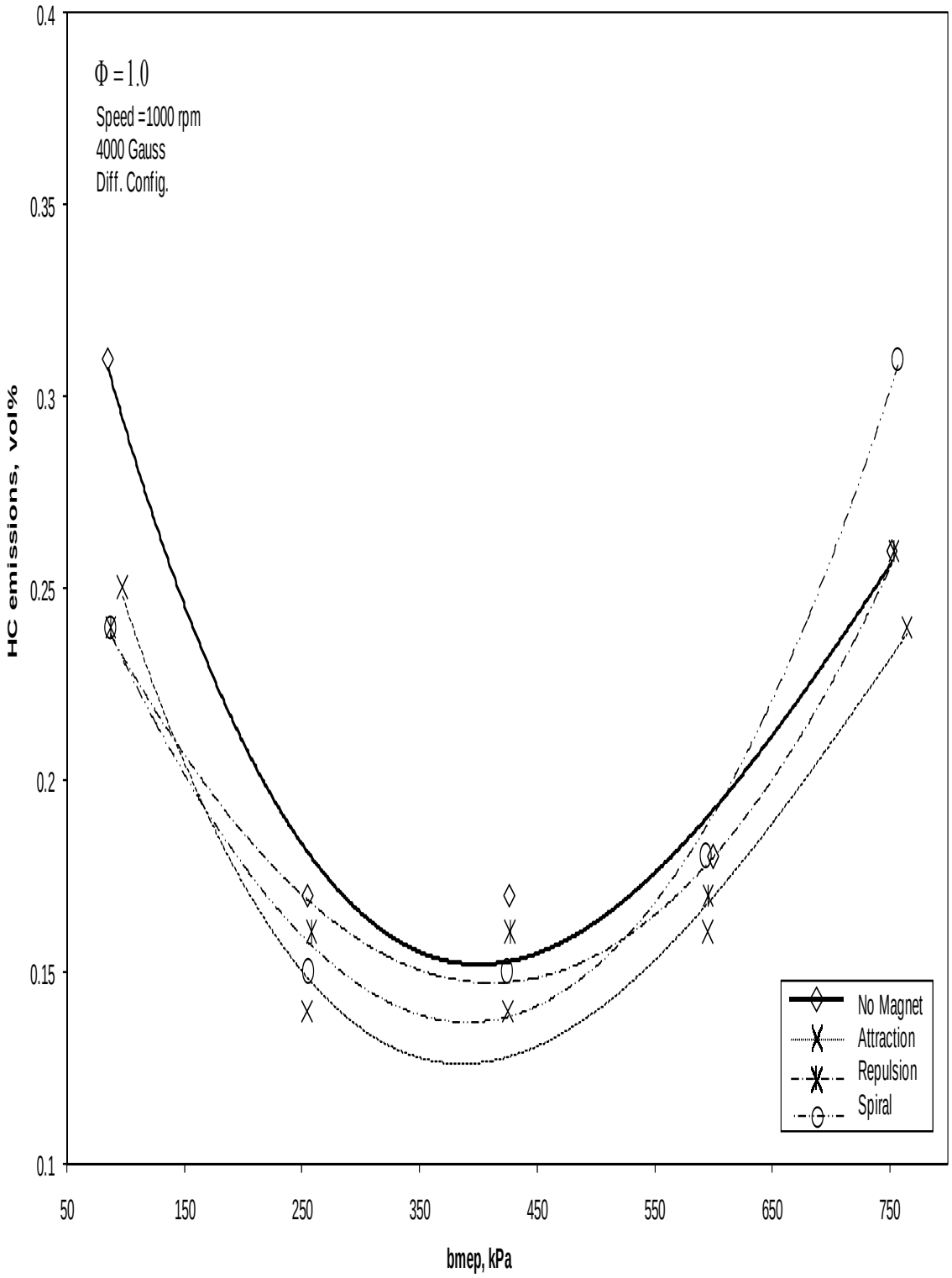

Figure 7-16: Magnetic configuration effect on HC at constant speed of 1000 rpm

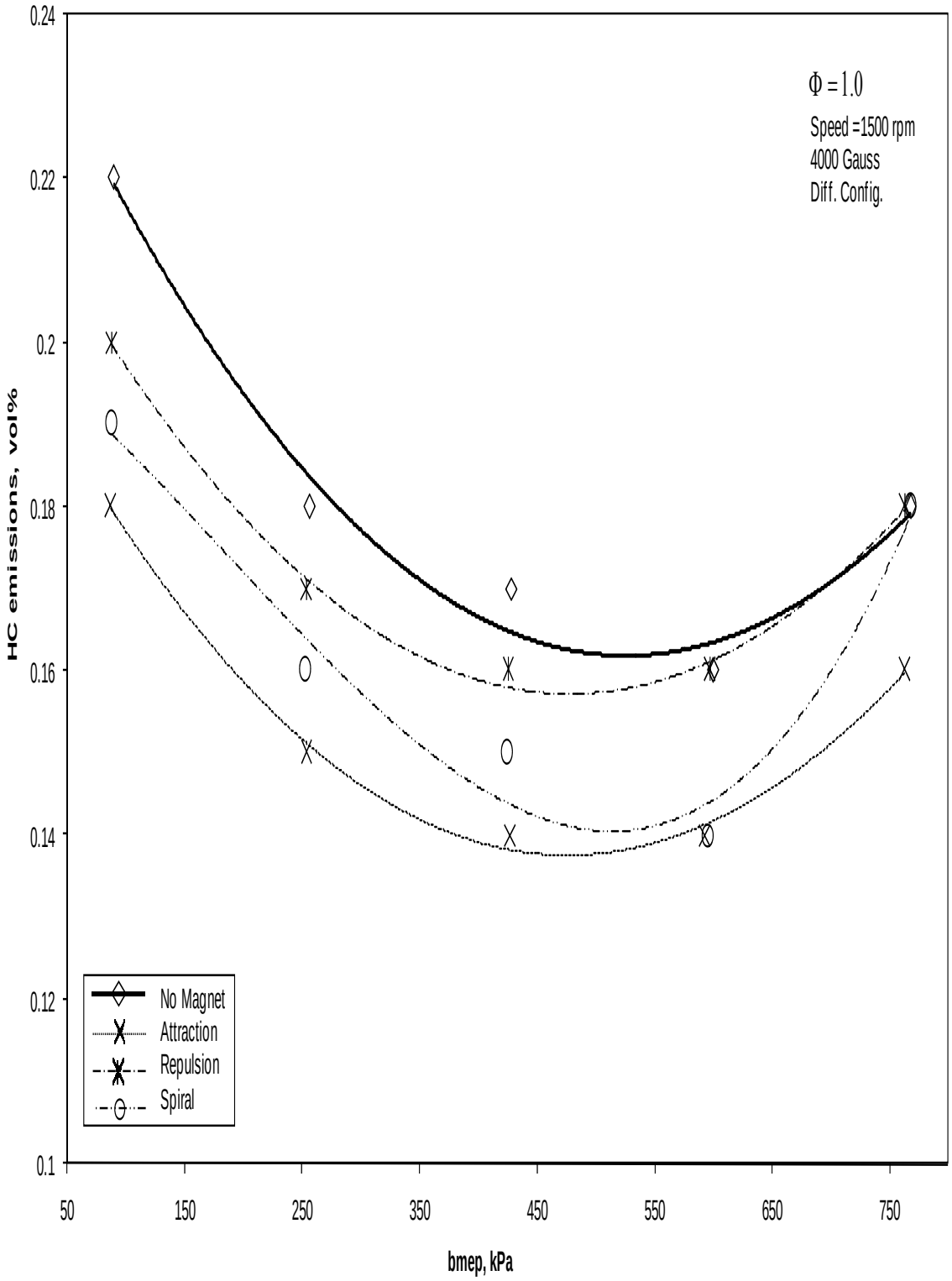

Figure 7-17: Magnetic configuration effect on HC at constant speed of 1500 rpm

Figure 7-18, Figure 7-19 and Figure 7-20 show the relationship of the same variables but at engine speeds of 2000, 2500 and 3000 rpm respectively. With no magnetic field, the overall trend of the HC emissions curve to become flatter can be observed obviously. Moreover, the difference between the maximum and the minimum values of HC emissions keeps decreasing with increasing engine speed. In addition, the 'Attraction' configuration is still turns out to be the best configuration for all engine speeds with an average reduction by 15% in HC emission level, whereas the 'Spiral' configuration nearly follows it. However, the application of a magnetic field shows a rather unusual behaviour at only 2000 rpm, where the 'Repulsion' and 'Spiral' configuration show a slight unfavourable effect at most engine loads.

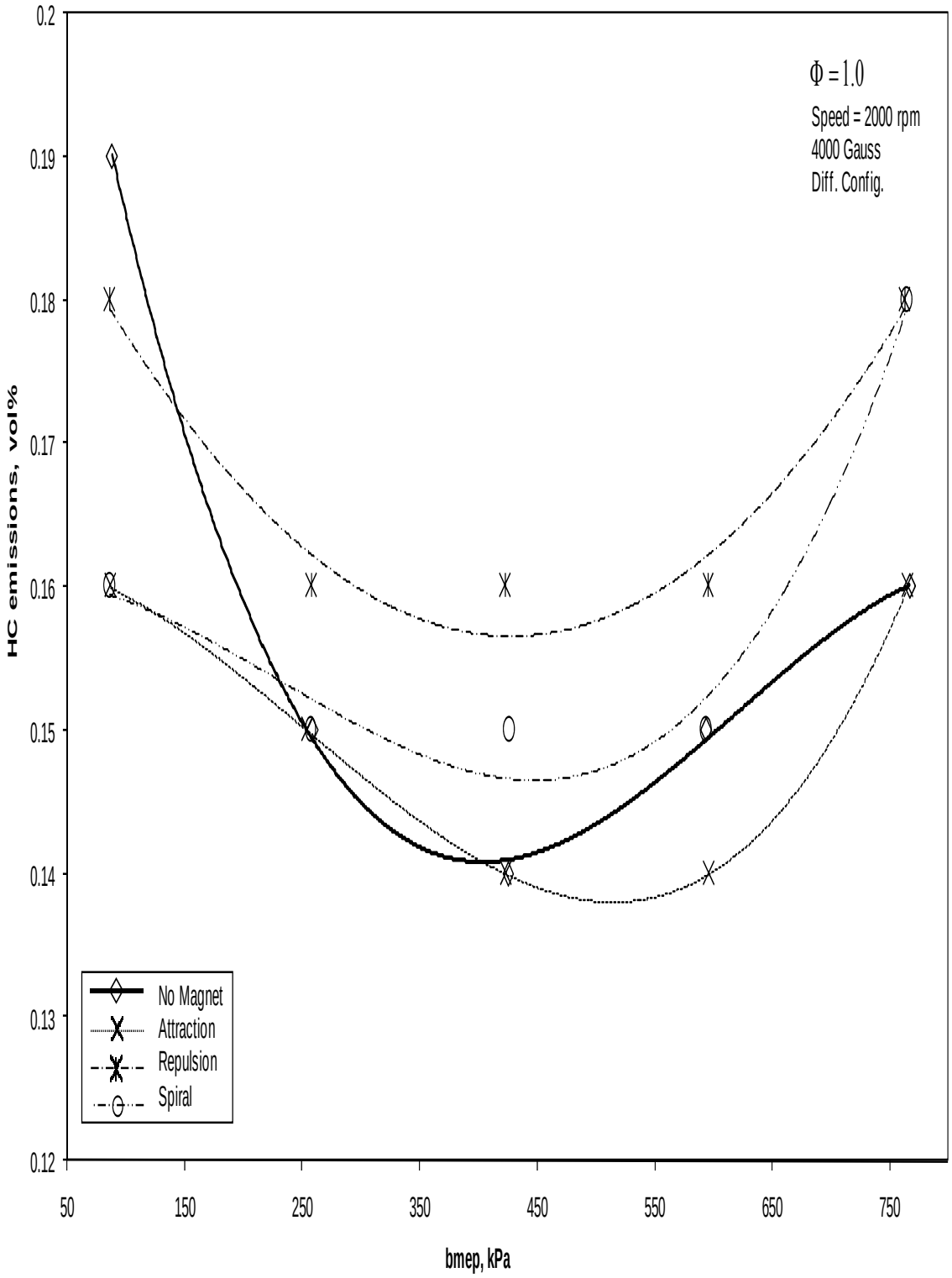

Figure 7-18: Magnetic configuration effect on HC at constant speed of 2000 rpm

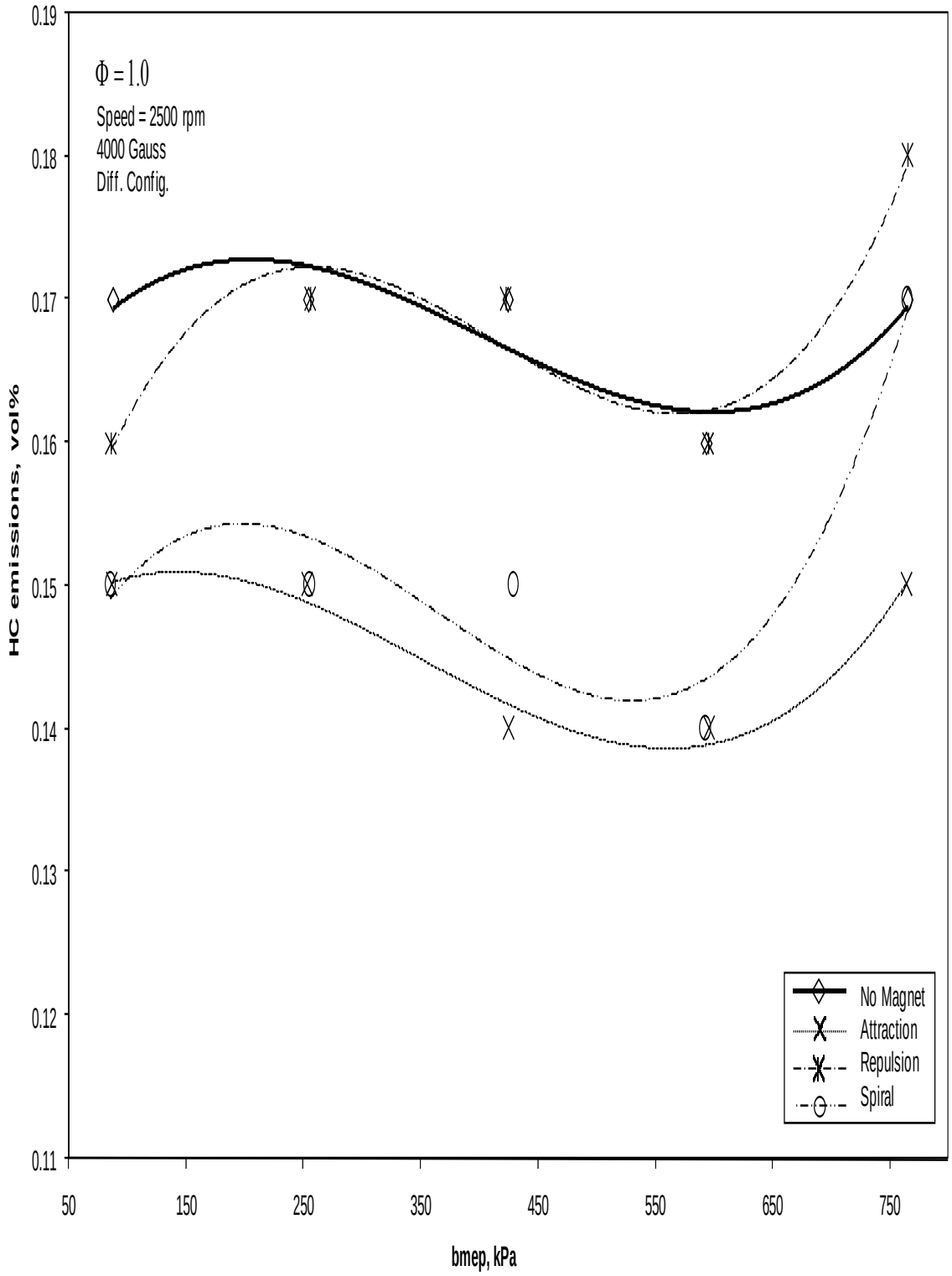

Figure 7-19: Magnetic configuration effect on HC at constant speed of 2500 rpm

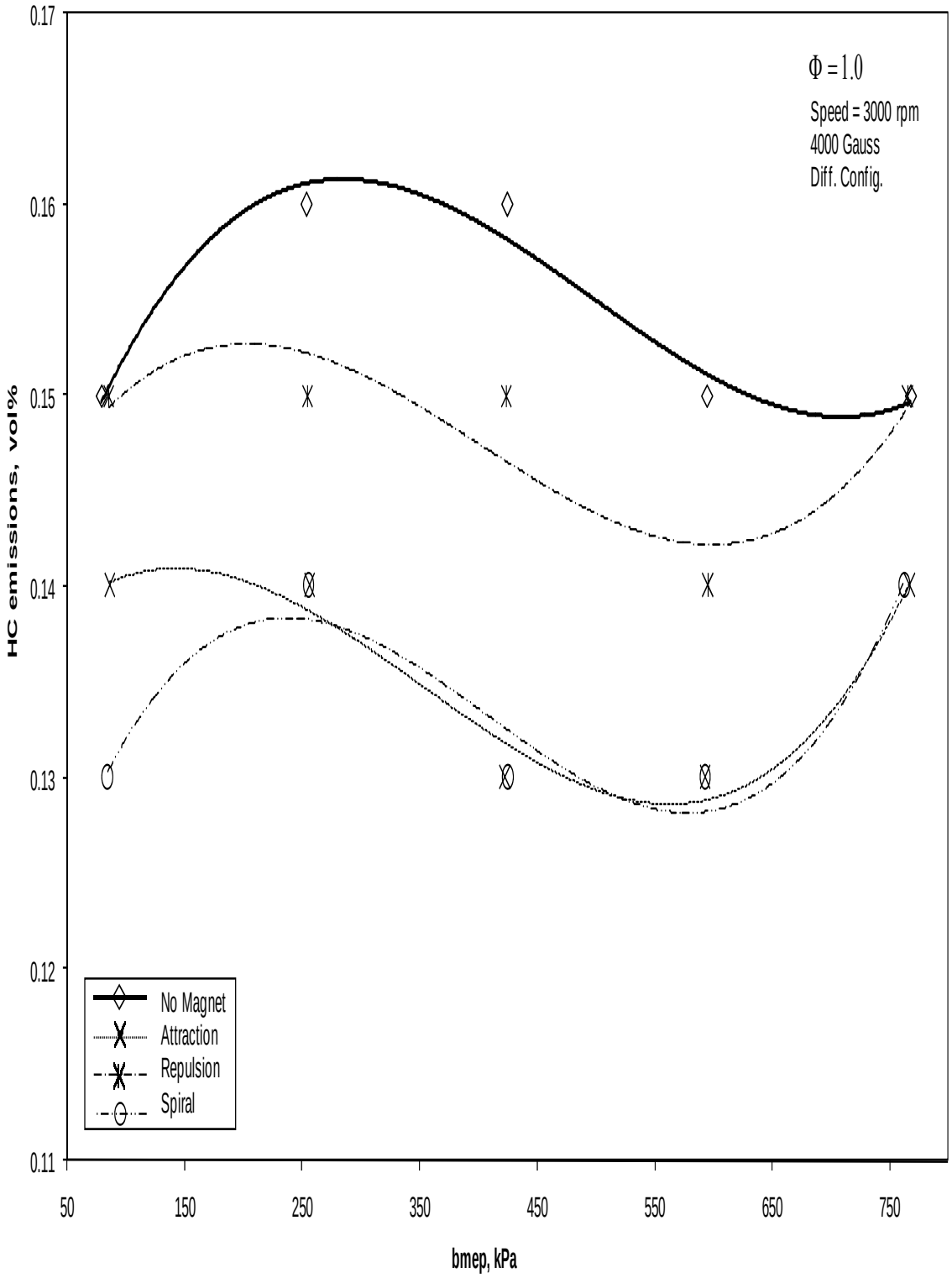

Figure 7-20: Magnetic configuration effect on HC at constant speed of 3000 rpm

CHAPTER 8

8 RESULTS AND DISCUSSIONS

8.1 Specific Fuel Consumption

8.1.1 Magnetic Field Strength Effect

There is little effect of magnetic field on the relationship of SFC to engine speed. In addition, the magnitude of magnetic field strength also has minimal effect to change this pattern at most engine speeds and loads. The difference between the maximum and minimum magnitude of SFC is small, depicting a relatively insensitive dependence of SFC on engine speed. The only considerable magnetic field effect can be observed at the lowest engine load of 20 Nm. This reduction by 10% is observed only at the lowest and highest engine speeds of 1000 rpm and 3000 rpm.

8.1.2 Magnetic Field Configuration Effect

An increase in load reduces the SFC at all engine speeds, whether the magnetic field is turned on or off. A marked decrease by 10 % in SFC occurs only at the lowest load of 20 Nm during the maximum and minimum engine speeds of 1000 rpm and 3000 rpm. It is more apparent for the ‘Attraction’ configuration, with a more favourable effect for the ‘Repulsion’ configuration at an engine load of 60 Nm. However, with the increase in load, this minimal improvement due to configuration is dissipating within the error.

8.2 Carbon Monoxide Emissions

8.2.1 Magnetic Field Strength Effect

The application of a magnetic field produces no qualitative change in the relationship of CO emissions level against engine speed at a constant load. However, it does produce an appreciable consistent decrease by 10% in the emissions level for most engine loads and speeds. It can also be reduce by 40% at the lowest engine speeds of 1000 rpm and engine loads of 20 Nm, 140 Nm, and 180 Nm. The magnitude of the magnetic field strength has virtually no obvious distinctive variation in the effect.

8.2.2 Magnetic Field Configuration Effect

With the increasing load, the CO emissions show a change in the qualitative behaviour for loads of 60 and 100 Nm. However, at the highest engine load of 180 Nm, the relationship reverts back to be similar to the lowest load of 20 Nm. Application of a magnetic field has an appreciable effect of 10% in decreasing the CO emissions at all engine speeds and loads. The influence of the different magnetic configurations is not pronounced, especially at the highest speed. Their effect is observed only below 1500 rpm and that too for the lowest and higher values of the load. In this regard, the 'Repulsion' and 'Attraction' configuration seems to perform better by achieving a reduction by 48% in CO emissions at extreme ends of the load settings.

8.3 Nitrogen Oxides Emissions

8.3.1 Magnetic Field Strength Effect

The application of the magnetic field decreases the NOx emissions considerably by an average of 15%. However, this is generally valid for intermediate ranges of the field strength from 1600 to 3200 Gauss where the reduction reaches 35% at the lowest engine load and speed. NOx emissions levels rise considerably with the increase of the load, and the dependence on the engine speed also changes, but then it settles down at a load of 140 Nm. The magnitude of the load also affects the influence of the magnetic field to produce enhanced performance, which can be clearly observed for the 100 Nm load setting.

8.3.2 Magnetic Field Configuration Effect

The NOx emissions trend against increasing engine speed changes considerably with each increase in the load value. Moreover, with each increase in the load value, the NOx emissions level increases considerably at all engine speeds. The application of the magnetic field reduces the emissions significantly by 35%, especially at the lowest engine speed of 1000 rpm. The ‘Spiral’ configuration continues to be the best performing setup for all engine loads, especially at the lowest engine speed with an average reduction by 15% in emissions level.

8.4 Hydrocarbons Emissions

8.4.1 Magnetic Field Strength Effect

Magnetic field strength has considerable influence on the emissions level reaching 30% reduction at higher magnetic field strengths. The best results are produced consistently by the strongest magnetic field at most engine loads and speeds, with an average of 15% reduction in NOx emission. The amount of reduction is generally following positively an increase in field strength. An isolated case occurs at an engine speed of 2000 rpm, where it is observed that the application of a magnetic field actually increases the HC emissions except at the highest field strength. It seems that the engine speed of 2000 rpm depicts a transition point.

8.4.2 Magnetic Field Configuration Effect

With increasing load the HC emissions go down at all engine speeds to a minimum at a load of 100 Nm, but thereafter the emissions start to increase again. Also, generally the relationship between the HC emissions and the engine speed is a linear one, with strong nonlinearity occurring only at lower engine speeds, and that too for the lowest and highest load values. Generally, the 'Attraction' and 'Spiral' configurations are seen to perform best with an average reduction by 15% in HC emissions. However, the 'Repulsion' configuration is seen to have very little or negative effect on the emissions at different loads.

CHAPTER 9

9 CONCLUSIONS AND RECOMMENDATIONS

The effect of magnetic field on the combustion efficiency and emissions formulation of a four-stroke internal combustion engine with spark ignition, six cylinders, and fuel injection was investigated experimentally with unleaded gasoline fuel. The equilibrium combustion characteristics can be influenced by applying a magnetic field with a sufficient strength and a certain configuration.

The magnetic force can affect the molecular energy and molecular arrangement of the fuel atoms. Moreover, the application of a magnetic field at the fuel injection point assures the impact on all combustion cycle processes. Furthermore, detailed experiments at different operating conditions and different magnetic field effects showed the effectiveness of applying a magnetic field on combustion efficiency and emissions formulation.

The effect of magnetism can be utilized in other individual and industrial applications. This effect can vary according to the application, fuel type, and equipment design. The effect of magnetism on combustion efficiency and exhaust emissions holds great promise for both the financial and the environmental perspectives. It will save individuals and companies a great amount of money by improvemening of the combustion efficiency. At the same time, by reducing the noxious emissions it will reduce air pollution and save the earth from these pollutants which harm all living organisms.

The specific fuel consumption was reduced by 10% for the lowest load of 20 Nm where it was observed at the lowest and highest speed of 1000 rpm and 3000 rpm respectively. The CO emissions were reduced by 48% with the 'Attraction' and 'Repulsion' configurations at the lowest speed or 1000 rpm for several loads settings (20 Nm, 140 Nm, and 180 Nm) with an average 10% reduction across most other settings. The NOx emissions were reduced by 35% with the 'Spiral' configuration at the lowest speed and load of 1000 rpm and 20 Nm respectively, with an average reduction of 15% across most other settings. The HC emissions were reduced by 30% with a magnetic field strength of 3200 Gauss at the lowest speed and load of 1000 rpm and 20 Nm, with an average of 15% reduction across most other settings.

In summary, the magnetic field effect is most useful while the engine is idling during warm-up, traffic jams, and at traffic lights at the lowest engine speed and load of 1000 rpm and 20 Nm respectively. Moreover, an appreciable reduction by 15% in exhaust emissions is achieved in almost all other settings, which will benefit the environment significantly. The magnetic field impact can be utilized in many other applications, equipment designs, and fuel types.

I recommend conducting more extensive experiments utilizing other magnetic field effects such as generating a stronger magnetic field concentrated at one point instead of spreading the strength across the line by using several magnets. The real effect on molecular arrangements and atoms energy needs to be studied further by physicists and chemists to clarify the relationship between combustion and magnetism.

APPENDICES

Table A-1: Experimental data of the base line without magnetic field effect

Test Results Data					Measured	Calculations		
Speed (rpm)	Load (Nm)	CO (ppm)	NOx (ppm)	HC (vol%)	Time (s)	Power (kW)	bmep (kPa)	SFC (g/kWh)
3001	180.92	1606	3249	0.15	45.7	56.86	768.08	260.66
2999.9	140.06	1768	2229	0.15	55.5	44.00	594.61	277.36
3000	100.09	2069	1465	0.16	71.0	31.44	424.92	303.38
3000	59.78	2297	835	0.16	97.0	18.78	253.79	371.79
2998.23	18.7	1958	513	0.15	151.3	5.87	79.39	762.44
2499.5	180.3	1718	3807	0.17	54.5	47.19	765.44	263.33
2499.34	139.99	1889	2756	0.16	67.0	36.64	594.31	275.90
2499.7	99.95	2265	1777	0.17	85.5	26.16	424.33	302.77
2499.8	59.9	2343	1013	0.17	117.3	15.68	254.30	368.23
2498.2	20.73	2185	549	0.17	183.7	5.42	88.01	679.85
1999.5	180.75	1797	3884	0.16	67.5	37.85	767.36	265.12
1999.3	139.9	1538	2927	0.15	84.0	29.29	593.93	275.28
1999.37	100.17	1865	1577	0.14	106.6	20.97	425.26	302.94
1999.77	61.06	2008	891	0.15	145.0	12.79	259.22	365.30
1999.34	20.75	2130	627	0.19	234.4	4.34	88.09	665.10
1499.8	180.9	1743	4018	0.18	86.7	28.41	767.99	274.95
1500.1	141.27	1189	3288	0.16	108.9	22.19	599.75	280.25
1499.71	100.82	1347	2248	0.17	140.3	15.83	428.02	304.89
1499.66	60.47	1611	1017	0.18	195.6	9.50	256.72	364.63
1499.2	21.15	2126	412	0.22	301.0	3.32	89.79	677.66
1000.85	177.1	3500	3458	0.26	123.5	18.56	751.86	295.46
1000.3	141.29	1800	3063	0.18	152.8	14.80	599.83	299.49
1000.27	100.53	967	2466	0.17	204.2	10.53	426.79	314.98
1000	60	900	1443	0.17	288.7	6.28	254.72	373.38
1000	20	3000	350	0.31	454.9	2.09	84.91	710.89

Table A-2: Experimental data after applying one (1) magnet (Attraction)

Test Results Data					Measured	Calculations		
Speed (rpm)	Load (Nm)	CO (ppm)	NOx (ppm)	HC (vol%)	Time (s)	Power (kW)	bmep (kPa)	SFC (g/kWh)
2999	180.45	1429	3563	0.15	45.5	56.67	766.08	262.67
3000.5	140.9	1566	2497	0.13	55.0	44.27	598.18	278.15
3000.6	99.9	1863	1584	0.14	71.0	31.39	424.12	303.89
3000	60.7	2067	944	0.14	96.0	19.07	257.70	369.97
3000.6	20.8	1800	502	0.14	148.0	6.54	88.30	700.19
2500	179.7	1555	3691	0.18	54.5	47.05	762.90	264.16
2501.5	141.35	1568	2961	0.15	66.7	37.03	600.09	274.24
2501.4	99.9	1977	1967	0.15	85.4	26.17	424.12	303.07
2501	60.06	2025	1138	0.15	117.1	15.73	254.98	367.70
2500	20.55	1912	604	0.15	182.2	5.38	87.24	690.96
2000.3	180.4	1321	3944	0.18	67.8	37.79	765.87	264.36
1999.8	139.8	1362	3194	0.15	84.5	29.28	593.51	273.78
1999.2	100.2	1608	1862	0.15	106.7	20.98	425.39	302.60
1998.8	60.5	1766	914	0.15	147.4	12.66	256.85	362.85
1999.7	20.5	1900	613	0.17	235.3	4.29	87.03	670.52
1499.4	180.6	1452	3779	0.19	87.6	28.36	766.72	272.65
1499.7	139.8	1092	3325	0.15	109.5	21.96	593.51	281.72
1499.4	100.15	1218	2310	0.15	142.5	15.73	425.18	302.25
1499.1	59.9	1456	1040	0.16	196.7	9.40	254.30	366.17
1498.8	20.5	1853	402	0.19	308.6	3.22	87.03	682.11
1000	178.13	3243	3229	0.32	124.4	18.65	756.23	291.87
999.9	139.7	1433	2969	0.18	156.4	14.63	593.08	296.05
1000	100.17	886	2428	0.15	205.3	10.49	425.26	314.50
999.9	59.46	885	1171	0.15	290.3	6.23	252.43	374.73
999.9	22.4	2424	259	0.28	448.8	2.35	95.10	643.42

Table A-3: Experimental data after applying two (2) magnets (Attraction)

Test Results Data					Measured	Calculations		
Speed (rpm)	Load (Nm)	CO (ppm)	NOx (ppm)	HC (vol%)	Time (s)	Power (kW)	Bmep (kPa)	SFC (g/kWh)
2999.5	180.09	1446	3238	0.15	45.6	56.57	764.55	262.57
2999.47	139.6	1589	2058	0.14	55.4	43.85	592.66	278.81
2999.77	100.87	1920	1310	0.14	70.4	31.69	428.23	303.62
3000.75	60.16	2070	740	0.15	96.1	18.90	255.40	372.81
3000.5	20.57	1770	440	0.14	147.4	6.46	87.33	710.93
2500	180.91	1418	3558	0.18	54.2	47.36	768.03	263.84
2499.92	140.04	1688	2556	0.16	66.2	36.66	594.53	279.07
2500.15	100.28	1991	1621	0.16	84.7	26.25	425.73	304.57
2499.97	60.2	2054	929	0.17	116.1	15.76	255.57	370.16
2499.86	19.45	1929	476	0.17	184.1	5.09	82.57	722.54
2000.19	179.86	1212	3669	0.19	68.1	37.67	763.58	264.00
1999.79	139.64	1427	2717	0.17	83.5	29.24	592.83	277.38
2000.09	99.63	1651	1463	0.16	106.4	20.87	422.97	305.05
1999.3	59.45	1717	710	0.17	147.0	12.45	252.39	370.17
1999.3	20.1	1886	552	0.19	238.4	4.21	85.33	675.10
1500	179.9	1189	3757	0.16	90.0	28.26	763.75	266.31
1500	139.73	1103	3183	0.14	111.0	21.95	593.21	278.00
1500.08	100.03	1267	2139	0.14	142.3	15.71	424.67	302.90
1500.15	60.47	1461	1081	0.15	197.1	9.50	256.72	361.73
1500.26	20.5	1995	422	0.19	309.8	3.22	87.03	678.81
999.9	180.1	2950	3310	0.27	124.9	18.86	764.60	287.55
999.7	140.22	1339	2990	0.16	157.8	14.68	595.29	292.39
999.6	100.64	929	2421	0.14	205.3	10.53	427.26	313.16
999.75	60.34	884	1440	0.14	290.8	6.32	256.17	368.69
999.46	23.3	2800	303	0.33	440.0	2.44	98.92	631.21

Table A-4: Experimental data after applying three (3) magnets (Attraction)

Test Results Data					Measured	Calculations		
Speed (rpm)	Load (Nm)	CO (ppm)	NOx (ppm)	HC (vol%)	Time (s)	Power (kW)	bmep (kPa)	SFC (g/kWh)
3000.2	180.45	1413	3428	0.15	46.1	56.69	766.08	259.14
3000.3	139.9	1528	2218	0.13	55.8	43.96	593.93	276.14
3000	100.07	1821	1377	0.14	71.2	31.44	424.84	302.58
3000.2	59.9	2039	772	0.15	96.2	18.82	254.30	374.11
3000.3	20.32	1826	449	0.14	147.5	6.38	86.27	719.23
2499.9	180.19	1441	3680	0.18	54.8	47.17	764.98	262.01
2500	140.28	1684	2807	0.15	66.6	36.73	595.54	276.91
2500	100.45	1993	1655	0.15	85.3	26.30	426.45	301.93
2500	59.79	2086	797	0.16	116.6	15.65	253.83	371.09
2500	20.3	1949	465	0.16	181.9	5.31	86.18	700.62
2000	180.1	1309	3750	0.19	68.1	37.72	764.60	263.67
2000	140.5	1395	2938	0.17	83.9	29.43	596.48	274.34
1999.9	100.59	1656	1588	0.15	107.1	21.07	427.04	300.19
2000	59.85	1800	695	0.16	146.6	12.53	254.09	368.57
2000	19.95	1891	483	0.17	238.7	4.18	84.70	679.09
1499.8	179.8	1229	3751	0.18	89.3	28.24	763.32	268.58
1499.8	140.1	1145	3090	0.15	110.7	22.00	594.78	278.06
1499.8	99.85	1308	1945	0.15	143.7	15.68	423.90	300.55
1499.77	59.76	1494	823	0.16	197.5	9.39	253.70	365.38
1499.7	19.98	1774	330	0.18	312.8	3.14	84.82	690.06
1000	179.77	2913	3237	0.29	125.1	18.83	763.19	287.59
1000.06	140.05	1320	2774	0.18	156.0	14.67	594.57	296.02
999.96	99.88	896	2138	0.16	203.9	10.46	424.03	317.59
1000	60.42	849	1294	0.14	291.9	6.33	256.51	366.72
1000	20.65	2276	237	0.27	454.8	2.16	87.67	688.67

Table A-5: Experimental data after applying four (4) magnets (Attraction)

Test Results Data					Measured	Calculations		
Speed (rpm)	Load (Nm)	CO (ppm)	NOx (ppm)	HC (vol%)	Time (s)	Power (kW)	Bmep (kPa)	SFC (g/kWh)
3000	180.09	1464	3633	0.14	46.2	56.58	764.55	259.12
3000.4	140.09	1619	2438	0.13	57.0	44.02	594.74	269.95
3000.2	99.86	1913	1570	0.13	72.2	31.37	423.95	299.00
2999.3	59.48	2071	867	0.14	97.8	18.68	252.52	370.70
3000.8	20.42	1858	482	0.14	148.7	6.42	86.69	709.82
2499.6	179.96	1448	3840	0.16	55.1	47.11	764.00	260.95
2499.5	140.04	1731	2968	0.14	67.6	36.66	594.53	273.34
2499.3	100.16	2025	1749	0.15	85.6	26.21	425.22	301.83
2500	60.56	2140	861	0.15	116.1	15.85	257.10	367.95
2499.9	20.09	2009	473	0.15	182.5	5.26	85.29	705.64
2000.1	180.01	1486	3607	0.19	68.0	37.70	764.21	264.18
2000.2	139.66	1452	2834	0.15	84.4	29.25	592.91	274.32
2000.1	100.1	1717	1551	0.15	106.8	20.97	424.96	302.48
2000.3	59.9	1855	680	0.15	146.5	12.55	254.30	368.46
2000.1	20.48	1983	454	0.17	236.3	4.29	86.95	668.20
1499.9	179.92	1583	3573	0.2	87.4	28.26	763.83	274.22
1500	139.7	1180	2941	0.15	110.6	21.94	593.08	279.07
1499.9	100.4	1321	1930	0.15	141.6	15.77	426.24	303.31
1500	60.34	1509	777	0.16	196.3	9.48	256.17	364.03
1500.2	20.2	1848	316	0.19	310.0	3.17	85.76	688.48
999.66	179.06	3350	3015	0.31	125.6	18.74	760.18	287.68
1000	139.94	1500	2690	0.19	154.7	14.65	594.10	298.76
999.94	99.94	921	2052	0.15	203.6	10.47	424.28	317.88
1000	60.8	910	1200	0.14	291.6	6.37	258.12	364.80
1000	20.7	1550	230	0.21	451.8	2.17	87.88	691.57

Table A-6: Experimental data after applying five (5) magnets (Attraction)

Test Results Data					Measured	Calculations		
Speed (rpm)	Load (Nm)	CO (ppm)	NOx (ppm)	HC (vol%)	Time (s)	Power (kW)	bmep (kPa)	SFC (g/kWh)
3000.16	180.72	1454	3291	0.14	45.9	56.78	767.23	259.89
2999.6	139.63	1630	2282	0.13	56.0	43.86	592.78	275.75
3000	99.72	1894	1426	0.13	71.0	31.33	423.35	304.50
2999.7	60.3	2085	804	0.14	95.0	18.94	256.00	376.38
3000.5	20.27	1778	484	0.14	147.7	6.37	86.05	719.98
2500.5	180.25	1425	3848	0.15	54.6	47.20	765.23	262.82
2500.1	140.52	1730	2713	0.14	66.4	36.79	596.56	277.26
2499.2	100.32	2020	1696	0.14	84.8	26.26	425.90	304.20
2499.4	59.83	2103	942	0.15	117.1	15.66	254.00	369.35
2499.26	20.59	1978	535	0.15	182.5	5.39	87.41	688.68
2000.4	180.45	1190	3997	0.16	68.0	37.80	766.08	263.49
2000.53	140.57	1458	2972	0.14	84.0	29.45	596.78	273.80
2000	99.92	1690	1631	0.14	107.2	20.93	424.20	301.91
2000	60.07	1789	800	0.15	146.9	12.58	255.02	366.47
2000.1	20.59	1898	615	0.16	237.4	4.31	87.41	661.55
1500	179.82	1095	3954	0.16	87.5	28.25	763.41	274.04
1499.73	139.74	1184	3190	0.14	109.6	21.95	593.25	281.58
1499.64	100.67	1304	2101	0.14	141.1	15.81	427.38	303.62
1499.5	59.72	1484	900	0.15	196.4	9.38	253.54	367.74
1499.65	20.57	1769	417	0.18	311.2	3.23	87.33	673.73
1000.7	180.08	1901	3540	0.24	124.9	18.87	764.51	287.35
1000.3	140.3	1074	3092	0.16	156.5	14.70	595.63	294.47
999.6	100.25	890	2427	0.14	206.4	10.49	425.60	312.70
1000.2	60	887	1480	0.14	292.4	6.28	254.72	368.58
999.8	22.9	2314	332	0.25	444.0	2.40	97.22	636.24

Table A-7: Experimental data after applying five (5) magnets (Repulsion)

Test Results Data					Measured	Calculations		
Speed (rpm)	Load (Nm)	CO (ppm)	NOx (ppm)	HC (vol%)	Time (s)	Power (kW)	bmep (kPa)	SFC (g/kWh)
3000	180.43	1470	3789	0.15	46.4	56.68	766.00	257.51
3000.2	140.3	1621	2528	0.14	55.9	44.08	595.63	274.87
2999.92	99.75	1927	1619	0.15	71.2	31.34	423.48	303.56
2999	59.89	2092	908	0.15	97.1	18.81	254.26	370.85
3000.65	20.07	1840	512	0.15	151.4	6.31	85.21	709.35
2500.5	180.45	1431	4042	0.18	54.6	47.25	766.08	262.53
2500.6	140.38	1760	2914	0.16	67.5	36.76	595.97	272.96
2500.5	99.7	2113	1688	0.17	85.7	26.11	423.27	302.72
2500.76	60.35	2143	894	0.17	116.9	15.80	256.21	366.60
2500.78	20.36	2025	511	0.16	182.4	5.33	86.44	696.42
2000.4	179.74	1224	4048	0.18	68.6	37.65	763.07	262.22
2000	140.23	1475	3107	0.16	84.0	29.37	595.33	274.54
2000	99.64	1723	1698	0.16	107.1	20.87	423.01	303.04
2000.66	60.75	1839	781	0.16	145.7	12.73	257.91	365.23
2000.5	20.36	1935	538	0.18	238.2	4.27	86.44	666.64
1500.25	179.75	1149	3974	0.18	88.6	28.24	763.11	270.70
1500.33	140.77	1220	3214	0.16	109.2	22.12	597.62	280.43
1500.14	100.18	1304	2323	0.16	141.2	15.74	425.30	304.79
1500	59.74	1526	855	0.17	197.2	9.38	253.62	366.00
1500	20.75	1797	368	0.2	306.1	3.26	88.09	678.86
999.9	177.5	1914	3508	0.26	126.0	18.59	753.56	289.22
1000	140.23	1073	3026	0.17	155.2	14.68	595.33	297.18
999.85	100.7	916	2295	0.16	202.9	10.54	427.51	316.59
1000.2	60.7	912	1369	0.16	289.2	6.36	257.70	368.36
1000.53	20.47	1527	335	0.24	455.6	2.14	86.90	693.14

Table A-8: Experimental data after applying five (5) magnets (Spiral)

Test Results Data					Measured	Calculations		
Speed (rpm)	Load (Nm)	CO (ppm)	NOx (ppm)	HC (vol%)	Time (s)	Power (kW)	bmep (kPa)	SFC (g/kWh)
2999.84	179.78	1410	3535	0.14	46.1	56.48	763.24	260.14
2999.8	139.6	1538	2346	0.13	55.8	43.85	592.66	276.78
2999.75	100.27	1810	1451	0.13	70.6	31.50	425.69	304.57
2999.4	60.13	2033	823	0.14	96.2	18.89	255.28	372.78
3000	19.98	1786	468	0.13	147.8	6.28	84.82	730.06
2499.82	180.08	1462	3787	0.17	54.5	47.14	764.51	263.62
2499.68	139.78	1680	2861	0.14	66.9	36.59	593.42	276.69
2499.45	100.95	1993	1787	0.15	84.2	26.42	428.57	304.43
2499.44	60.25	2083	831	0.15	116.1	15.77	255.79	369.93
2498.4	20.04	1953	472	0.15	182.1	5.24	85.08	709.38
1999.6	180.15	1286	3796	0.18	67.4	37.72	764.81	266.39
1999.34	139.88	1367	3047	0.15	83.5	29.29	593.85	276.96
1999.69	100.53	1663	1630	0.15	106.5	21.05	426.79	302.09
1999.6	60.5	1790	708	0.15	144.8	12.67	256.85	369.22
1999.2	20.38	1877	514	0.16	235.8	4.27	86.52	673.20
1499.9	180.95	1288	3776	0.18	87.3	28.42	768.20	272.97
1499.6	140.3	1208	3106	0.14	108.7	22.03	595.63	282.81
1500.26	100.13	1264	2081	0.15	141.2	15.73	425.09	304.92
1499.68	59.67	1460	848	0.16	195.8	9.37	253.32	369.13
1499	20.74	1768	350	0.19	304.8	3.26	88.05	682.54
1000.68	178.35	3033	3192	0.31	124.7	18.69	757.17	290.61
1000.45	139.95	1264	2794	0.18	155.7	14.66	594.14	296.68
1000.5	100.03	866	2090	0.15	204.0	10.48	424.67	316.79
1000.2	60.18	855	1188	0.15	290.7	6.30	255.49	369.63
1001.56	20.56	1792	222	0.24	455.0	2.16	87.29	690.30

NOMENCLATURE

Φ	Equivalence Ratio
BC	Bottom Centre
bmep	Brake mean effective pressure
CI	Compression Ignition
CL	Chemi-Luminescent Analyzer
CO	Carbon Monoxide
HFID	Heated Flame Ionization Detector
HC	Hydrocarbons
ICE	Internal Combustion Engine
Gauss	Magnetic Strength Unit
kWh	Kilo Watt per hour
LHV	Low Heating Value
NDIR	Non-Dispersive Infra-Red Analyzer
Nm	Newton meter
NOx	Nitrogen Oxides
ppm	part per million
rpm	Revolution per minute
SFC	Specific Fuel Consumption
SI	Spark Ignition
T	Tulsa (Magnetic Strength Unit)
TC	Top Centre

REFERENCES

1. AL-Dawood, A. M., "Effects of Blending MTBE, Methanol, or Ethanol with Gasoline on Performance and Exhaust Emissions of SI Engines", *KFUPM, Mechanical Engineering Thesis*, Dhahran, Saudi Arabia, 1998.
2. Heywood, J. B., *Internal Combustion Engine Fundamentals*, McGraw-Hill, New York, 1988.
3. Obert, E. D., "*Internal Combustion Engines and Air Pollution*", Harper & Row Publishers, 1973.
4. Taylor, C. F., "*The Internal Combustion Engines in Theory and Practice*", Vol 1 & 2, MIT Press, 2nd Edition, 1985.
5. Stone, R., "*Introduction to Internal Combustion Engines*", SAE International, 2nd Edition, 1992.
6. Wark, K., and Warner, C. F., *Air Pollution, its Origin and Control*, Harber and Row Publishers, New York.
7. Masterton, W. L., Hurley, C. N., "*Chemistry: Principles and Reactions*", Saunders, College Publishing, 1989.
8. Jiles, D., *Introduction to Magnetism and Magnetic Materials*, Chapman and Hall, New York, 1991.
9. Ulaby, F. T., *Fundamentals of Applied Electromagnetics,* Prentice Hall, Upper Saddle River, New Jersey, 2001.
10. Ueno, S., and Harada, K., "Experimental Difficulties in Observing the Effect of Magnetic Fields on Biological and Chemical Processes," *IEEE Transactions on Magnetics*, MAG-22, No.5, 1986, pp. 868-873.
11. Ueno, S., and Harada, K., "Effects of Magnetic Fields on Flames and Gas Flow," *IEEE Transactions on Magnetics*, MAG-23, No.5, 1987, pp. 2752-2754.
12. Aoki, T., "Radicals Emissions and Butane Diffusion Flames Exposed to Upward Decreasing Magnetic Fields," *Japanese Journal of Applied Physics*, Vol. 28, No. 5, 1989, pp.776-785.
13. Aoki, T., "Radicals Emissions and Butane Diffusion Flames Exposed to Uniform Magnetic Fields Encircled by Magnetic Gradient Fields," *Japanese Journal of Applied Physics*, Vol. 29, No. 5, 1990, pp.952-957.
14. Wakayama, N. I., "Magnetic Promotion of Combustion in Diffusion Flames," *Combustion and Flame*, Vol. 93, 1993, pp.207-214.
15. Wakayama, N. I., Ito, H., Kurida, Y., Fujita, O., and Ito, K., "Magnetic Support of Combustion in Diffusion Flames under Microgravity," *Combustion and Flame*, Vol. 107, 1996, pp.187-192.

16. Energy Management Solution, “Magnetism Making Fuel Burn More Completely?” *Metallurgia*, Vol. 63, July 1996, p. 244.
17. Nayyar, N., “Combustion Efficiency with Magnetism,” *Metallurgia*, Vol. 65, No. 7, July 1998, pp. 233-234.
18. Baker J., and Saito K., “Magnetocombustion: A Thermodynamic Analysis,” *Journal of Propulsion and Power*, Vol. 16, No. 2, March 2000, pp. 263-268.
19. Pankhurst, Q., and Parkin I, “Magnetism Adds Sparkle to Combustion,” *Physics World*, Vol. 14, Issue. 11, 2001, pp. 20-21.

VITA

Name of Student : Rashid Mohammed Ali Al-Dossary
Date of Birth : April 7, 1975
Nationality : Saudi Arabian

- Bachelor of Science, Mechanical Engineering (1999), Oregon State University, Corvallis, OR, USA.
    - GPA: 3.69
    - Major: Mechanical Engineering
    - Minor: Computer Science
- Currently working as a Utility Operation Engineer for Abqaiq Plants, Saudi Aramco, Abqaiq, KSA.